Interplay between n→π^* Interactions and Dynamic Covalent Bonds: Quantification and Modulation by Solvent Effects

Hao Zheng,[a, c] Hebo Ye,[a, b] Xiaoxia Yu,[a, c] and Lei You[a, b, *]

a. State Key Laboratory of Structural Chemistry, Fujian Institute of Research on the Structure of Matter, Chinese Academy of Sciences, Fuzhou 350002, China.

b. University of Chinese of Academy of Sciences, Beijing 100049, China.

c. College of Chemistry and Material Science, Fujian Normal University, Fuzhou 350007, China.

Table of Contents

1. General Methods

^{1}H NMR and ^{13}C NMR spectra were recorded on a 400 MHz Bruker Biospin Avance III spectrometer or a 400 MHz JEOL JNM-ECZ400S spectrometer. The chemical shifts (δ) for ^{1}H NMR spectra, given in ppm, are referenced to the residual proton signal of the deuterated solvent. Mass spectra were recorded on a Bruker IMPACT-II spectrometer. Crystallographic data was collected on a Mercury single crystal diffractometer at room temperature. The structures were solved with direct methods by using SHELXS-97 and refined with the full-matrix least-squares technique based on F2. Deuterium solvents were purchased from Aldrich. All other reagents were obtained from commercial sources and were used without further purification, unless indicated otherwise. The experimental details of dynamic covalent reactions, computational studies, and imine formation in water are shown in page S15, S42, and S59, respectively.

2. Synthesis and Characterization

(1) Synthesis of 1(X) and 1(*p*-X)

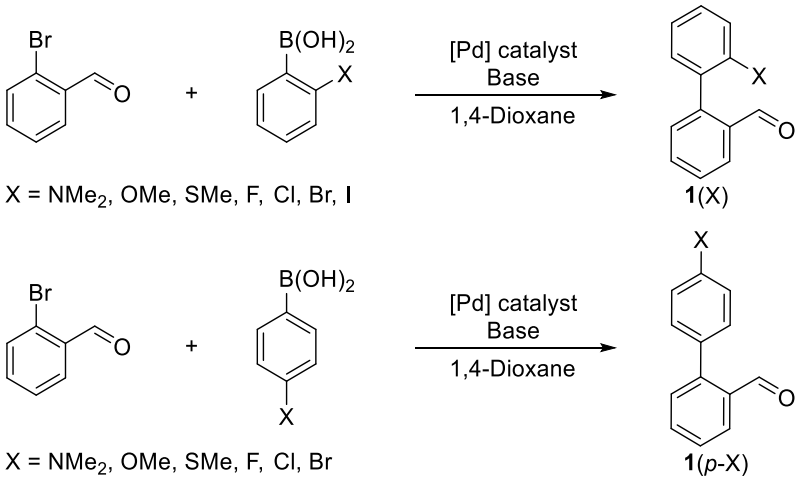

Scheme S1. General synthetic routes of **1**(X) and **1**(*p*-X).

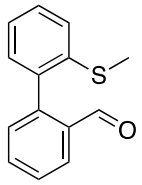

2'-(methylthio)-[1,1'-biphenyl]-2-carbaldehyde: To a mixture of 2-bromobenzaldehyde (1.0 mmol, 185 mg), (2-(methylthio)phenyl)boronic acid (1.2 mmol, 202 mg), potassium carbonate (2.0 mmol, 276 mg), and tetrakis(triphenylphosphine)palladium (0.005 mmol, 58 mg), was added 1,4-dioxane (10 mL) under N_2 atmosphere. The reaction was stirred at 80 ℃ for 12 h. After the reaction was cooled to room temperature, H_2O (25 ml) was added, and the mixture was extracted with ethyl acetate (EA; 25 ml × 3). The combined organic layer was washed with saturated aqueous NH_4Cl (50 ml × 3) and dried over anhydrous Na_2SO_4. After removal of solvent under vacuum and further purification performed on the column chromatography (silica gel, petroleum ether (PE) / EA = 40:1 to 20:1), the title compound was obtained as a white solid (216 mg, 95%). ^{1}H NMR (DMSO-d_6): δ 9.61 (s, 1H), 7.91 (dd, *J* = 7.7, 1.1 Hz, 1H), 7.77 (td, *J* = 7.5, 1.3 Hz, 1H), 7.61 (t, *J* = 7.6 Hz, 1H), 7.48 (t, *J* = 6.6 Hz, 1H), 7.35 (t, *J* = 8.2 Hz, 2H), 7.32-7.23 (m, 2H), 2.36 (s, 3H). ^{13}C NMR ($CDCl_3$): δ 191.9, 143.8, 138.3, 136.3, 133.9, 133.9, 131.0, 130.4, 129.0, 128.5, 127.0, 124.7, 124.6, 15.5. ESI-HRMS: m/z calcd for $C_{14}H_{12}OSNa$ [M + Na^+]: 251.0501; found: 251.0501.

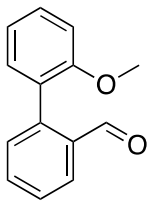

2'-methoxy-[1,1'-biphenyl]-2-carbaldehyde: The reported procedure[S1] was used to afford the title compound as a white crystal (yield: 90%). ^{1}H NMR ($CDCl_3$): δ ^{1}H NMR ($CDCl_3$) δ 9.81 (s, 1H), 8.02 (dd, *J* = 7.8, 1.3 Hz, 1H), 7.67 (td, *J* = 7.5, 1.4 Hz, 1H), 7.51 (t, *J* = 7.6 Hz, 1H), 7.48-7.42 (m, 1H), 7.39 (d, *J* = 7.7 Hz, 1H), 7.32 (dd, *J* = 7.5, 1.7 Hz, 1H), 7.11 (t, *J* = 7.0 Hz, 1H), 7.01 (d, *J* = 8.1 Hz, 1H), 3.77 (s, 3H).

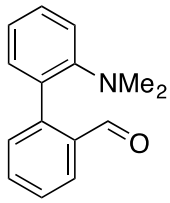

2'-(dimethylamino)-[1,1'-biphenyl]-2-carbaldehyde: The reported procedure[S2] was used to afford the title compound as a yellow solid (yield: 96%). ^{1}H NMR (CD_3CN): 9.54 (s, 1H), 7.88 (dd, *J* = 7.7, 1.2 Hz, 1H), 7.74 (td, *J* = 7.5, 1.4 Hz, 1H), 7.52 (t, *J* = 7.5 Hz, 1H), 7.48-7.45 (m, 1H), 7.42 (td, *J* = 7.9, 1.7 Hz, 1H), 7.38 (dd, *J* = 7.5, 1.6 Hz, 1H), 7.23-7.14 (m, 2H), 2.37 (s, 6H).

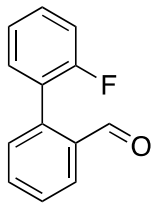

2'-fluoro-[1,1'-biphenyl]-2-carbaldehyde: The reported procedure[S3] was used to afford the title compound as a colorless oil (yield: 60%). ^{1}H NMR (DMSO-d_6): δ 9.83 (s, 1H), 7.96 (d, *J* = 7.3 Hz, 1H), 7.80 (t, *J* = 7.5 Hz, 1H), 7.65 (t, *J* = 7.5 Hz, 1H), 7.56-7.46 (m, 3H), 7.38-7.32 (m, 2H).

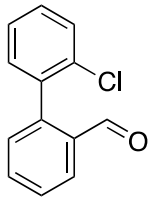

2'-chloro-[1,1'-biphenyl]-2-carbaldehyde: The reported procedure[S3] was used to afford the title compound as a white solid (yield: 55%). ^{1}H NMR ($CDCl_3$): δ 9.83 (s, 1H), 8.07 (dd, *J* = 7.8, 1.1 Hz, 1H), 7.70 (td, *J* = 7.5, 1.4 Hz, 1H), 7.58 (t, *J* = 7.6 Hz, 1H), 7.55-7.51 (m, 1H), 7.45-7.39 (m, 2H), 7.37 (m, 2H).

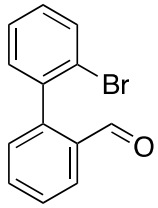

2'-bromo-[1,1'-biphenyl]-2-carbaldehyde: The reported procedure[S3]

was used to afford the title compound as a yellow solid (yield: 63%). ^{1}H NMR (DMSO-d_6): δ 9.71 (s, 1H), 7.95 (dd, *J* = 7.7, 1.1 Hz, 1H), 7.81-7.74 (m, 2H), 7.65 (t, *J* = 7.5 Hz, 1H), 7.52 (td, *J* = 7.5, 1.1 Hz, 1H), 7.47-7.35 (m, 3H).

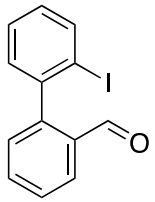

2'-iodo-[1,1'-biphenyl]-2-carbaldehyde: The reported procedure[S4] was used to afford the title compound as a drab solid (yield: 57%). ^{1}H NMR (DMSO-d_6): δ 9.68 (s, 1H), 8.00 (dd, *J* = 7.9, 0.9 Hz, 1H), 7.95 (dd, *J* = 7.8, 1.1 Hz, 1H), 7.78 (td, *J* = 7.5, 1.4 Hz, 1H), 7.64 (t, *J* = 7.6 Hz, 1H), 7.53 (td, *J* = 7.5, 1.1 Hz, 1H), 7.41 (dd, *J* = 7.6, 1.6 Hz, 1H), 7.31 (d, *J* = 7.6 Hz, 1H), 7.21 (td, *J* = 7.7, 1.7 Hz, 1H).

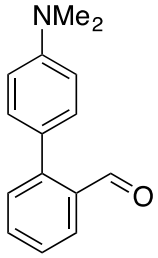

4'-(dimethylamino)-[1,1'-biphenyl]-2-carbaldehyde: The reported procedure[S5] was used to afford the title compound as a yellow solid (yield: 97%). ^{1}H NMR ($CDCl_3$): δ 10.03 (s, 1H), 7.99 (dd, *J* = 7.8, 1.2 Hz, 1H), 7.60 (td, *J* = 7.7, 1.5 Hz, 1H), 7.45 (d, *J* = 8.5 Hz, 1H), 7.41 (t, *J* = 7.5 Hz, 1H), 7.27 (d, *J* = 8.8 Hz, 2H), 6.81 (d, *J* = 8.8 Hz, 2H), 3.03 (s, 6H).

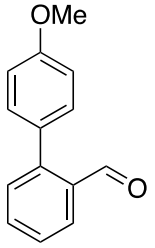

4'-methoxy-[1,1'-biphenyl]-2-carbaldehyde: The reported procedure[S5] was used to afford the title compound as a white solid (yield: 95%). ^{1}H NMR ($CDCl_3$): δ 10.02 (s, 1H), 8.05 (dd, *J* = 7.8, 1.1 Hz, 1H), 7.66 (td, *J* = 7.5, 1.5 Hz, 1H), 7.52 (t, *J*

= 7.6 Hz, 1H), 7.48 (d, *J* = 7.7 Hz, 1H), 7.43 – 7.37 (t, *J* = 7.5 Hz, 1H), 7.04 – 6.93 (m, 3H), 3.88 (s, 3H).

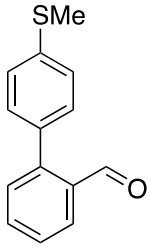

4'-(methylthio)-[1,1'-biphenyl]-2-carbaldehyde: The reported procedure[S6] was used to afford the title compound as a white solid (yield: 96%). ^{1}H NMR ($CDCl_3$) δ 9.99 (s, 1H), 8.02 (d, *J* = 7.8 Hz, 1H), 7.64 (t, *J* = 7.5 Hz, 1H), 7.49 (t, *J* = 7.4 Hz, 1H), 7.43 (d, *J* = 7.7 Hz, 1H), 7.33 (q, *J* = 8.3 Hz, 4H), 2.55 (s, 3H).

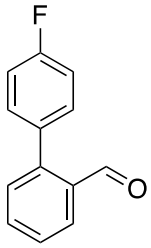

4'-fluoro-[1,1'-biphenyl]-2-carbaldehyde: The reported procedure[S3] was used to afford the title compound as a white solid (yield: 58%). ^{1}H NMR ($CDCl_3$) δ 9.97 (s, 1H), 8.05 – 8.00 (m, 1H), 7.64 (td, *J* = 7.5, 1.4 Hz, 1H), 7.51 (t, *J* = 7.6 Hz, 1H), 7.42 (d, *J* = 7.7 Hz, 1H), 7.35 (m, 2H), 7.17 (t, *J* = 8.6 Hz, 2H).

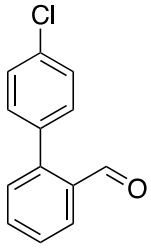

4'-chloro-[1,1'-biphenyl]-2-carbaldehyde: The reported procedure[S3] was used to afford the title compound as a white solid (yield: 70%). ^{1}H NMR ($CDCl_3$) δ 9.97 (s, 1H), 8.03 (dd, *J* = 7.8, 1.3 Hz, 1H), 7.65 (td, *J* = 7.5, 1.4 Hz, 1H), 7.52 (t, *J* = 7.6 Hz, 1H), 7.46 (d, *J* = 8.4 Hz, 2H), 7.41 (dd, *J* = 7.7, 0.9 Hz, 1H), 7.32 (d, *J* = 8.4 Hz, 2H).

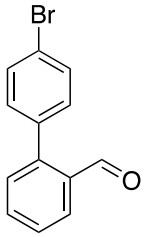

4'-bromo-[1,1'-biphenyl]-2-carbaldehyde: The reported procedure[S3] was used to afford the title compound as a yellow solid (yield: 66%). ^{1}H NMR ($CDCl_3$) δ 9.97 (s, 1H), 8.03 (dd, *J* = 7.8, 1.1 Hz, 1H), 7.68 – 7.59 (m, 3H), 7.52 (t, *J* = 7.6 Hz, 1H), 7.41 (d, *J* = 7.7 Hz, 1H), 7.27 – 7.25 (m, 2H).

(2) Synthesis of water soluble compounds

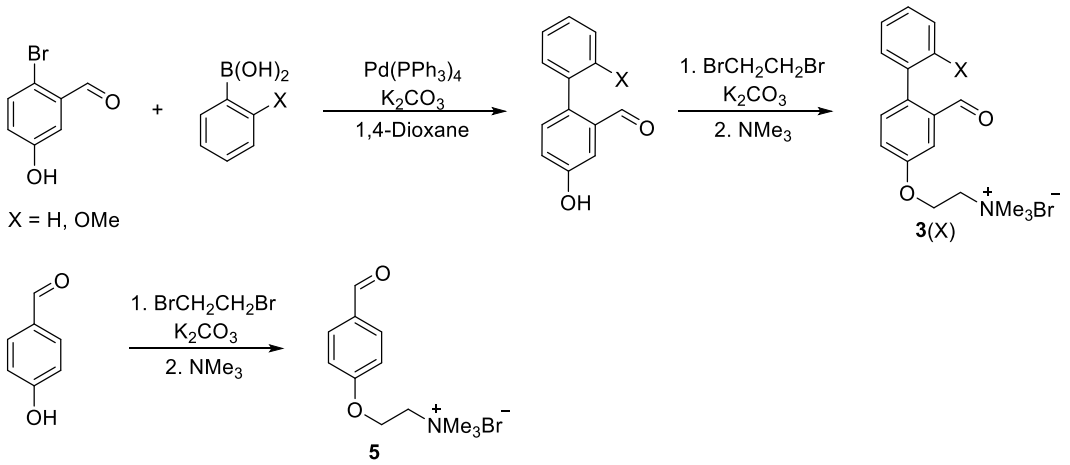

Scheme S2. General Synthetic routes of water soluble compounds **3**(X) and **5**.

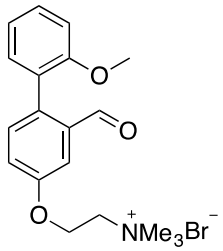

2-((2-formyl-2'-methoxy-[1,1'-biphenyl]-4-yl)oxy)-*N*,*N*,*N*-trimethylethan-1-aminium bromide: To a suspension of 4-hydroxy-2'-methoxy-[1,1'-biphenyl]-2-carbaldehyde (1.0 mmol, 228 mg) and potassium carbonate (3.0 mmol, 414 mg) in 10 ml anhydrous DMF, was added 1,2-dibromoethane (2.0 mmol, 376 mg) was added dropwise. The reaction was stirred at 90 ℃ until the starting material was completely consumed. After the reaction was cooled to room temperature, H_2O (50 mL) was added, and the mixture was extracted

with EA (25 ml × 3). The combined organic layer was washed with brine (50 ml × 3), dried over anhydrous Na_2SO_4, and concentrated under vacuum. Toluene (7 mL), a solution of trimethylamine (2 M in THF, 3 mL) was added to the resulting residue, and the mixture was transferred to a sealed tube. The reaction was stirred at 60 ℃ for 2 days, and H_2O (20 mL) was next added. The aqueous layer was washed with PE (20 ml × 3) and EA (20 ml × 3), concentrated under vacuum, and dried to afford the title compound as a white solid (389 mg, 96%). ^{1}H NMR (D_2O): δ 9.57 (s, 1H), 7.50-7.47 (m, 2H), 7.37-7.30 (m, 3H), 7.15 (t, *J* = 6.6 Hz, 2H), 4.58 (br, 2H), 3.85 (t, *J* = 4.5 Hz, 2H), 3.71 (s, 3H), 3.26 (s, 9H). ^{13}C NMR (D_2O): δ 194.9, 156.7, 155.8, 134.8, 134.2, 132.8, 131.1, 130.2, 125.6, 121.5, 121.3, 111.5, 111.3, 64.9, 62.1, 55.2, 54.0. ESI-HRMS: m/z calcd for $C_{19}H_{24}NO_3^+$ [M^+]: 314.1751; found: 314.1751.

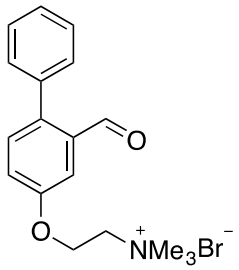

2-((2-formyl-[1,1'-biphenyl]-4-yl)oxy)-*N,N,N*-trimethylethan-1-aminium bromide: To a suspension of 4-hydroxy-[1,1'-biphenyl]-2-carbaldehyde (1.0 mmol, 198 mg) and potassium carbonate (3.0 mmol, 414 mg) in 10 ml anhydrous DMF, was added 1,2-dibromoethane (2.0 mmol, 376 mg) was added dropwise. The reaction was stirred at 90 ℃ until the starting material was completely consumed. After the reaction was cooled to room temperature, H_2O (50 mL) was added, and the mixture was extracted with EA (25 ml × 3). The combined organic layer was washed with brine (50 ml × 3), dried over anhydrous Na_2SO_4, and concentrated under vacuum. Toluene (7 mL), a solution of trimethylamine (2 M in THF, 3 mL) was added to the resulting residue, and the mixture was transferred to a sealed tube. The reaction was stirred at 60 ℃ for 2 days, and H_2O (20 mL) was next added. The aqueous layer was washed with PE (20 ml × 3) and EA (20 ml × 3), concentrated under vacuum, and dried to afford the title compound as a yellowish solid (360 mg, 95%). ^{1}H NMR (D_2O): δ 9.73 (s, 1H), 7.50-7.43 (m, 5H), 7.36-7.31 (m, 3H), 4.53 (br, 2H), 3.83 (br,

2H), 3.24 (s, 9H). ^{13}C NMR (D_2O): δ 193.9, 156.5, 139.4, 136.7, 133.5, 132.3, 130.0, 128.4, 127.9, 121.4, 111.7, 64.9, 62.1, 54.0. ESI-HRMS: m/z calcd for $C_{18}H_{22}NO_2^+$ [M^+]: 284.1645; found: 284.1645.

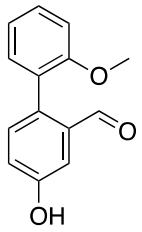

4-hydroxy-2'-methoxy-[1,1'-biphenyl]-2-carbaldehyde: The reported procedure[S7] was used to afford the title compound as a white solid (yield: 90%). ^{1}H NMR (DMSO-d_6): δ 9.98 (br, 1H), 9.55 (s, 1H), 7.40 (t, *J* = 8.1 Hz, 1H), 7.25 (d, *J* = 7.2 Hz, 1H), 7.21-7.18 (m, 2H), 7.12-7.05 (m, 3H), 3.67 (s, 3H).

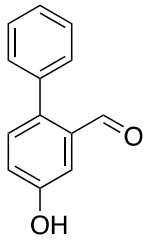

4-hydroxy-[1,1'-biphenyl]-2-carbaldehyde: The reported procedure[S8] was used to afford the title compound as a yellowish solid (yield: 92%). ^{1}H NMR (DMSO-d_6): δ 10.05 (br, 1H), 9.81 (s, 1H), 7.50 - 7.41 (m, 3H), 7.41 - 7.36 (m, 3H), 7.35 - 7.28 (m, 2H), 7.16 (dd, *J* = 8.2, 2.2 Hz, 1H).

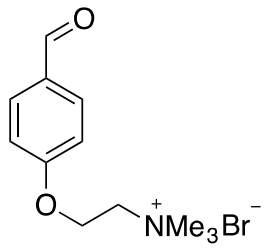

2-(4-formylphenoxy)-*N*,*N*,*N*-trimethylethan-1-aminium bromide: The reported procedure[S9] was used to afford the title compound as a white solid (yield: 98%). ^{1}H NMR (D_2O): δ 9.77 (s, 1H), 7.93 (d, *J* = 8.5 Hz, 2H), 7.16 (d, *J* = 8.4 Hz, 2H), 4.61 (br, 2H), 3.86 (t, *J* = 4.1 Hz, 2H), 3.24 (s, 9H).

(3) NMR spectrum of synthetic compounds

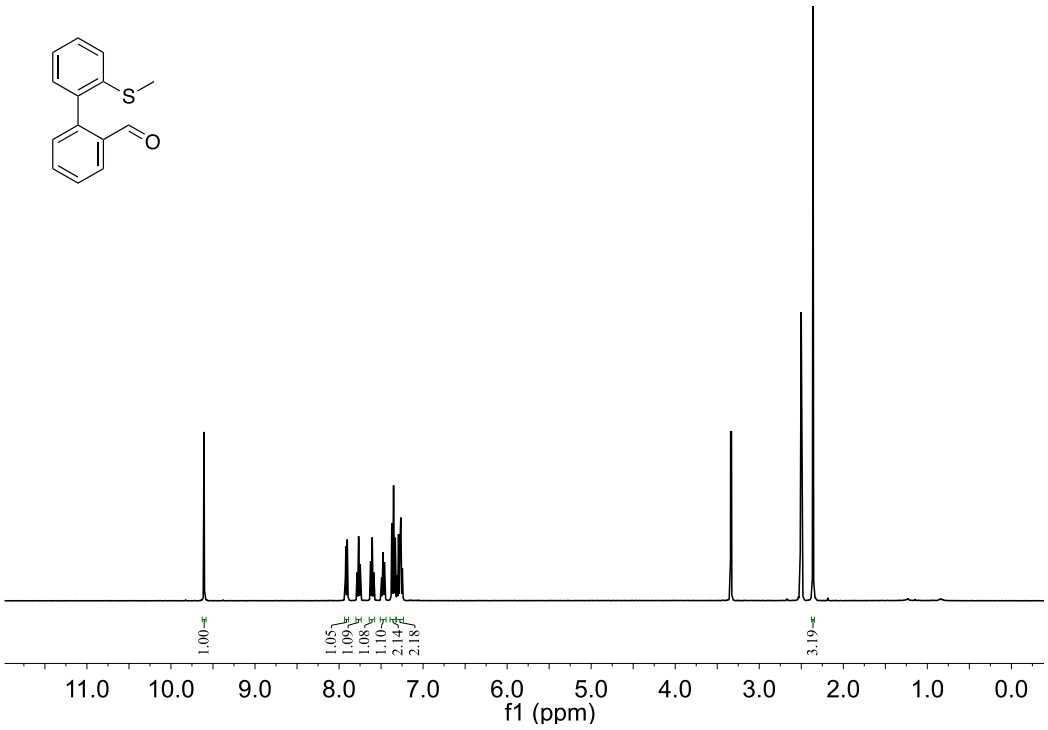

Figure S1. ^{1}H NMR spectrum of **1**(SMe) in DMSO-d_6.

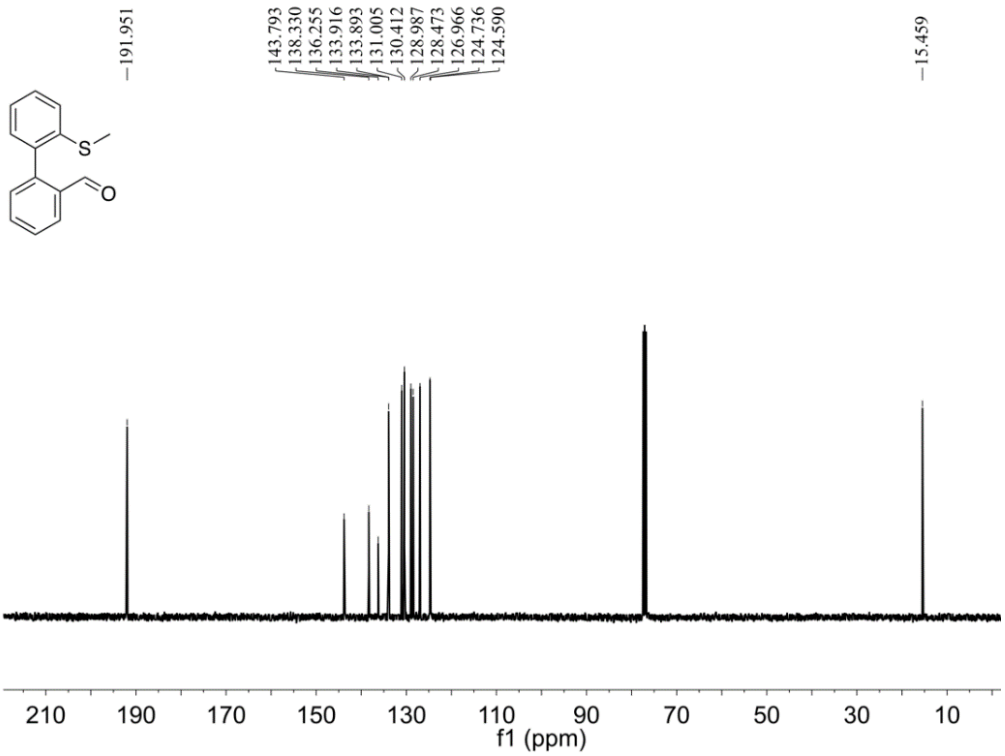

Figure S2. ^{13}C NMR spectrum of **1**(SMe) in $CDCl_3$.

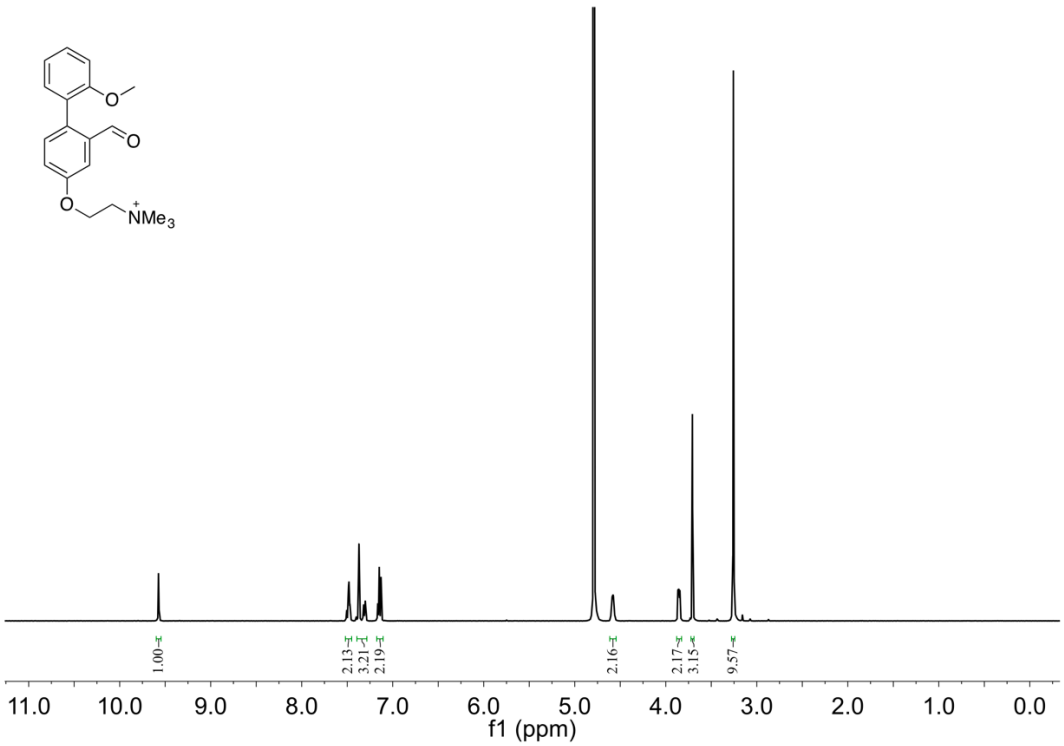

Figure S3. ^{1}H NMR spectrum of **3**(OMe) in D_2O.

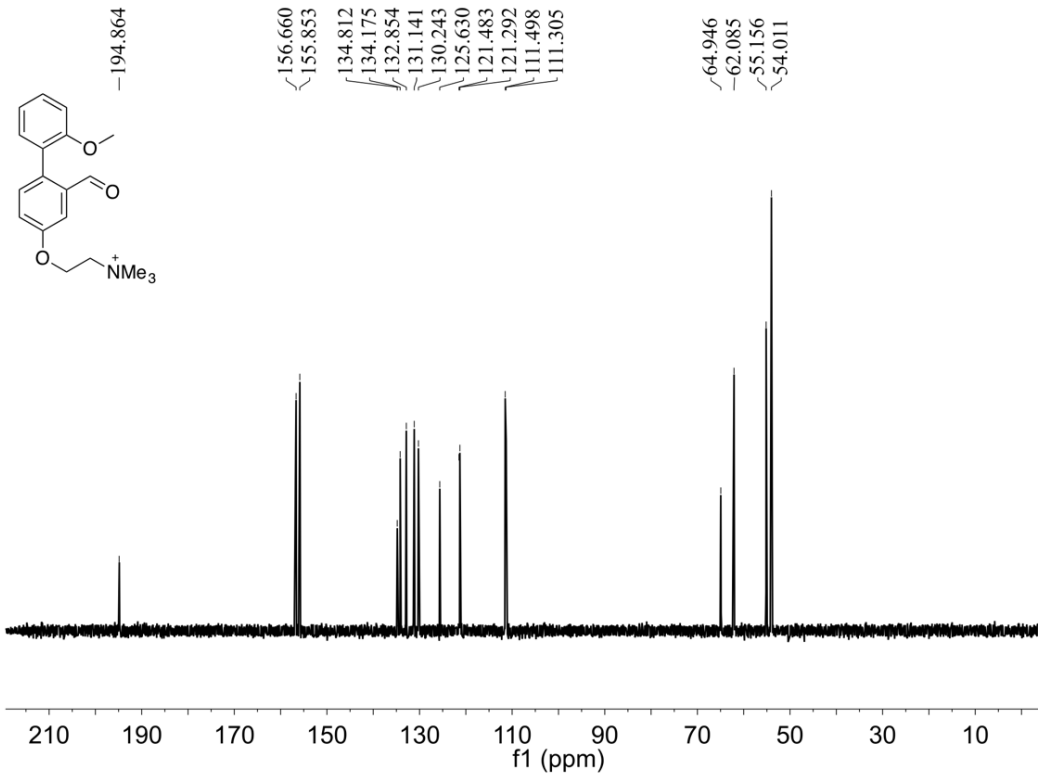

Figure S4. ^{13}C NMR spectrum of **3**(OMe) in D_2O.

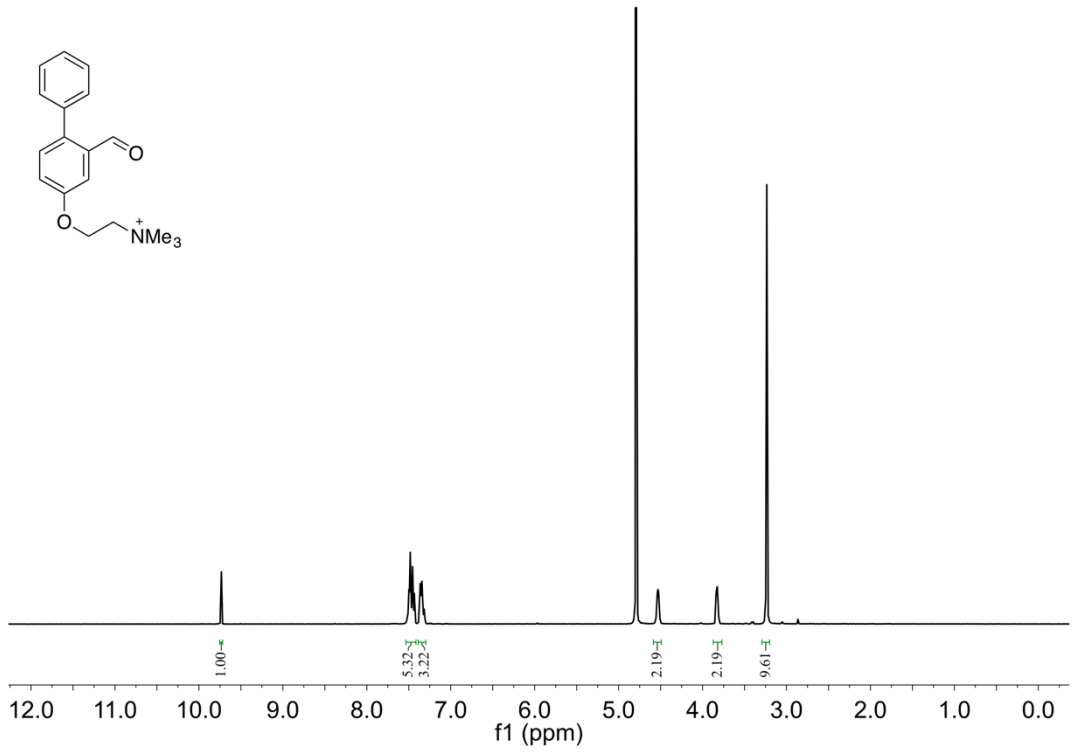

Figure S5. ^{1}H NMR spectrum of **3**(H) in D_2O.

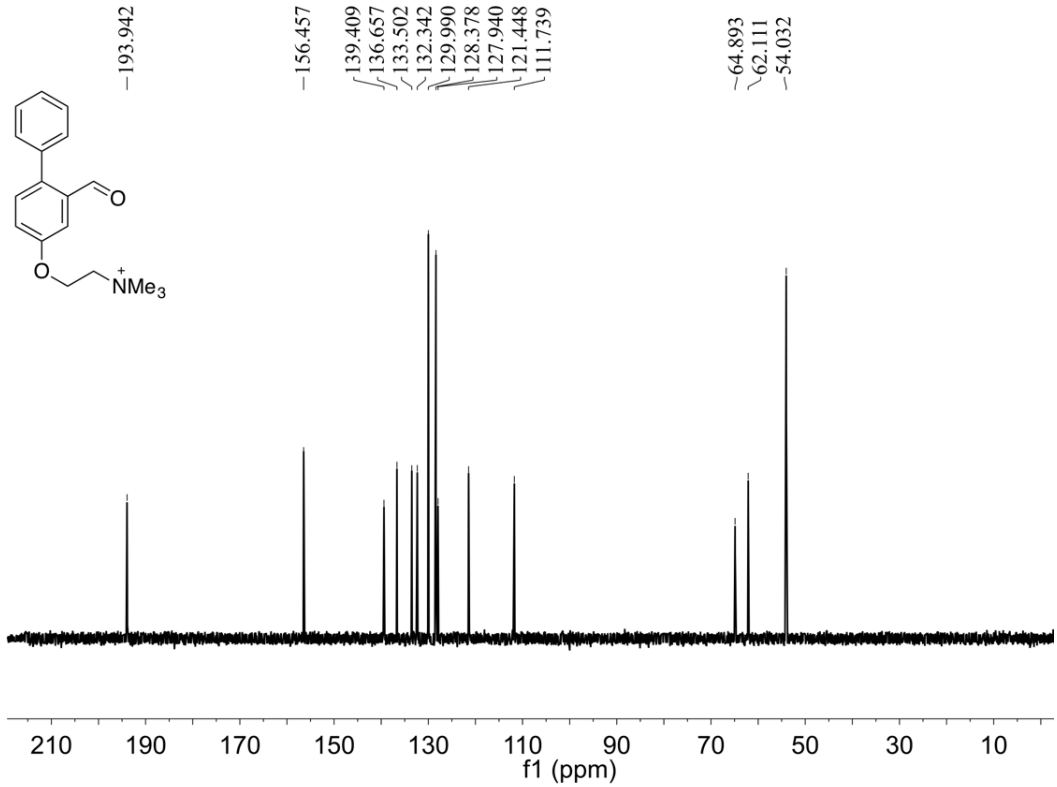

Figure S6. ^{13}C NMR spectrum of **3**(H) in D_2O.

(4) Crystal structures of 1(X)

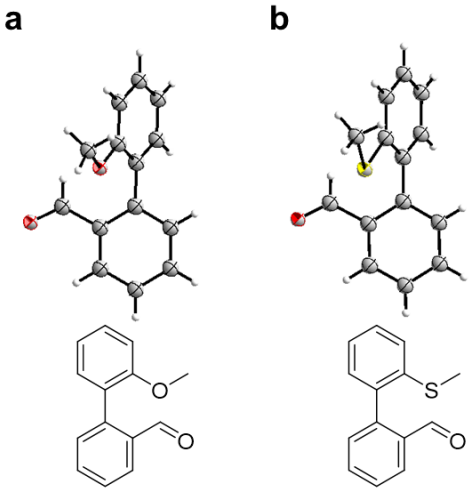

Figure S7. Crystal structure of **1**(OMe) (a) and **1**(SMe) (b).

Table S1. Summary of crystallographic data for **1**(OMe) and **1**(SMe).

	1(OMe)	**1**(SMe)
Formula	$C_{14}H_{12}O_2$	$C_{14}H_{12}OS$
Formula weight	212.24	228.30
T / K	100	293
Crystallization solvent	Cyclohexane	Cyclohexane
Color	Colorless	Colorless
Crystal system	monoclinic	monoclinic
Space group	P 1 21 1	P 1 21/c 1
a / Å	7.6256(4)	10.530(4)
b / Å	7.4766(3)	7.555(3)
c / Å	9.9777(5)	15.466(6)
α / °	90.00	90.00
β / °	108.663(2)	105.601(5)
γ / °	90.00	90.00
V / Å^3	538.95(4)	1185.1(8)
Z	2	4
D_x / g cm^{-3}	1.308	1.280
μ / mm^{-1}	0.087	0.247
F(000)	224.0	480.0
θ range / °	2.950 to 25.414	2.7167 to 27.5126
GOF on F^2	1.294	1.049
R_1 [$I > 2\sigma(I)$]	0.0269	0.0359
wR_2 (all data)	0.0970	0.1029

3. Dynamic Covalent Reactions

Dynamic Covalent Reactions (DCRs) were performed in *situ* in CD_3CN without isolation and purification. To a stirred solution of **1** (20 mM, 1.0 equiv.) in CD_3CN (0.60 mL), were added 1-butylamine (22 mM, 1.2 equiv.) and activated 3 Å molecular sieves (MS, 4-8 mesh). The mixture was stirred at room temperature overnight and characterized by ^1H NMR and ESI-MS. For imine exchange, another aldehyde (20 mM, 1.0 equiv.) was then added, and the exchange was monitored by ^1H NMR. For competition experiments, both aldehydes (20 mM each, 1.0 equiv.) were mixed with 1-butylamine (24 mM, 1.2 equiv.) in CD_3CN (0.60 mL), and the mixture was stirred overnight and characterized by ^1H NMR. To ensure reproducibility all competition experiments were performed twice.

(1) Imine formation

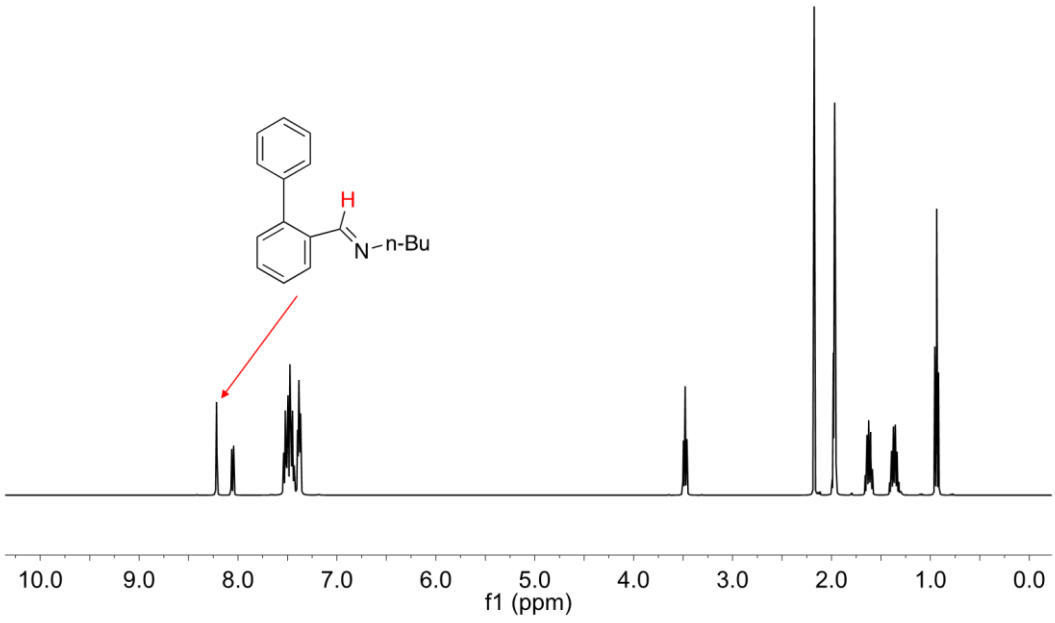

Figure S8. ^1H NMR spectrum of the reaction of **1**(H) and 1-butylamine in CD_3CN.

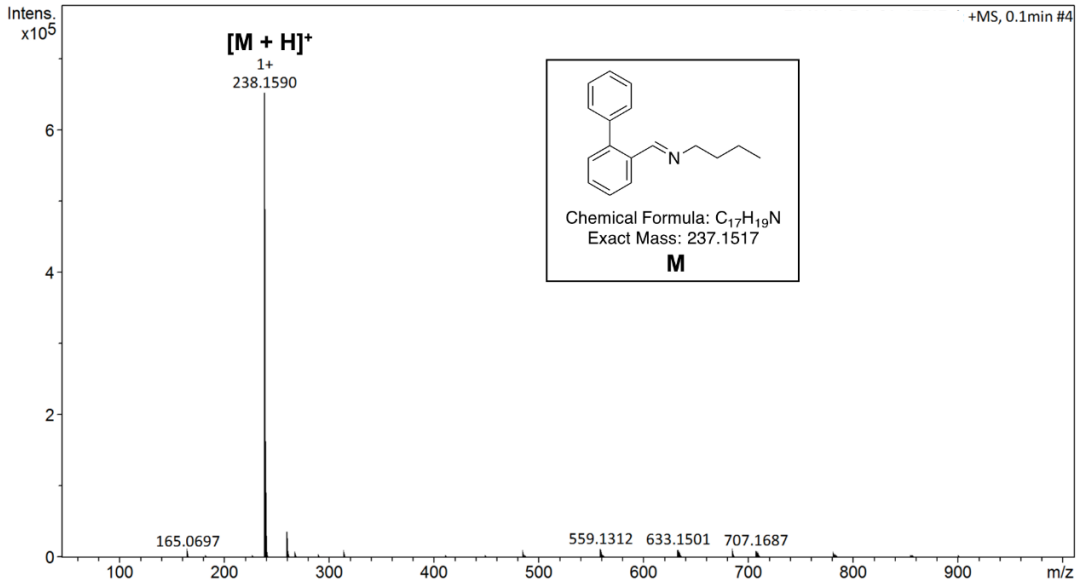

Figure S9. ESI-MS spectrum of the reaction of **1**(H) and 1-butylamine in CD_3CN.

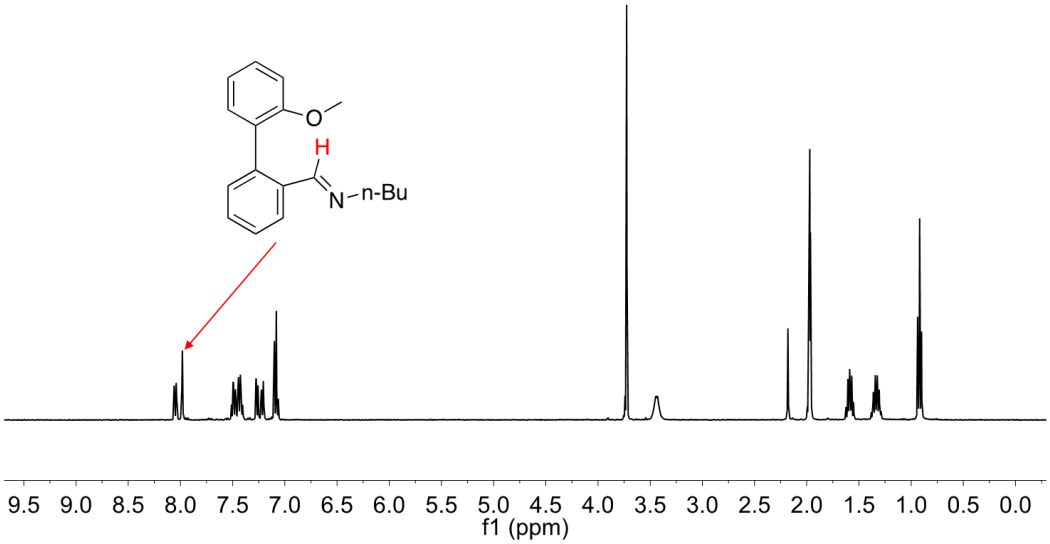

Figure S10. ^1H NMR spectrum of the reaction of **1**(OMe) and 1-butylamine in CD_3CN.

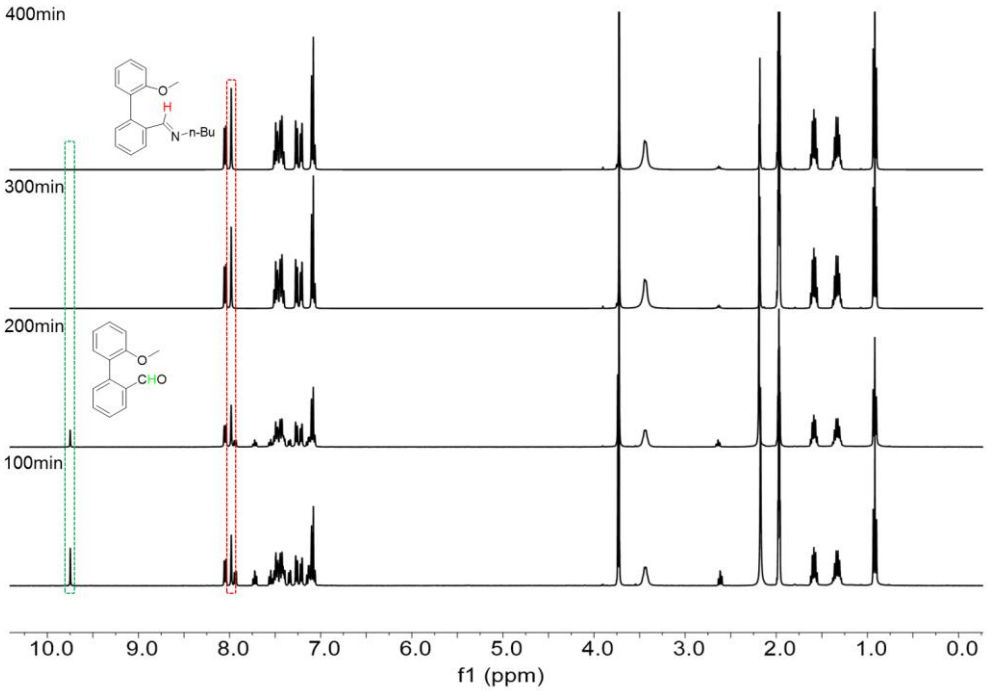

Figure S11. ^{1}H NMR spectra of the reaction between **1**(OMe) (20 mM, 1.0 equiv.) and 1-butylamine (24 mM, 1.2 equiv.) in CD_3CN at varied time. The reaction was complete in 300 min.

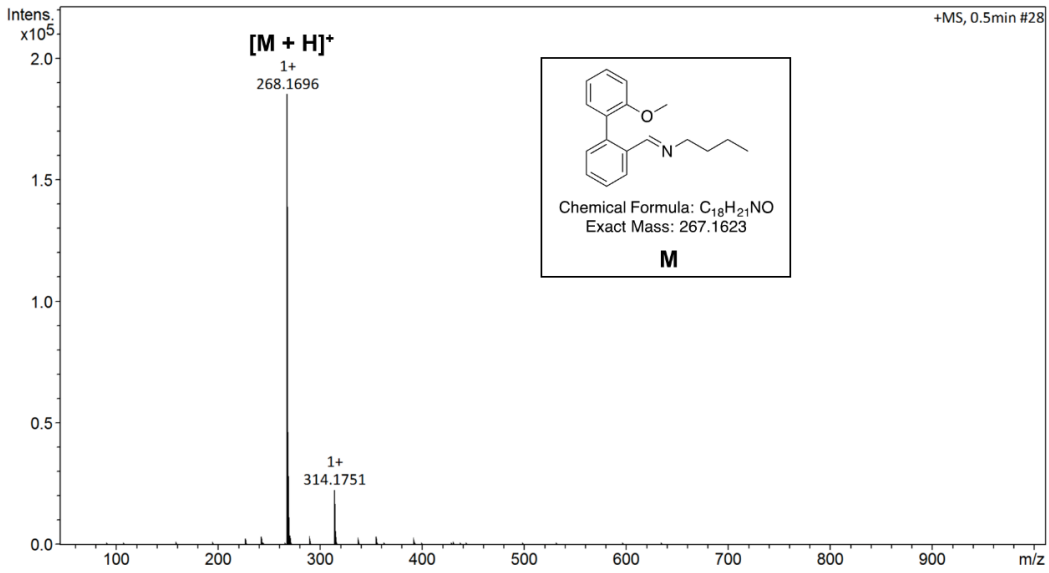

Figure S12. ESI-MS spectrum of the reaction of **1**(OMe) and 1-butylamine in CD_3CN.

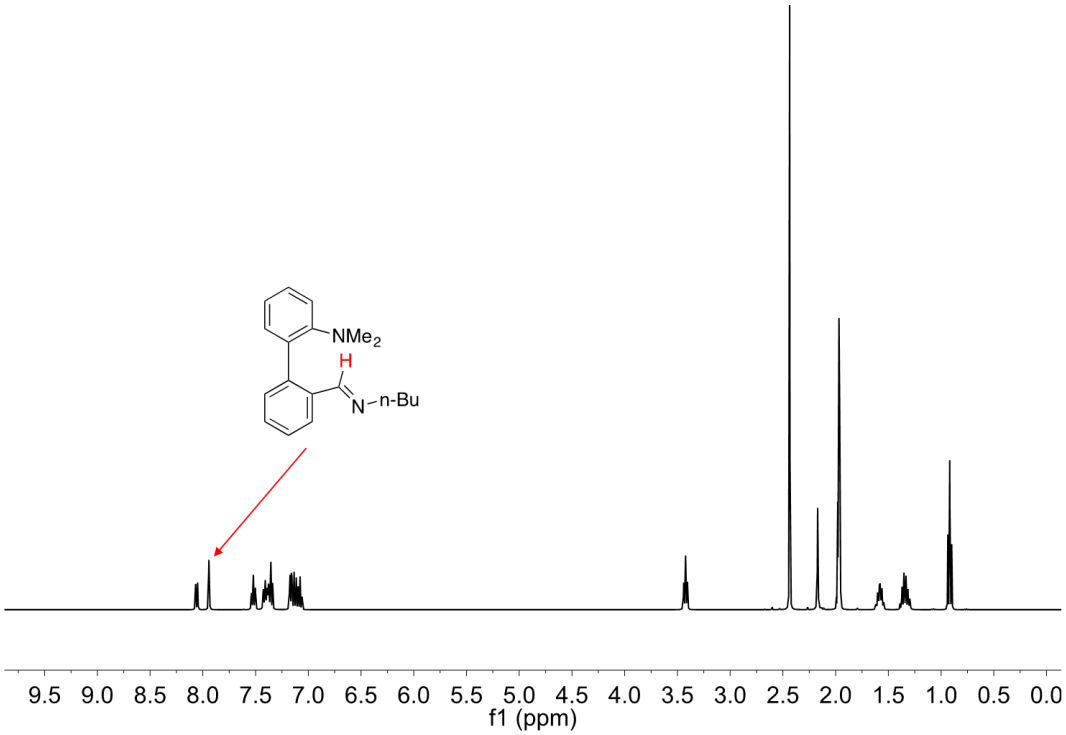

Figure S13. ^{1}H NMR spectrum of the reaction of **1**(NMe_2) and 1-butylamine in CD_3CN.

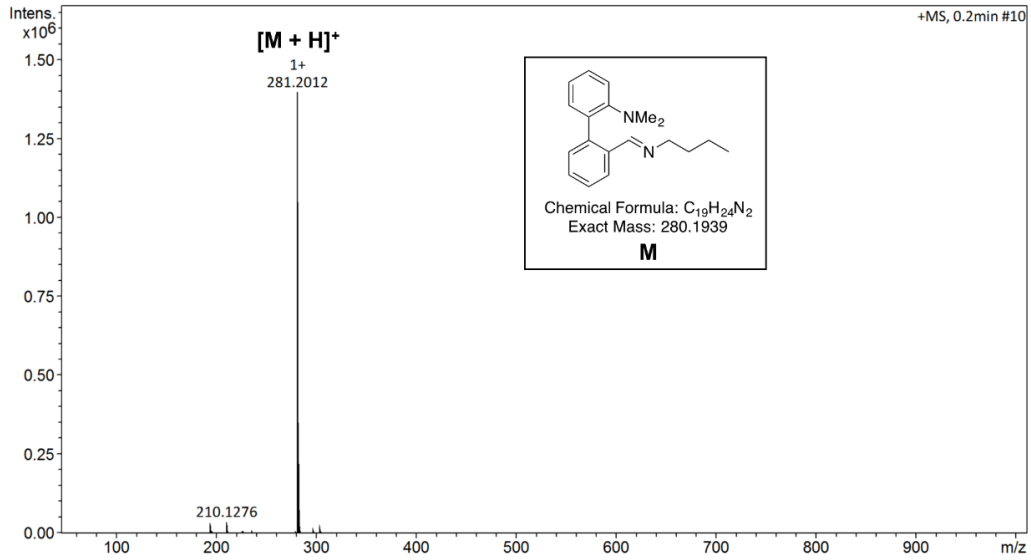

Figure S14. ESI-MS spectrum of the reaction of **1**(NMe_2) and 1-butylamine in CD_3CN.

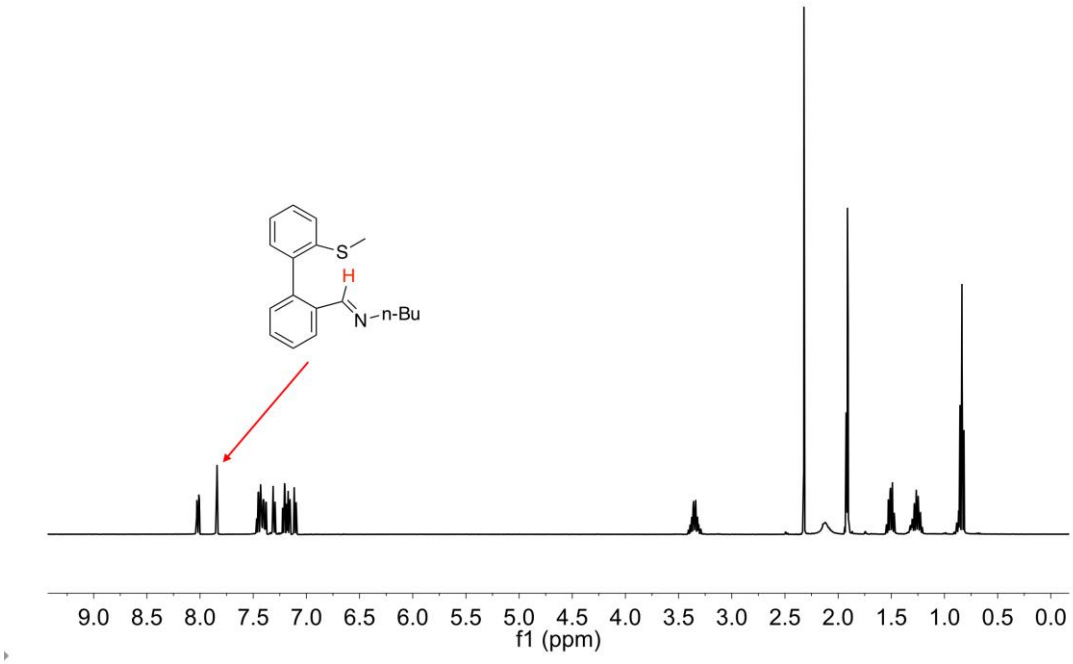

Figure S15. ^{1}H NMR spectrum of the reaction of **1**(SMe) and 1-butylamine in CD_3CN.

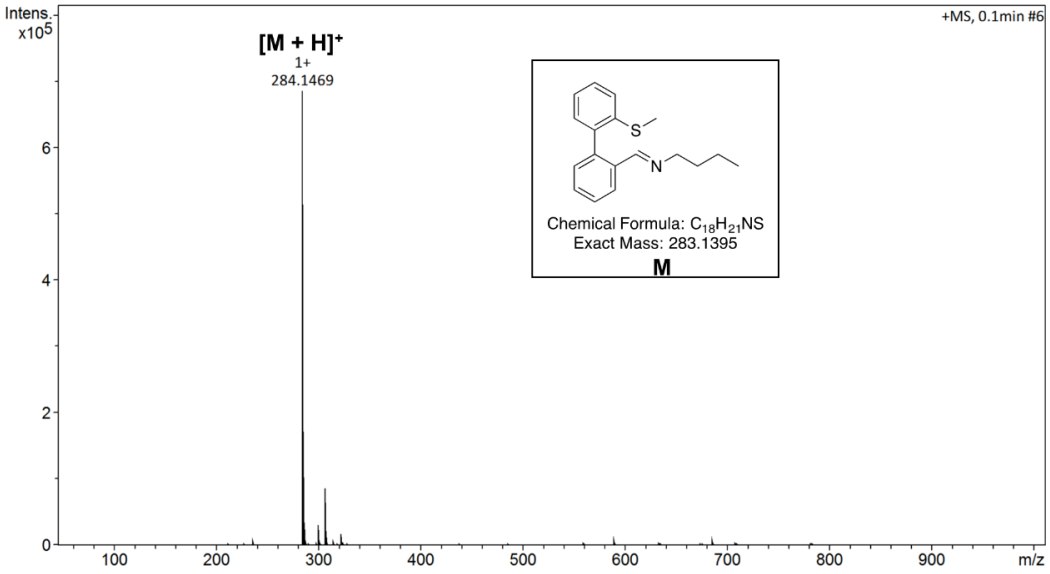

Figure S16. ESI-MS spectrum of the reaction of **1**(SMe) and 1-butylamine in CD_3CN.

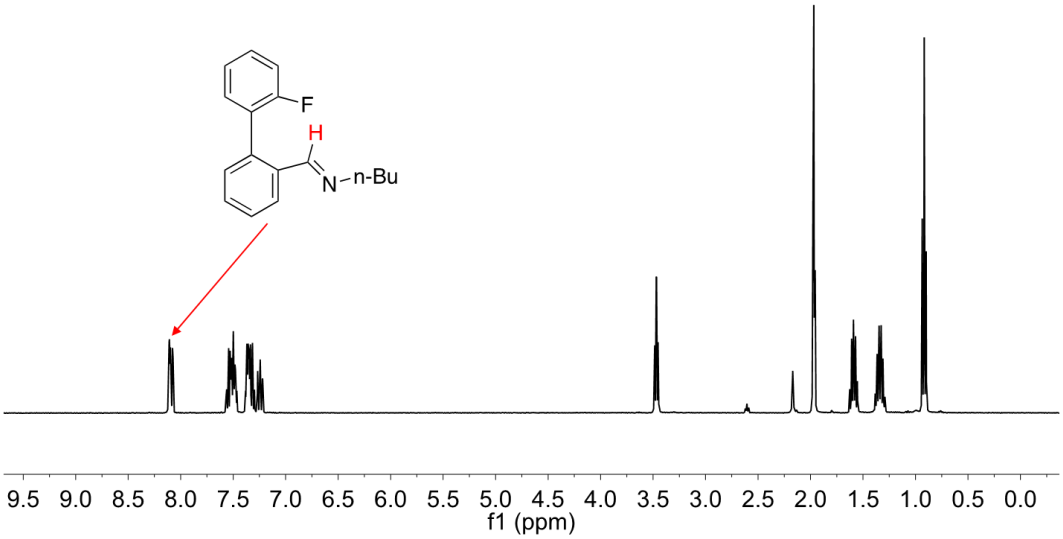

Figure S17. ^{1}H NMR spectrum of the reaction of **1**(F) and 1-butylamine in CD_3CN.

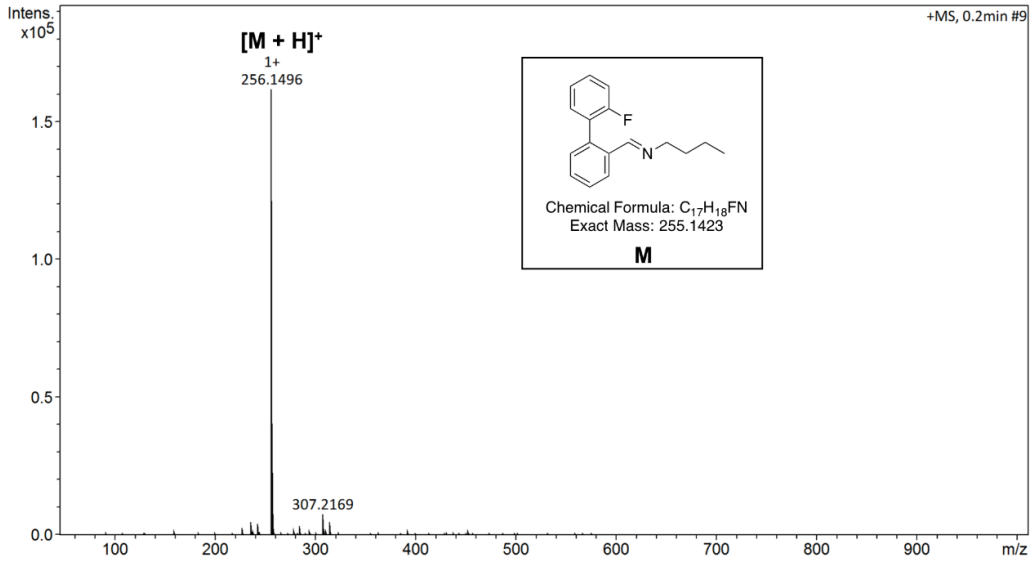

Figure S18. ESI-MS spectrum of the reaction of **1**(F) and 1-butylamine in CD_3CN.

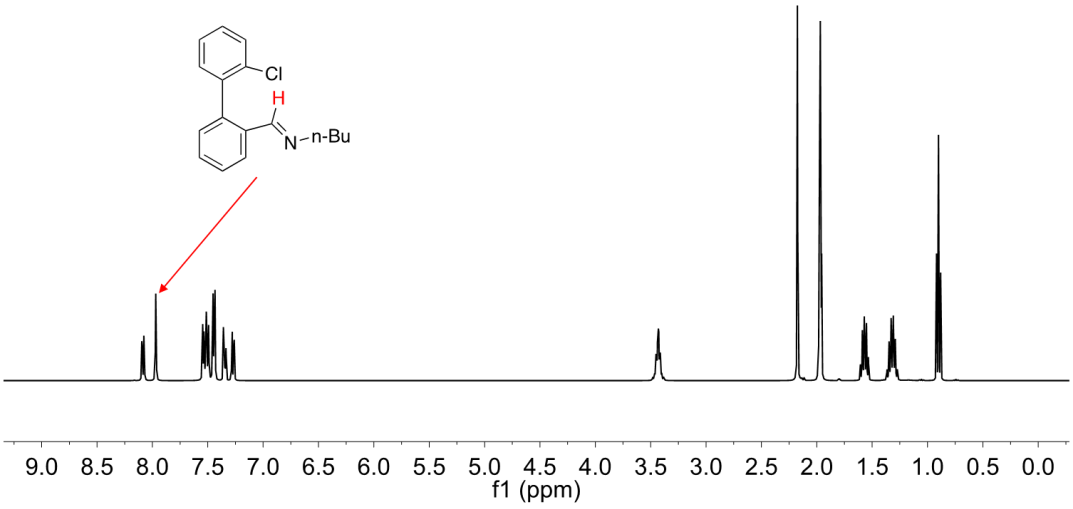

Figure S19. ^{1}H NMR spectrum of the reaction of **1**(Cl) and 1-butylamine in CD_3CN.

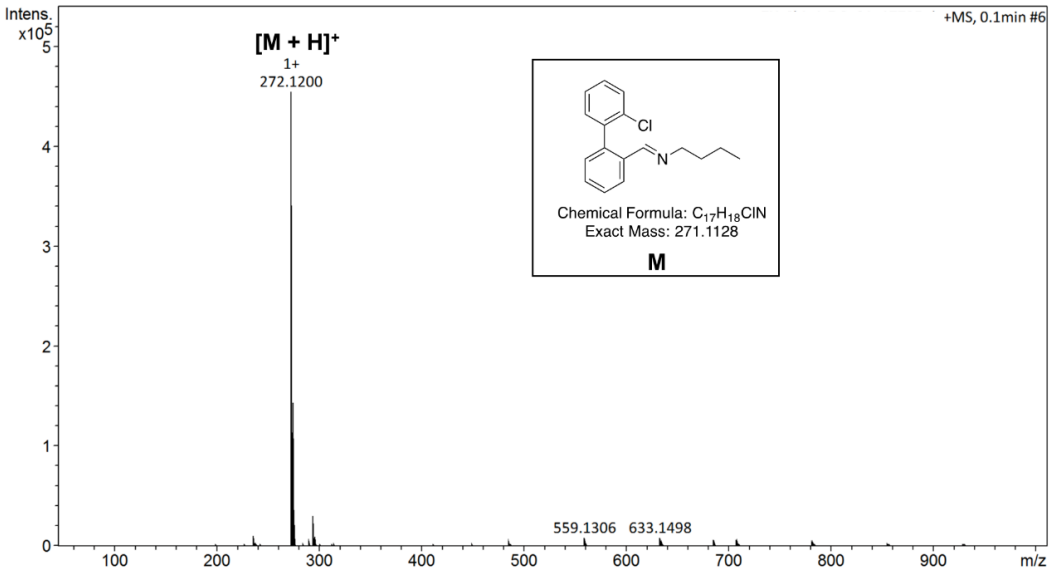

Figure S20. ESI-MS spectrum of the reaction of **1**(Cl) and 1-butylamine in CD_3CN.

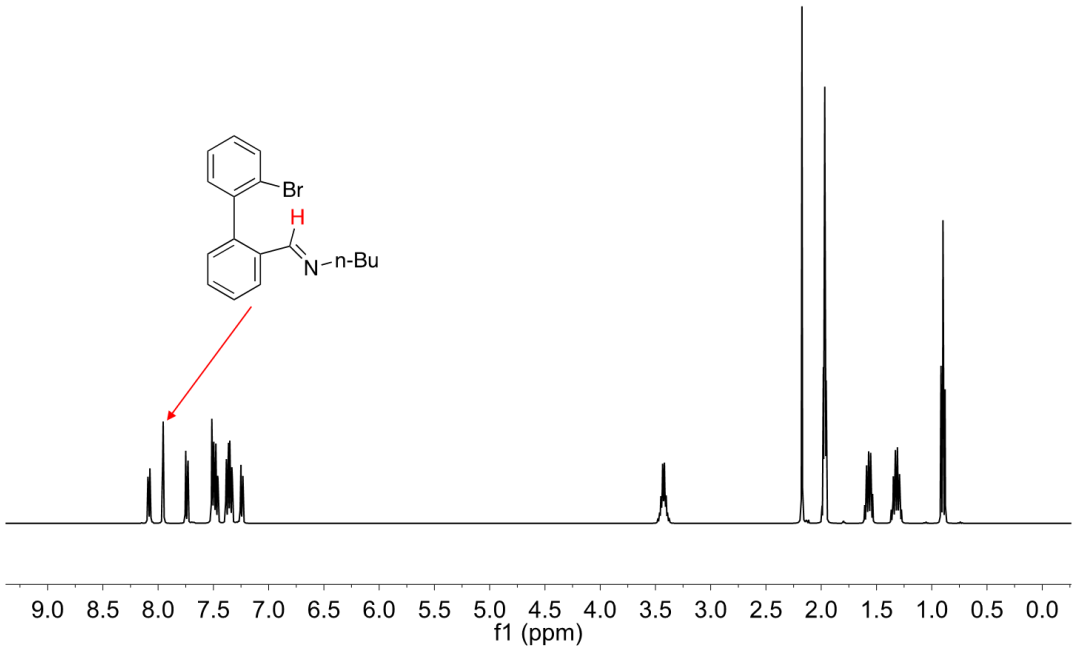

Figure S21. ^{1}H NMR spectrum of the reaction of **1**(Br) and 1-butylamine in CD_3CN.

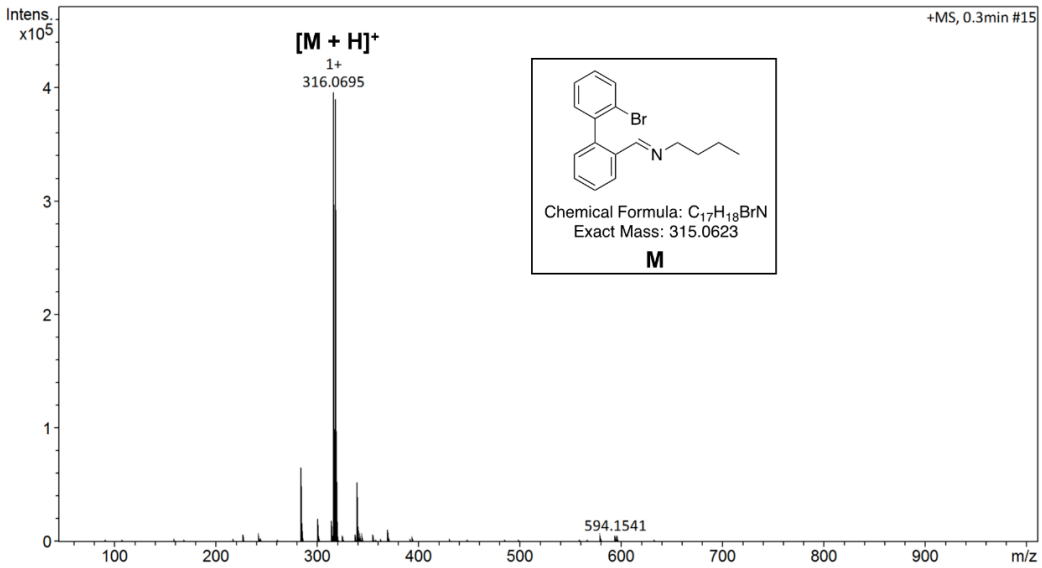

Figure S22. ESI-MS spectrum of the reaction of **1**(Br) and 1-butylamine in CD_3CN.

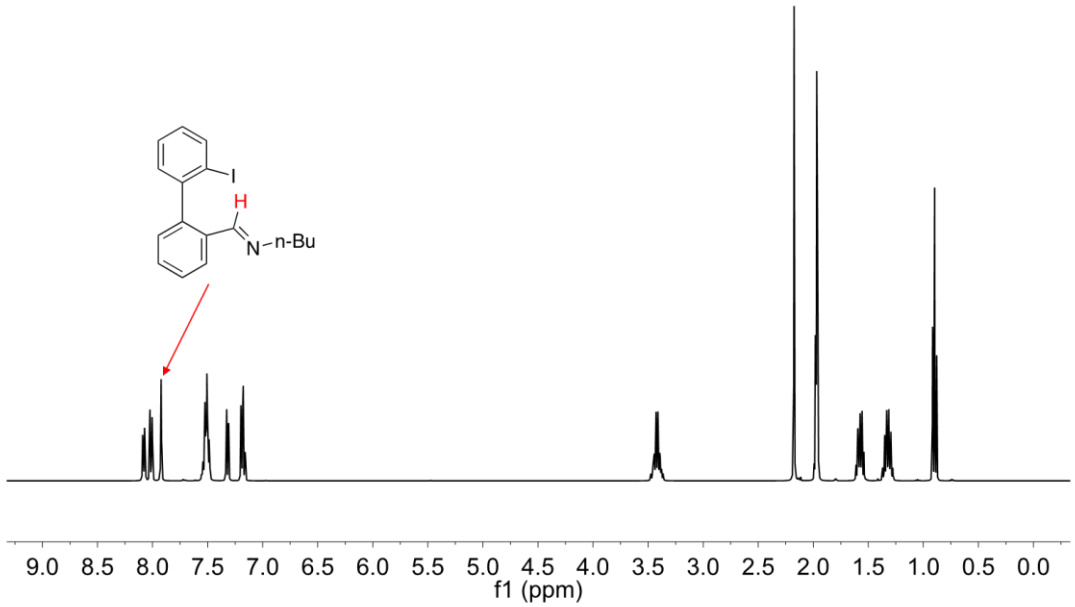

Figure S23. ^{1}H NMR spectrum of the reaction of **1**(I) and 1-butylamine in CD_3CN.

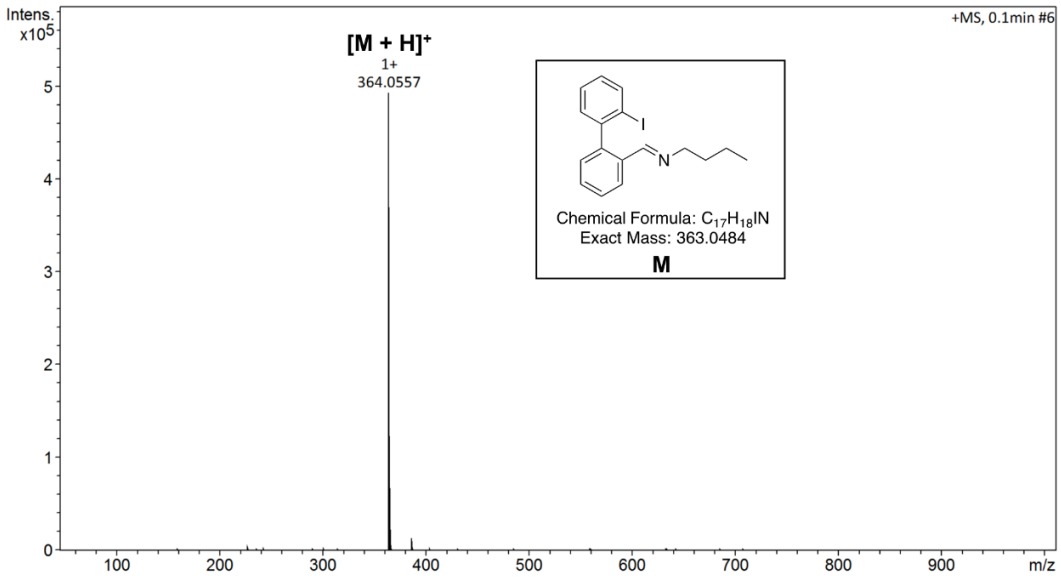

Figure S24. ESI-MS spectrum of the reaction of **1**(I) and 1-butylamine in CD_3CN.

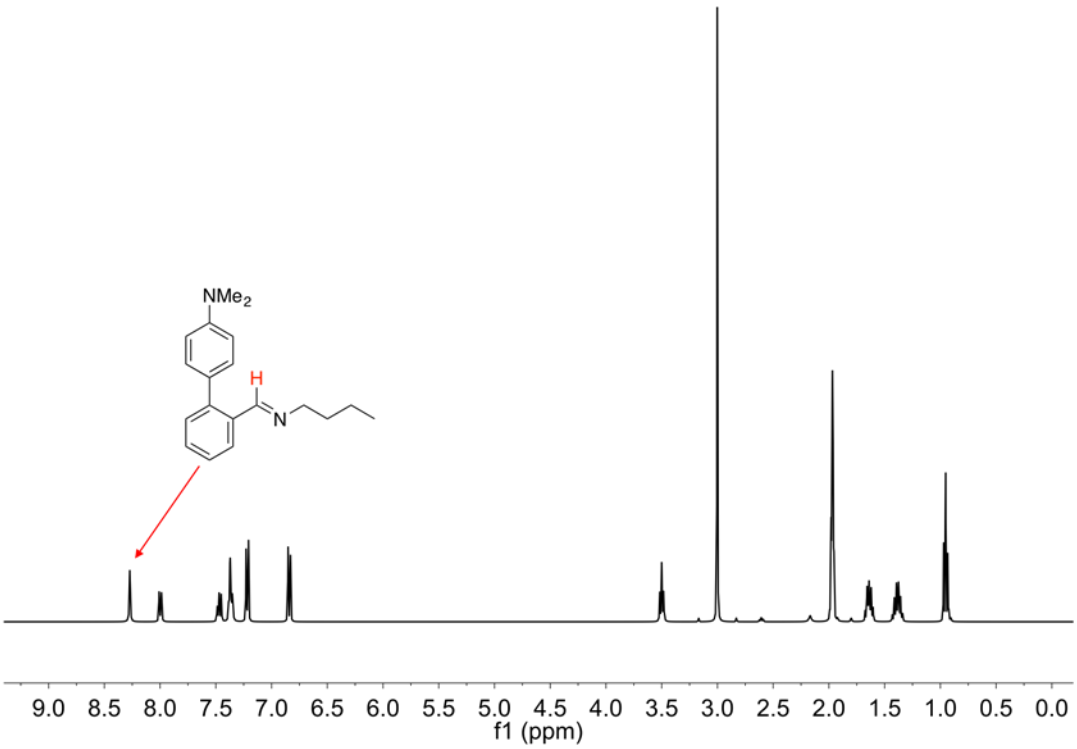

Figure S25. ^{1}H NMR spectrum of the reaction of **1**(*p*-NMe_2) and 1-butylamine in CD_3CN.

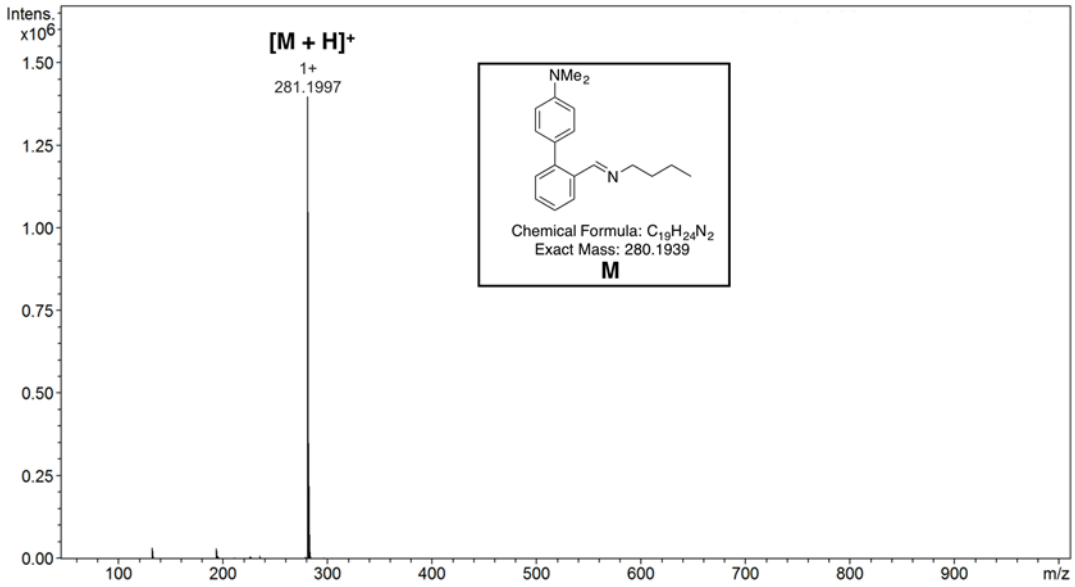

Figure S26. ESI-MS spectrum of the reaction of **1**(*p*-NMe_2) and 1-butylamine in CD_3CN.

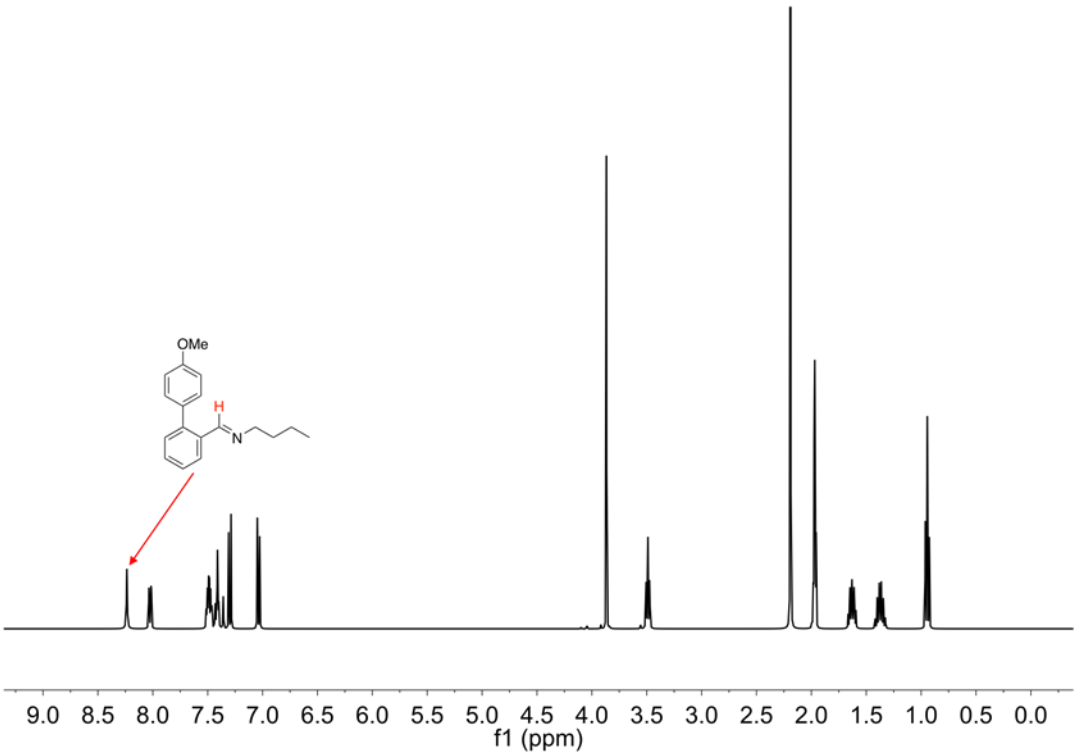

Figure S27. ^{1}H NMR spectrum of the reaction of **1**(*p*-OMe) and 1-butylamine in CD_3CN.

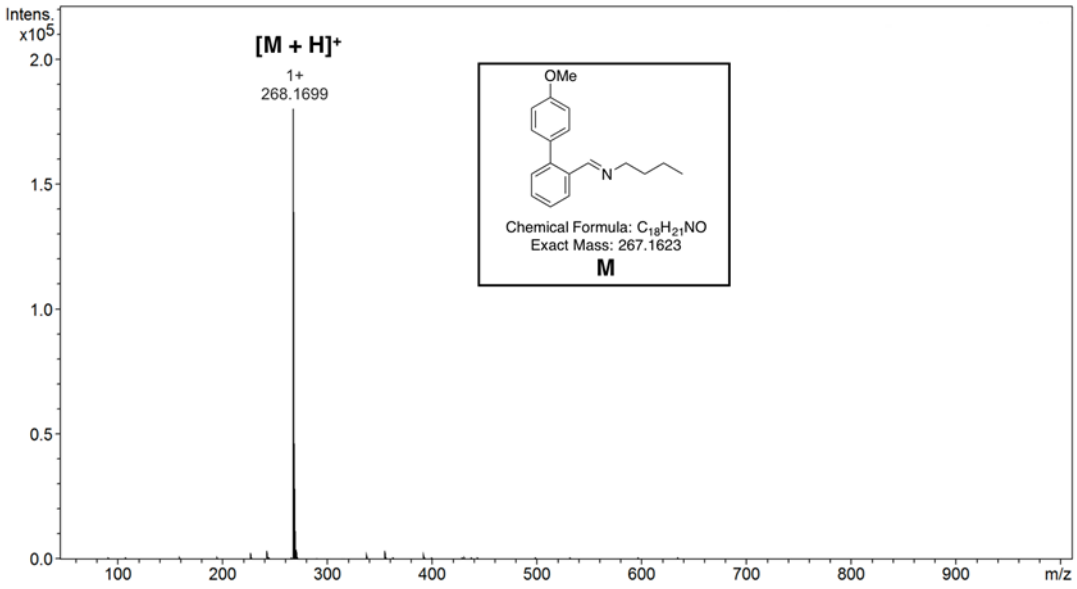

Figure S28. ESI-MS spectrum of the reaction of **1**(*p*-OMe) and 1-butylamine in CD_3CN.

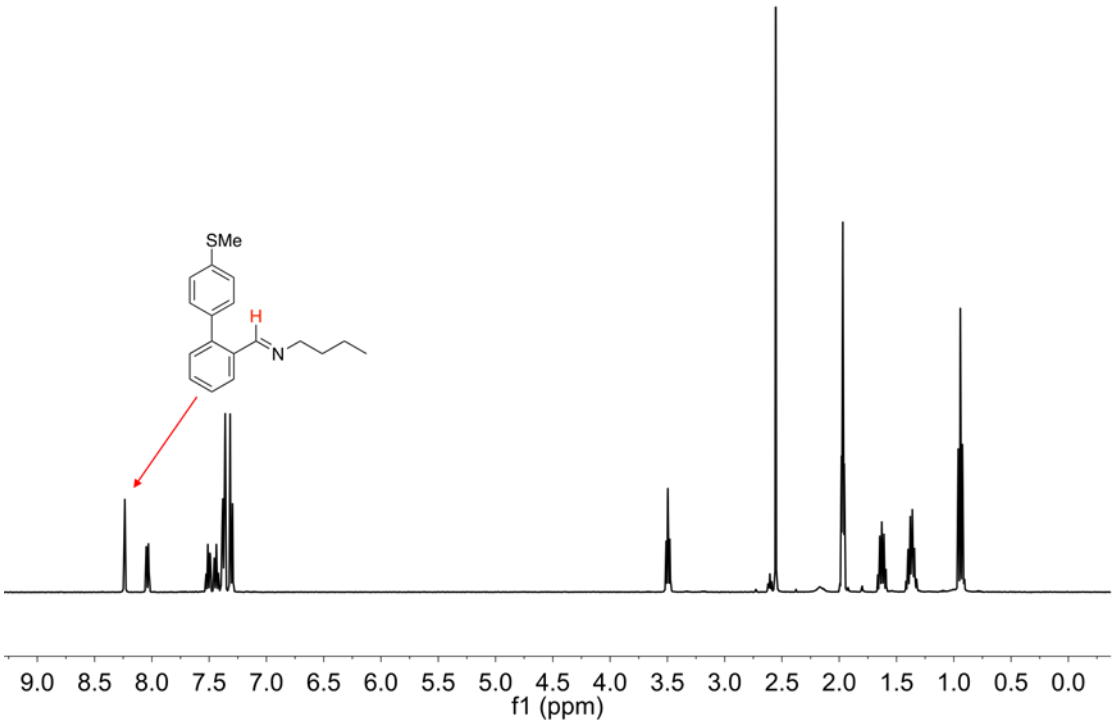

Figure S29. ^{1}H NMR spectrum of the reaction of **1**(*p*-SMe) and 1-butylamine in CD_3CN.

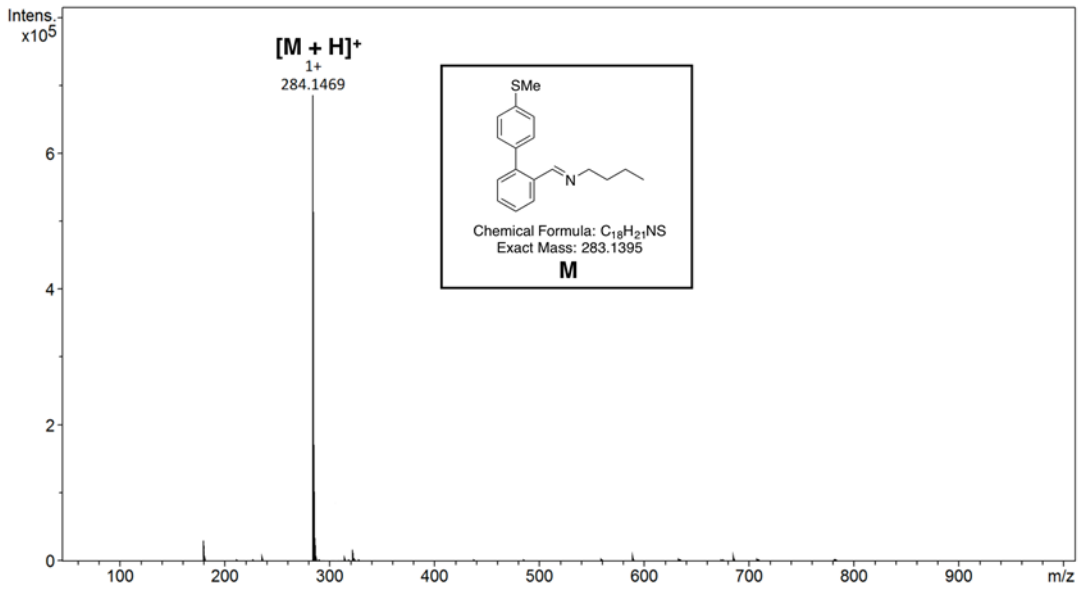

Figure S30. ESI-MS spectrum of the reaction of **1**(*p*-SMe) and 1-butylamine in CD_3CN.

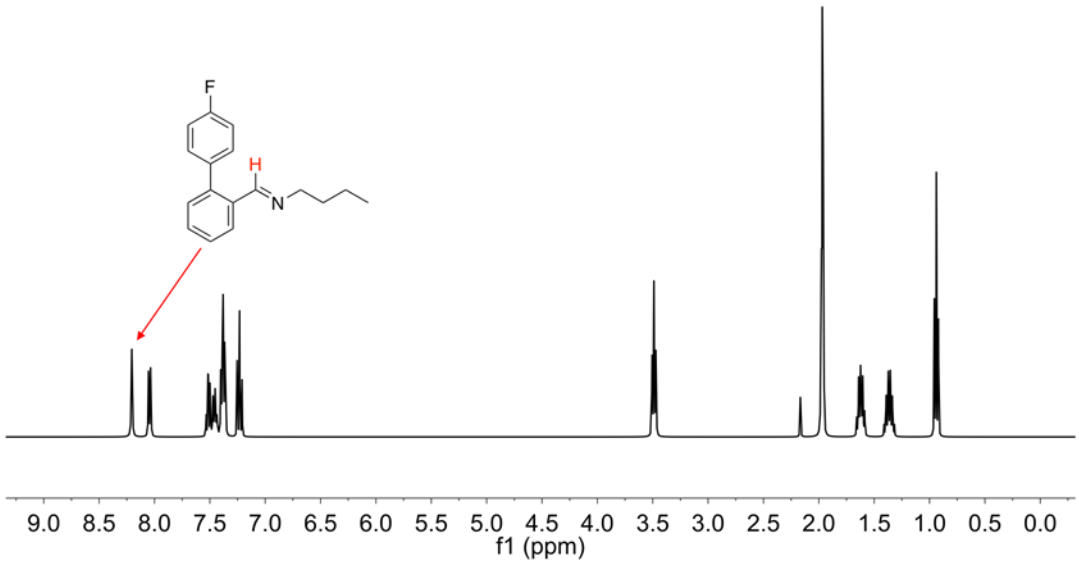

Figure S31. ^{1}H NMR spectrum of the reaction of **1**(*p*-F) and 1-butylamine in CD_3CN.

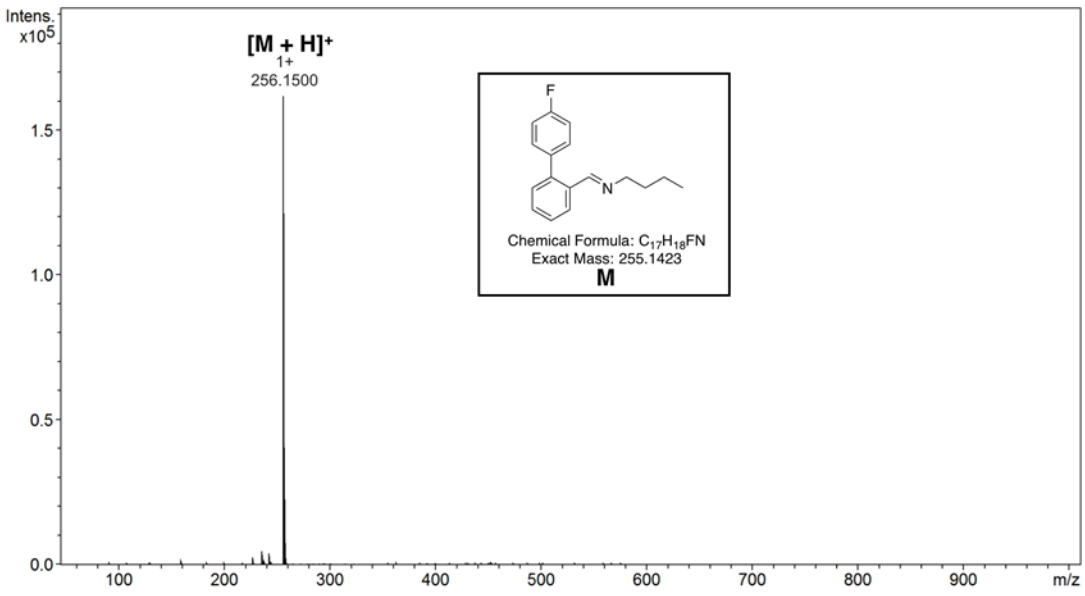

Figure S32. ESI-MS spectrum of the reaction of **1**(*p*-F) and 1-butylamine in CD_3CN.

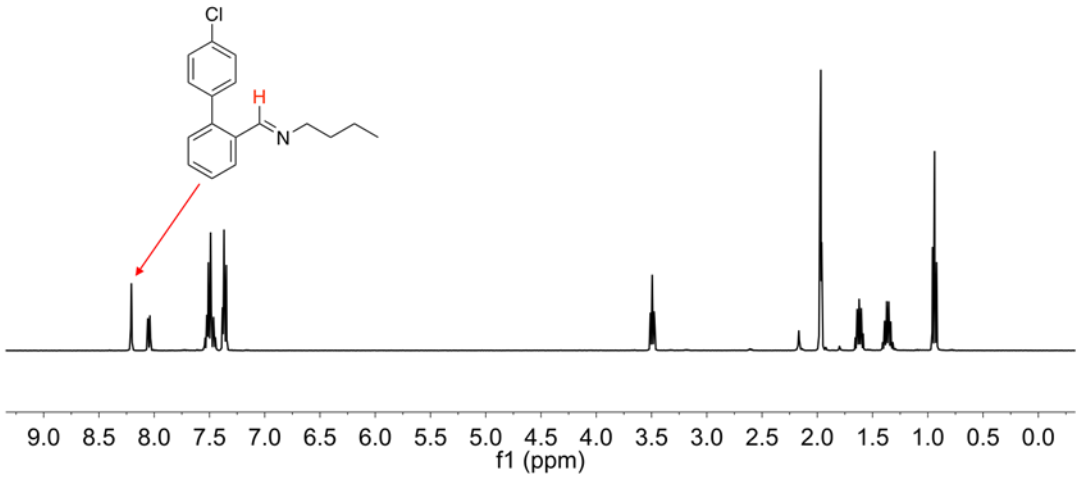

Figure S33. ^{1}H NMR spectrum of the reaction of **1**(*p*-Cl) and 1-butylamine in CD_3CN.

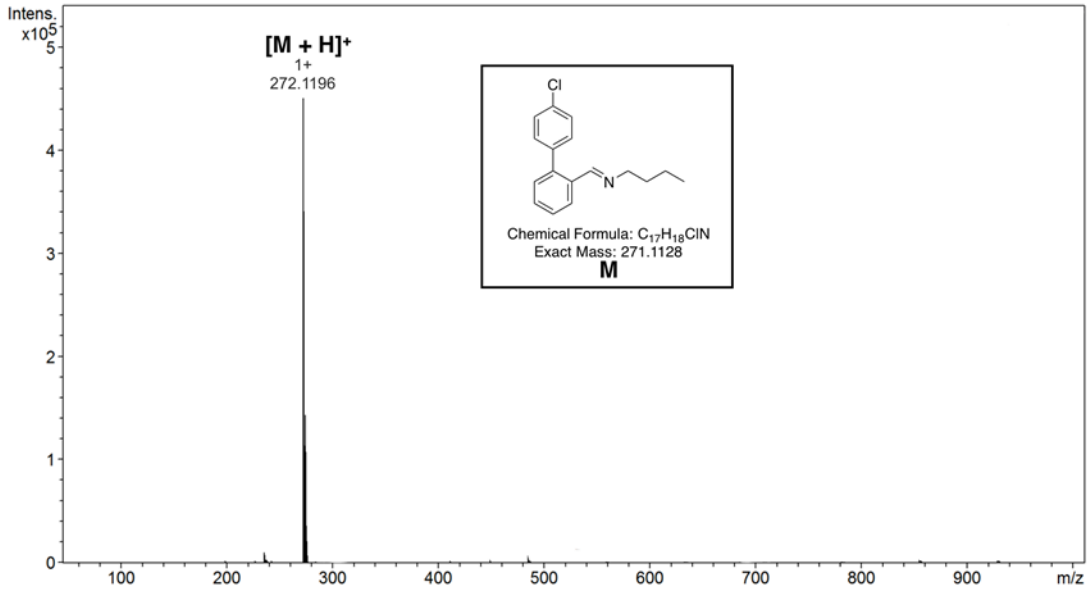

Figure S34. ESI-MS spectrum of the reaction of **1**(*p*-Cl) and 1-butylamine in CD_3CN.

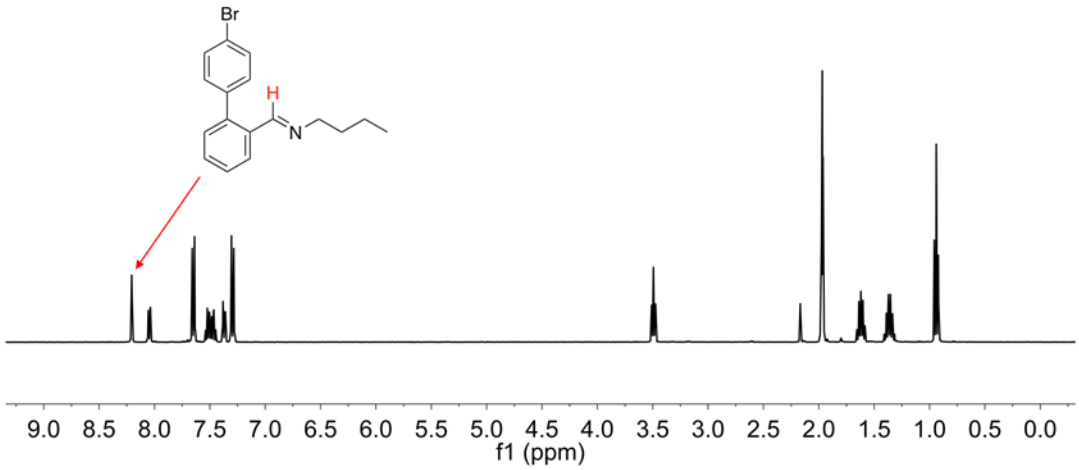

Figure S35. ^{1}H NMR spectrum of the reaction of **1**(*p*-Br) and 1-butylamine in CD_3CN.

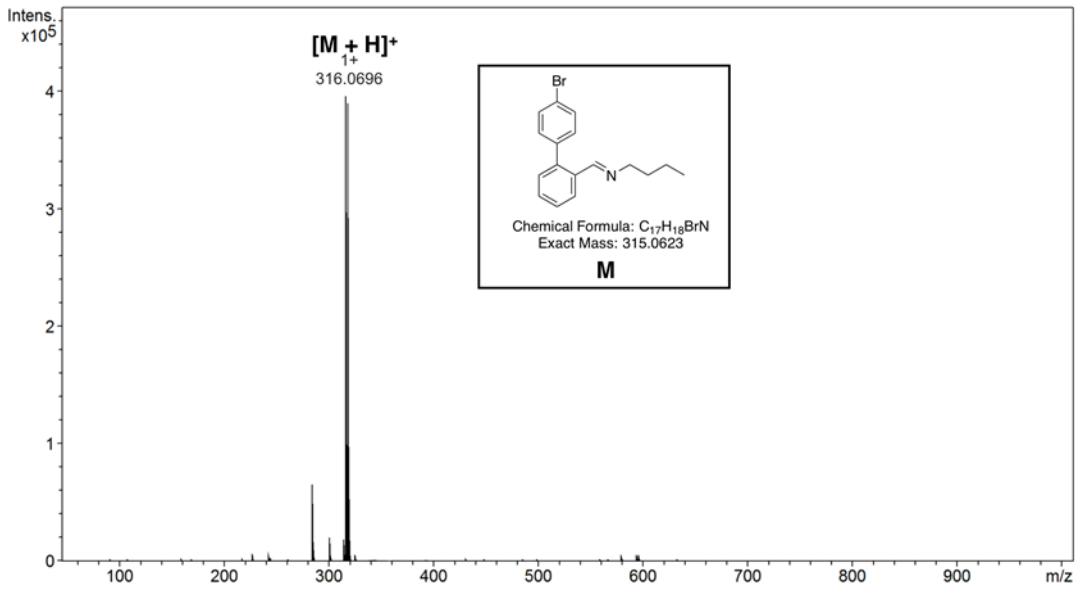

Figure S36. ESI-MS spectrum of the reaction of **1**(*p*-Br) and 1-butylamine in CD_3CN.

(2) Imine exchange

Table S2. The equilibrium constant and equilibrating time of the imine exchange with different sequence of reagents addition in different solvents.

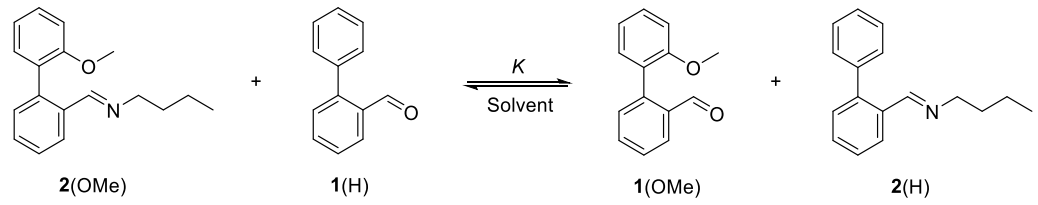

2(OMe) **1**(H) **1**(OMe) **2**(H)

Panel	Sequence of adding reagents	Solvent	*K*	Equilibrating time
a	Generate **2**(OMe) *in situ*, then add **1**(H)	CD_3CN	1.63	180 day
b		5% D_2O 95% CD_3CN	1.53	100 day
c		10% D_2O 90% CD_3CN	1.44	55 day
d	Generate **2**(H) *in situ*, then add **1**(OMe)	CD_3CN	1.64	150 day
e		5% D_2O 95% CD_3CN	1.54	58 day
f		10% D_2O 90% CD_3CN	1.44	30 day
g	**1**(H) and **1**(OMe) simultaneously reacted with 1-butylamine	CD_3CN	1.64	1 day
h		5% D_2O 95% CD_3CN	1.52	1 day
i		10% D_2O 90% CD_3CN	1.45	1 day

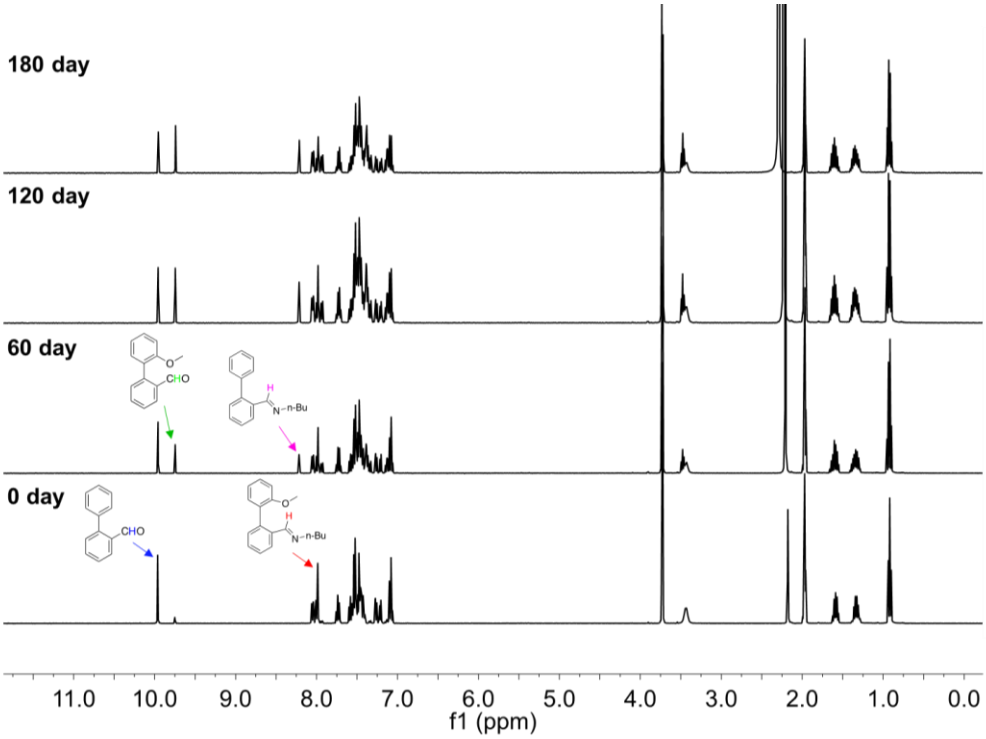

Figure S37. ^{1}H NMR spectra of the reaction of preformed **2**(OMe) and **1**(H) in CD_3CN at varied time (the corresponding spectra of panel a in Table S2).

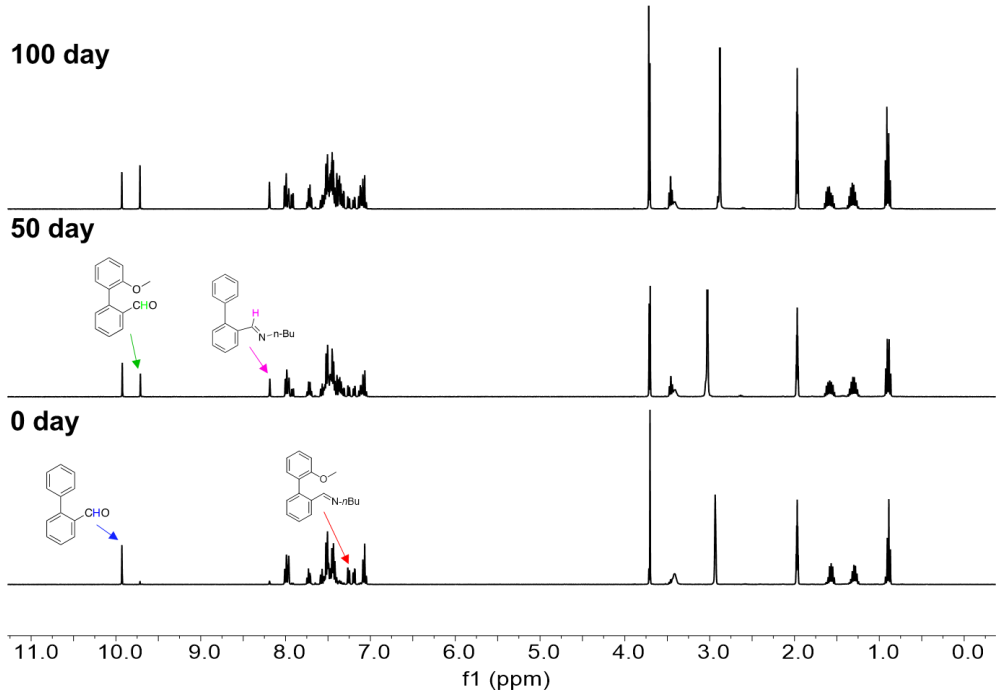

Figure S38. ^{1}H NMR spectra of the reaction of preformed **2**(OMe) and **1**(H) in mixed solvent (5% D_2O, 95% CD_3CN) at varied time (the corresponding spectra of panel b in Table S2).

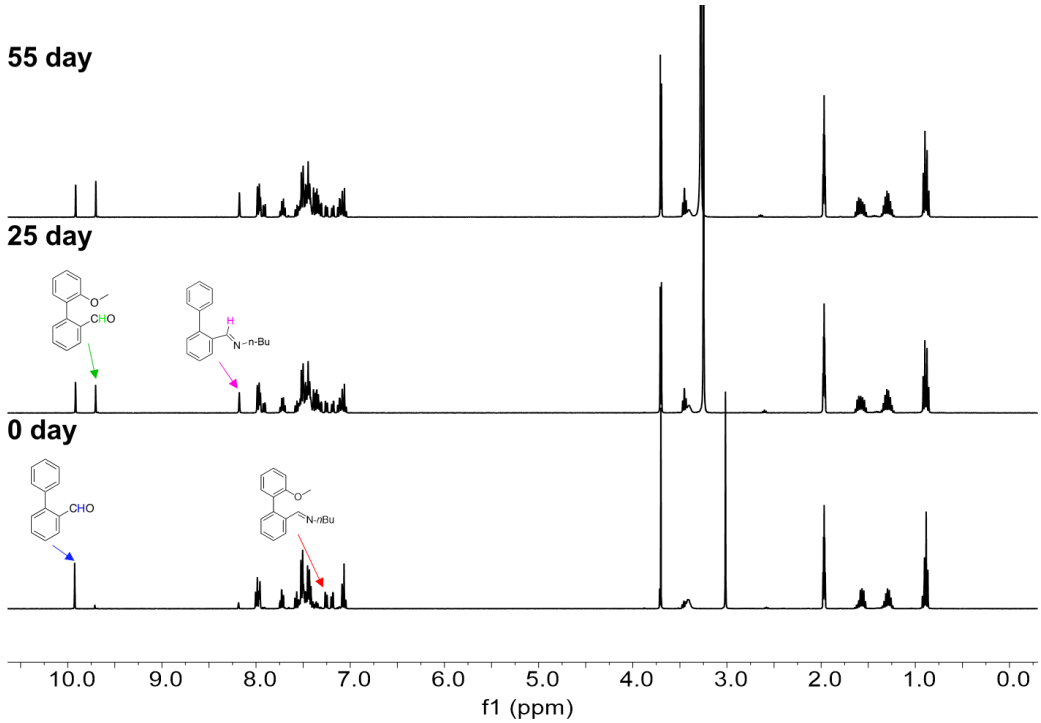

Figure S39. ^{1}H NMR spectra of the reaction of preformed **2**(OMe) and **1**(H) in mixed solvent (10% D_2O, 90% CD_3CN) at varied time (the corresponding spectra of panel c in Table S2).

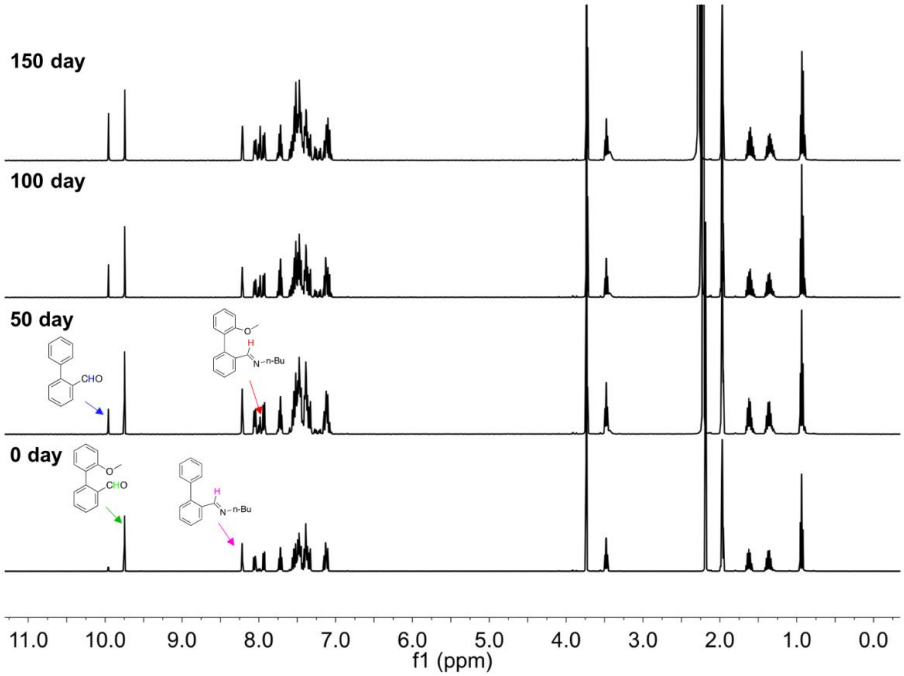

Figure S40. ^{1}H NMR spectra of the reaction of preformed **2**(H) and **1**(OMe) in CD_3CN at varied time (the corresponding spectra of panel d in Table S2).

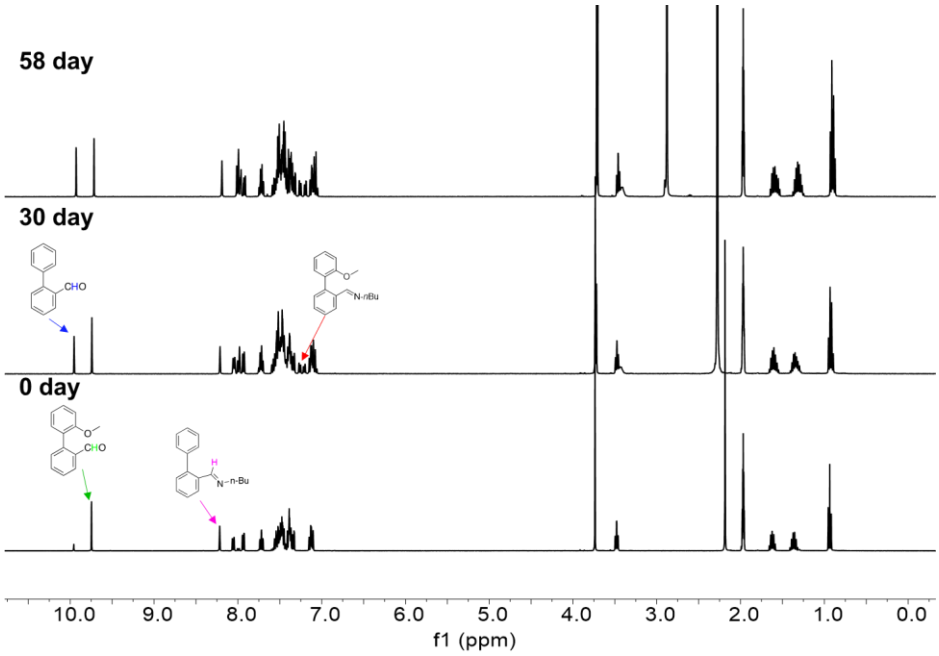

Figure S41. ^{1}H NMR spectra of the reaction of preformed **2**(H) and **1**(OMe) in mixed solvent (5% D_2O, 95% CD_3CN) at varied time (the corresponding spectra of panel e in Table S2).

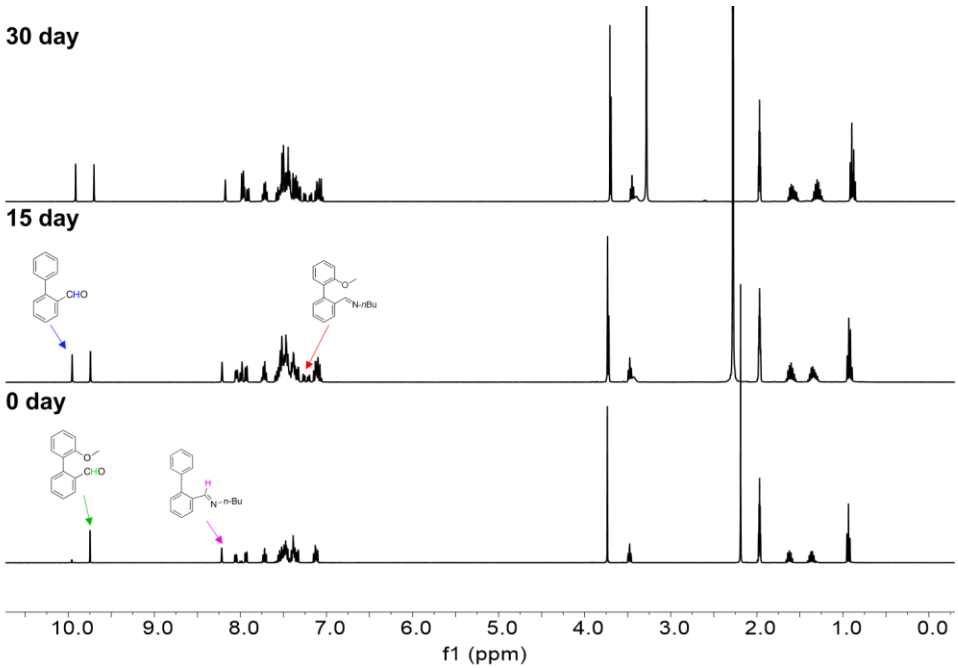

Figure S42. ^{1}H NMR spectra of the reaction of preformed **2**(H) and **1**(OMe) in mixed solvent (10% D_2O, 90% CD_3CN) at varied time (the corresponding spectra of panel f in Table S2).

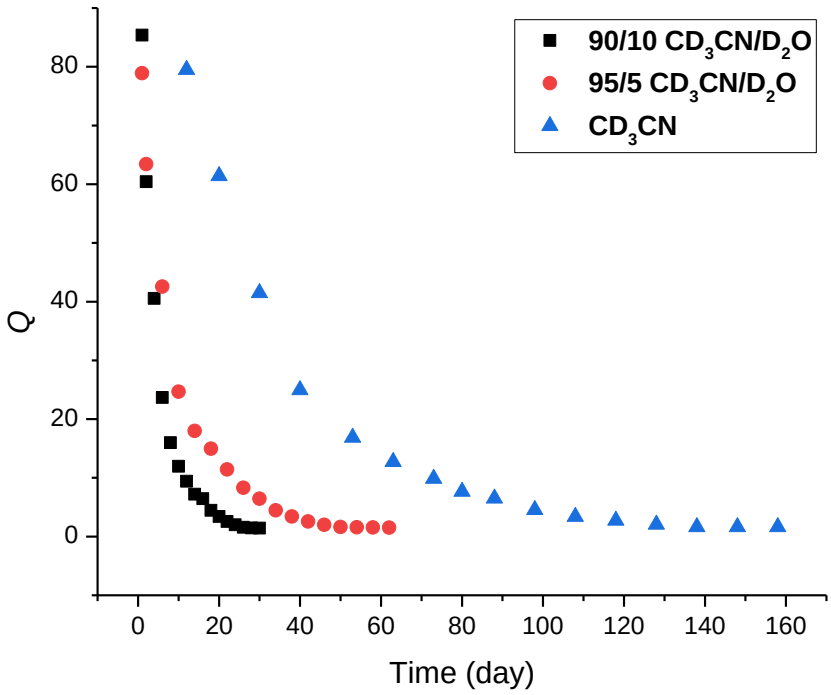

Figure S43. Kinetic profile of the reaction of preformed **2**(H) and **1**(OMe) in different solvent.

Table S3. The equilibrium constants of imine exchange reactions. The representative NMR spectrums were shown in Figures S44-S56.

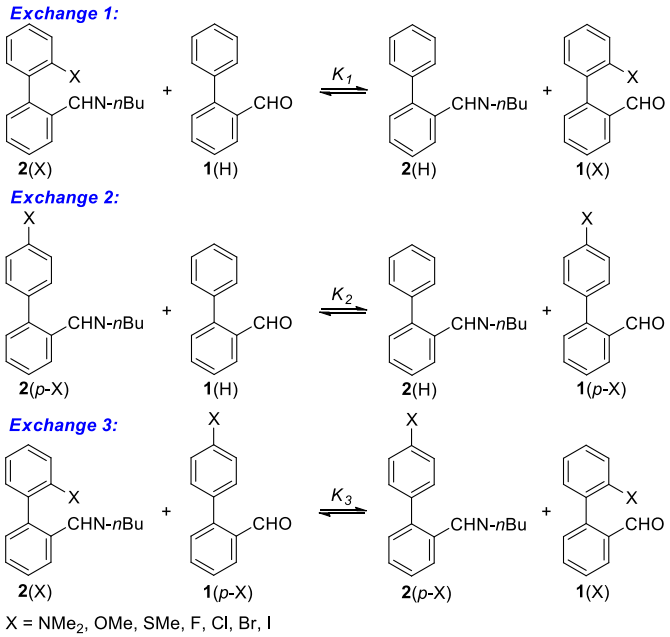

X	K_1	K_2	K_3
NMe_2	2.42	0.98	2.38

OMe	1.64	1.04	1.58
SMe	1.39	1.04	1.33
F	1.19	1.03	1.13
Cl	1.06	1.01	1.08
Br	1.04	0.99	1.06
I	1.02	-	-
H	1	1	1

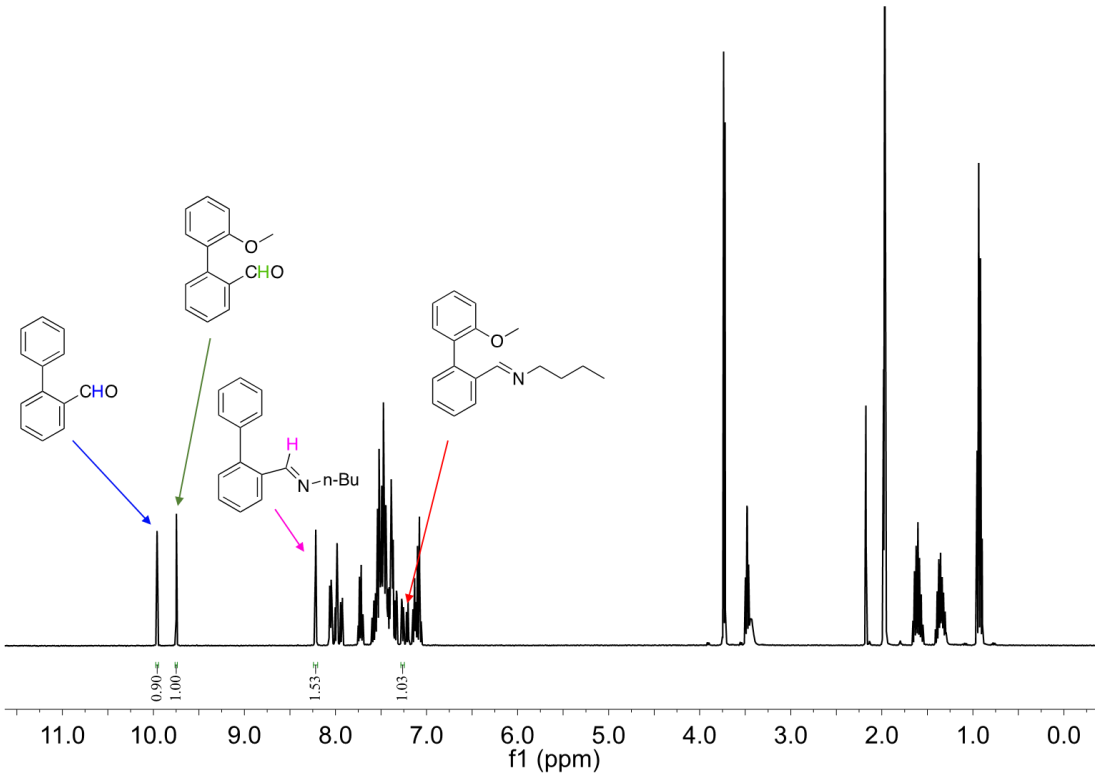

Figure S44. ^{1}H NMR spectrum of the competition between **1**(H) and **1**(OMe) for the reaction with 1-butylamine in CD_3CN.

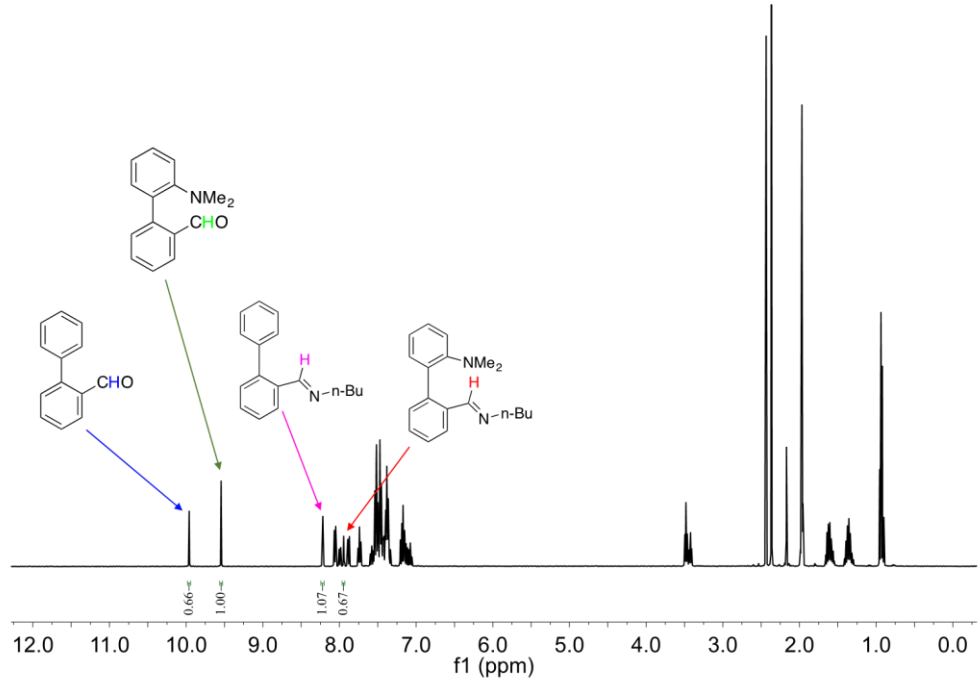

Figure S45. ^{1}H NMR spectrum of the competition between **1**(H) and **1**(NMe_2) for the reaction with 1-butylamine in CD_3CN.

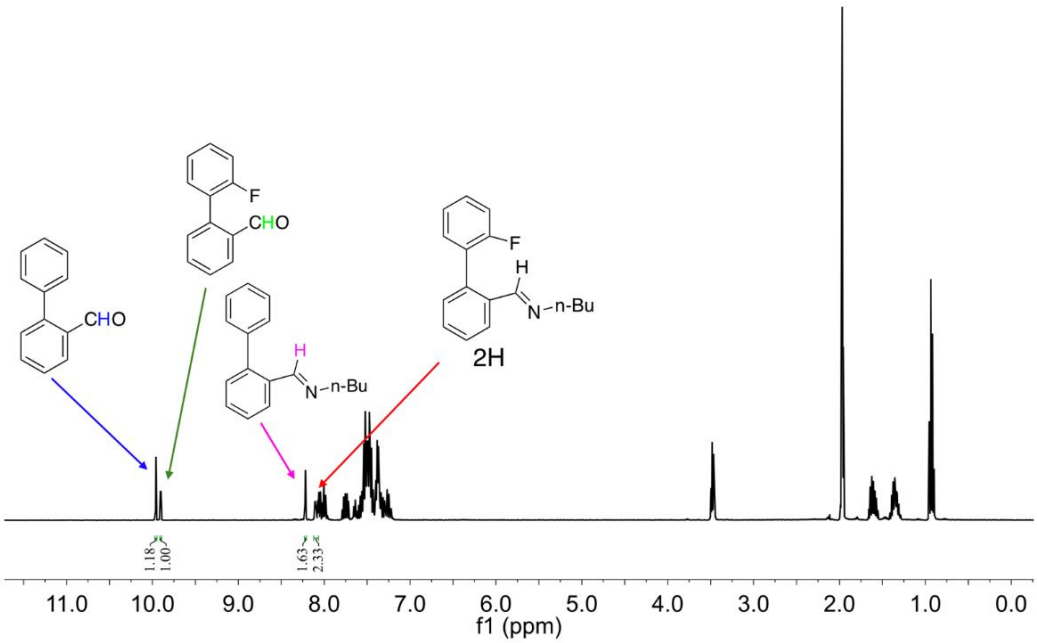

Figure S46. ^{1}H NMR spectrum of the competition between **1**(H) and **1**(F) for the reaction with 1-butylamine in CD_3CN.

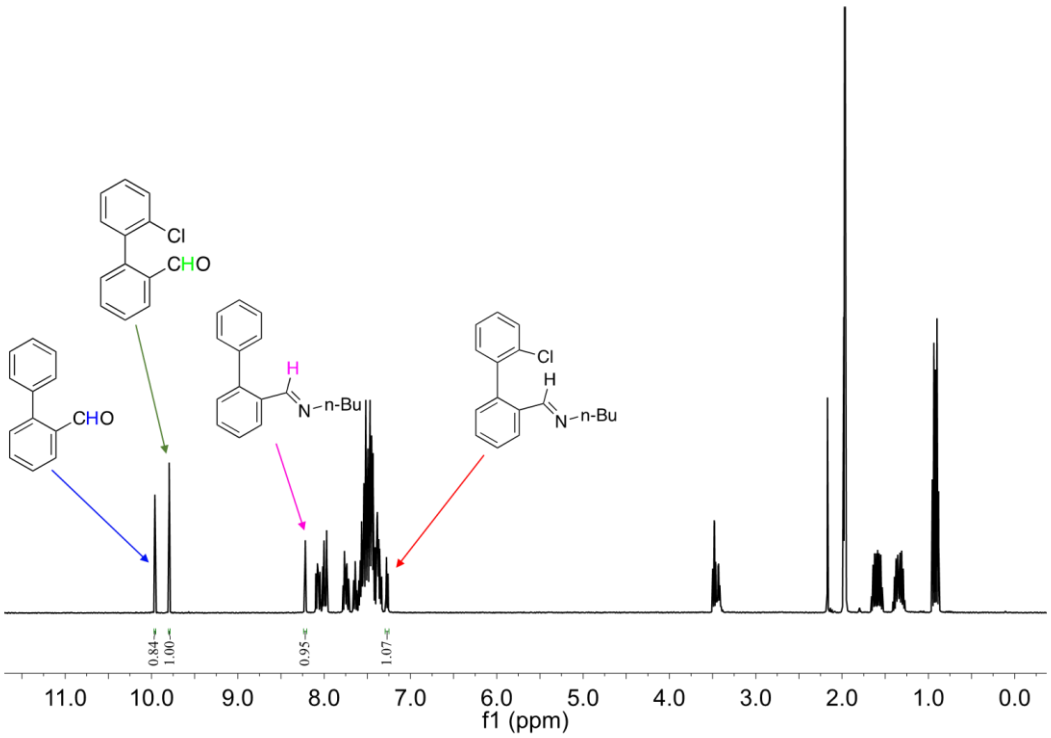

Figure S47. ^{1}H NMR spectrum of the competition between **1**(H) and **1**(Cl) for the reaction with 1-butylamine in CD_3CN.

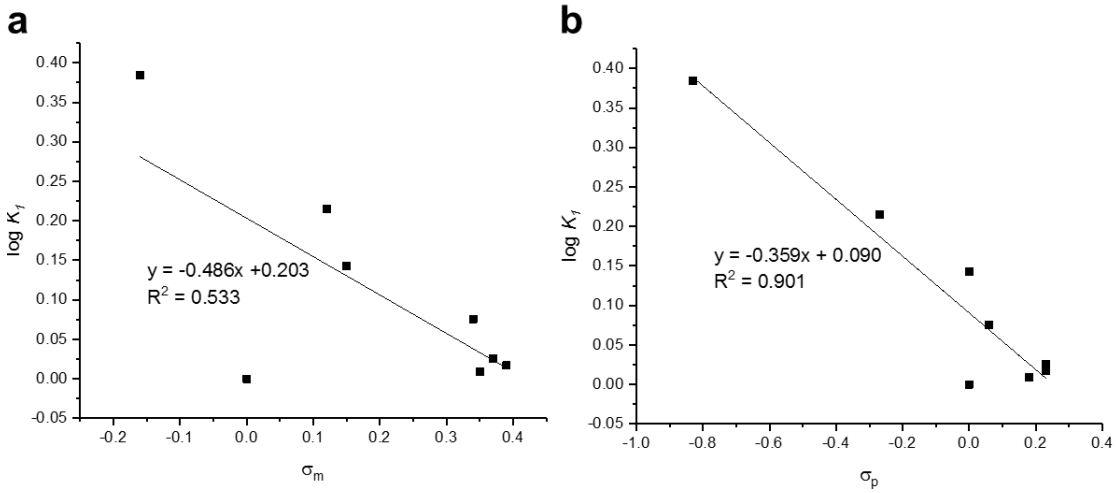

Figure S48. (a) log *K* of imine exchange 1 (Figure 2 and Table S3) versus σ_m. (b) log *K* of imine exchange 1 versus σ_p.

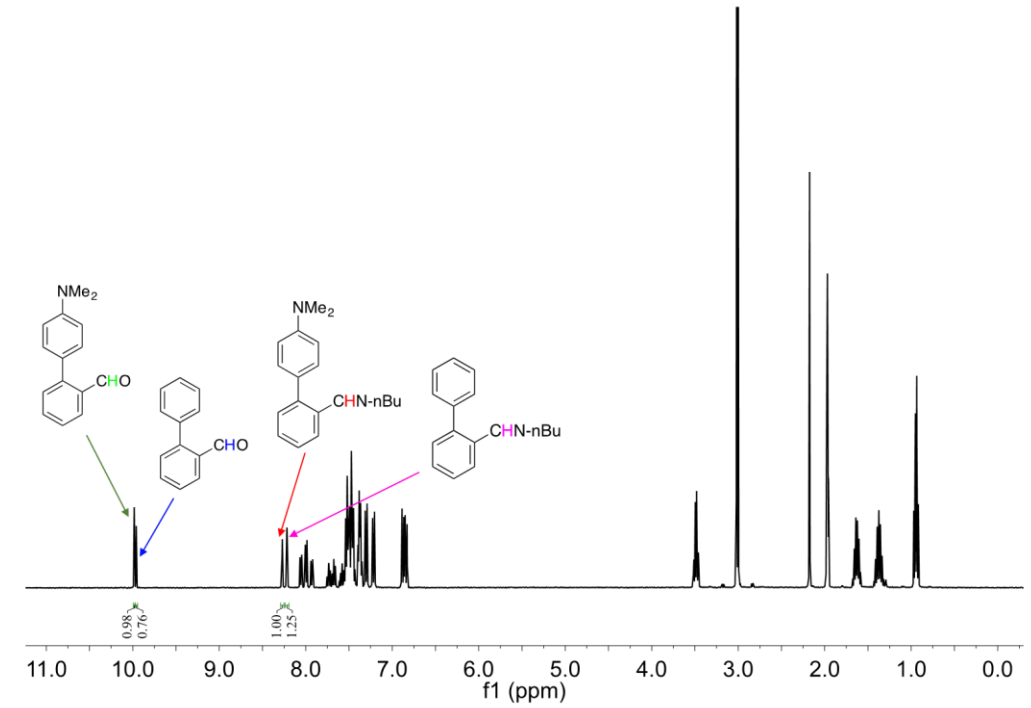

Figure S49. ^{1}H NMR spectrum of the competition between **1**(H) and **1**(*p*-NMe_2) for the reaction with 1-butylamine in CD_3CN.

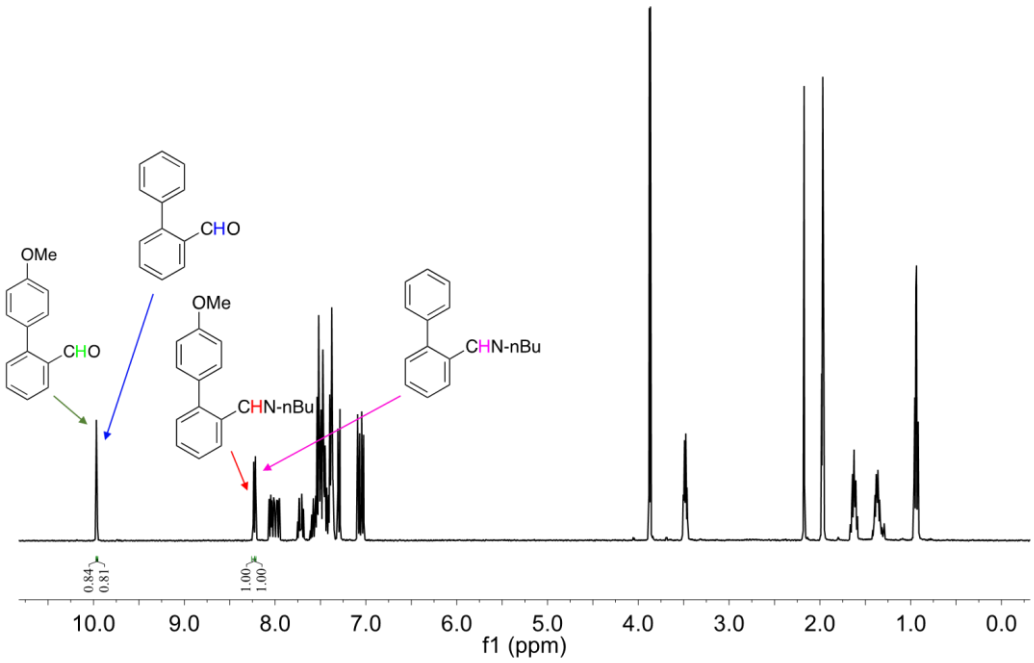

Figure S50. ^{1}H NMR spectrum of the competition between **1**(H) and **1**(*p*-OMe) for the reaction with 1-butylamine in CD_3CN.

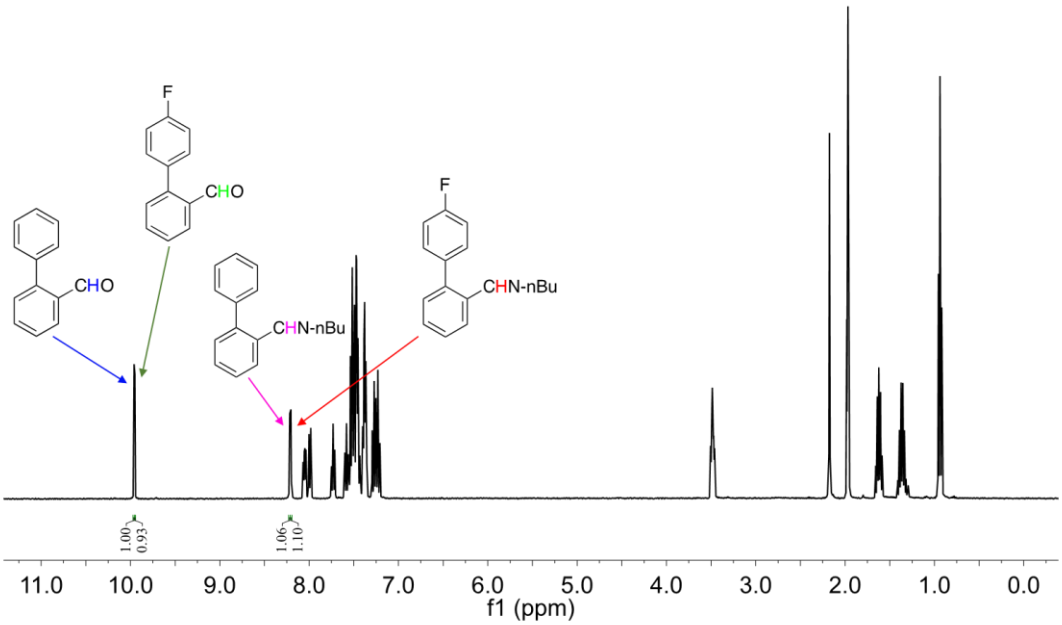

Figure S51. ^{1}H NMR spectrum of the competition between **1**(H) and **1**(*p*-F) for the reaction with 1-butylamine in CD_3CN.

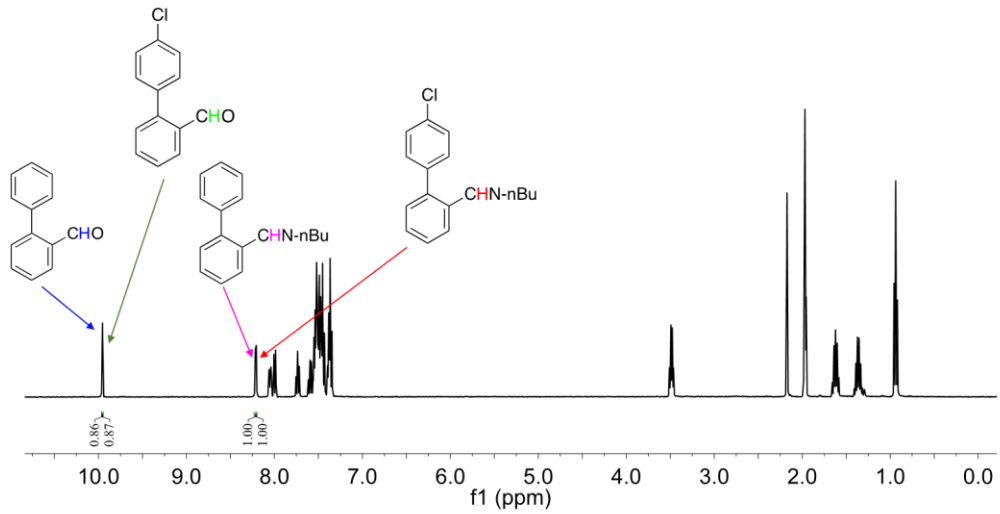

Figure S52. ^{1}H NMR spectrum of the competition between **1**(H) and **1**(*p*-Cl) for the reaction with 1-butylamine in CD_3CN.

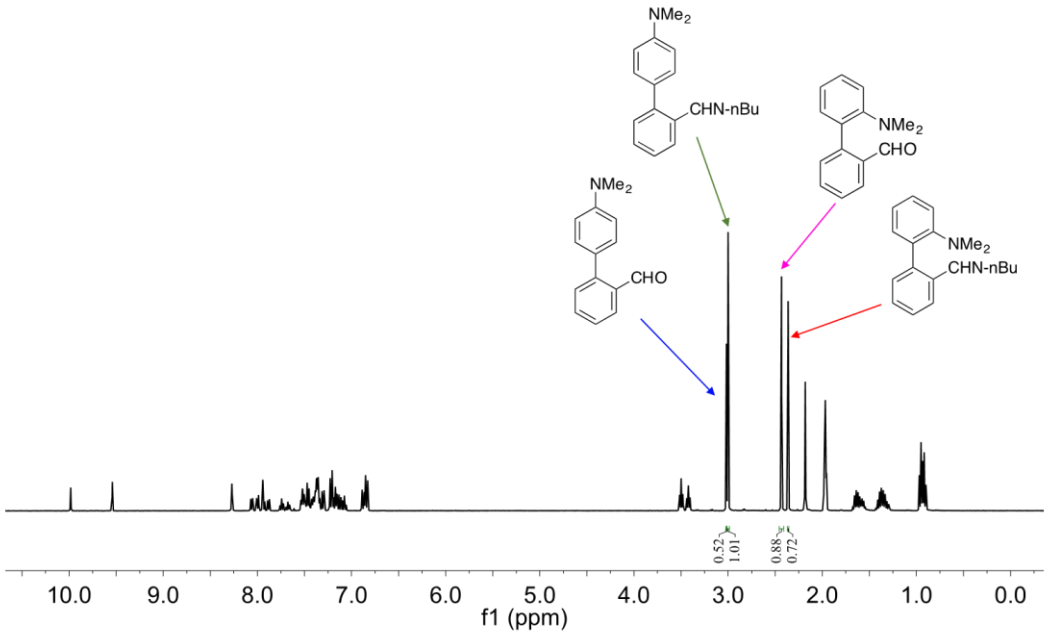

Figure S53. ^{1}H NMR spectrum of the competition between **1**(NMe$_2$) and **1**(*p*-NMe$_2$) for the reaction with 1-butylamine in CD_3CN.

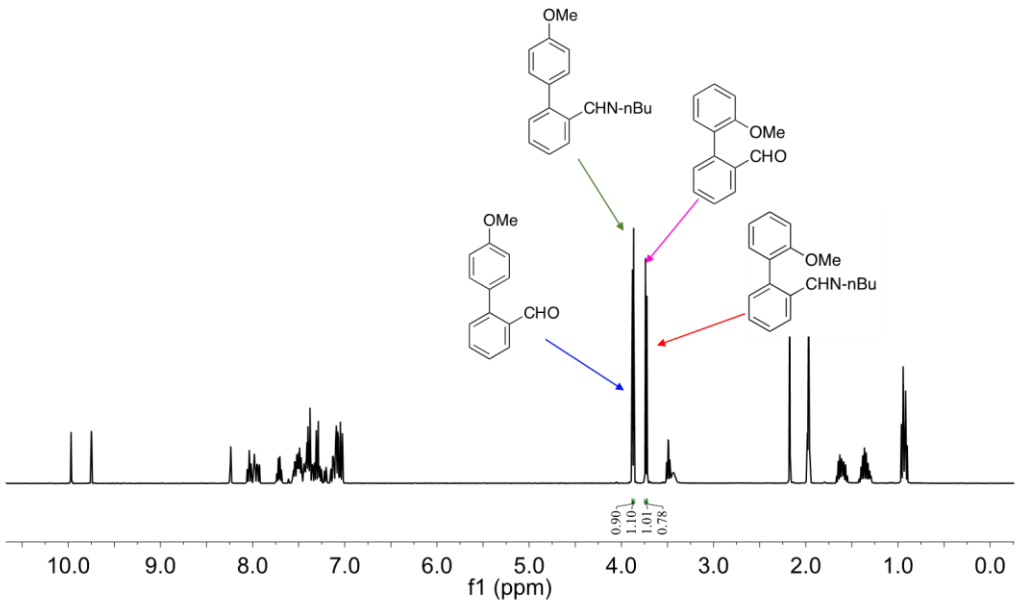

Figure S54. ^{1}H NMR spectrum of the competition between **1**(OMe) and **1**(*p*-OMe) for the reaction with 1-butylamine in CD_3CN.

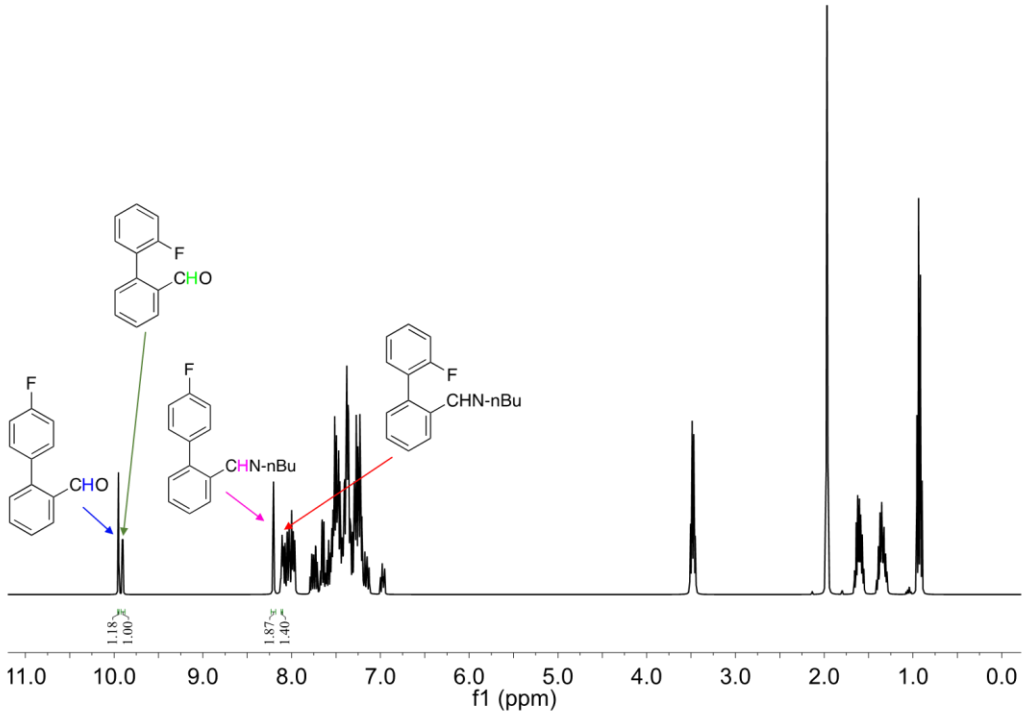

Figure S55. ^{1}H NMR spectrum of the competition between **1**(F) and **1**(*p*-F) for the reaction with 1-butylamine in CD_3CN.

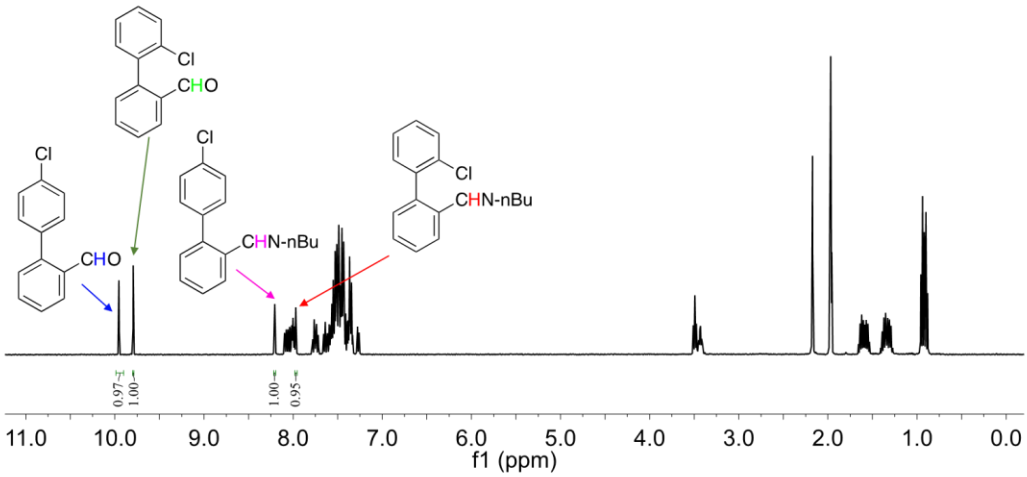

Figure S56. ^{1}H NMR spectrum of the competition between **1**(Cl) and **1**(*p*-Cl) for the reaction with 1-butylamine in CD_3CN.

4. Correlation with $n\rightarrow\pi^*$ Interaction

All calculations were performed by using Gaussian 09 packages.[S10] The method and basis set of M062X-D3/Def2-TZVP, M062X/Def2-TZVP, and B3LYP/Def2-TZVP was employed for the optimization and frequency analysis of model compounds **1**(X) and **2**(X) (X = NMe_2 and OMe), respectively. PCM solvent model is also included for acetonitrile. By frequency analysis, the number of imaginary frequencies for minima is 0. Conformers 1 and 2 (with or without $n\rightarrow\pi^*$ interaction, Figure 3) were found, and the corresponding G were calculated. Conformers 1 and 2 were also revealed to account for more than 95% of the population of **1**(OMe) and **2**(OMe), respectively, and other isomers, such as *Z*-isomer of **2**(OMe) and structures in which the carbonyl/imine points toward the other phenyl plane, were not considered further. $\triangle G$ of the exchange reaction was then calculated based on Boltzmann distribution of conformers, and summarized in Table S4. Both M062X and M062X-D3 were able to correctly predict the trend of experimental substituent effect, but with D3 correction, $\triangle G_{cacld}$ from M062X-D3 is more close to $\triangle G_{exp}$ than M062X. Therefore, M062X-D3/Def2-TZVP (with an ultrafine integration grid) was employed for the subsequent Natural bond orbital (NBO) calculation, nocovalent interaction (NCI) analysis. In order to focus on $n\rightarrow\pi^*$ interaction, only conformer 1 was calculated for other X substituents. NBO was implemented by NBO 3.1 module[S11] in Gaussian 09 packages. The electronic density cubes for NCI[S12] were generated by Multiwfn 3.38 using the optimized structures.[S13] NBO and NCI plot were presented by VMD1.90.[S14]

Table S4. Summary of calculated $\triangle G$ with different DFT functions.

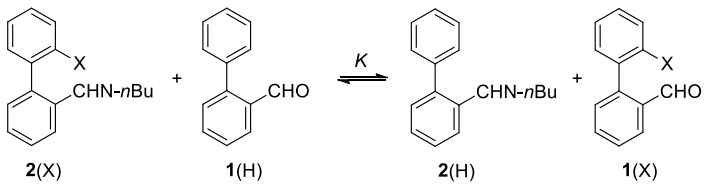

X	M062X-D3 (kcal/mol)	M062X (kcal/mol)	B3LYP (kcal/mol)	Experimental $\triangle G$ (kcal/mol)
NMe_2	-0.464	-0.779	-0.345	-0.524
OMe	-0.252	0.282	-0.348	-0.293

Table S5. The values of second order stabilization energy (kcal/mol) for each natural bond orbital (based on the number of lone pairs of X) and their sums for conformer 1 of **1**(X).

1(X)		NBO1	NBO2	NBO3	SUM
I	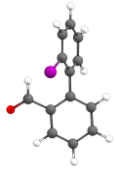	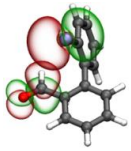 -0.78	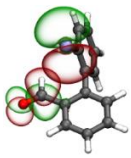 -0.22	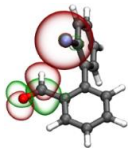 -0.07	**-1.07**
Br	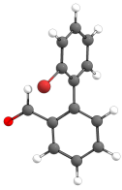	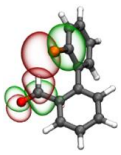 -0.86	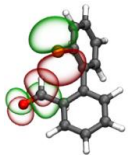 -0.32	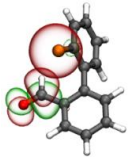 -0.11	**-1.29**
Cl	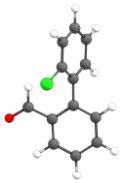	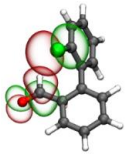 -0.81	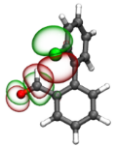 -0.38	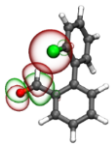 -0.14	**-1.33**
F	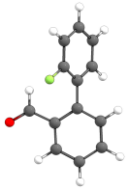	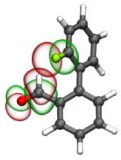 -0.47	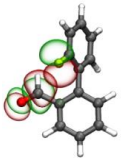 -0.36	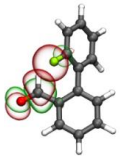 -0.22	**-1.05**
SMe	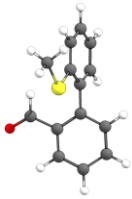	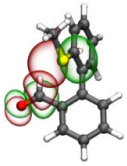 -1.37	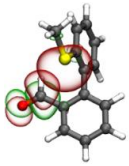 -0.31		**-1.68**
OMe	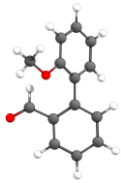	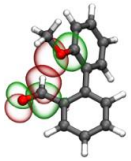 -0.96	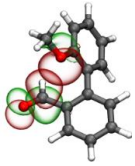 -0.78		**-1.74**
NMe_2	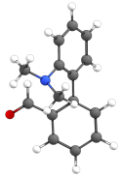	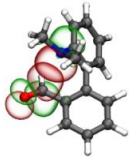 -4.59			**-4.59**

Table S6. The comparison of the values of NBOs (kcal/mol) and their sums of conformer 1 of **2**(OMe) incorporating 1-butylamine or methylamine.

Conformer 1	NBO1	NBO2	SUM
methylamine	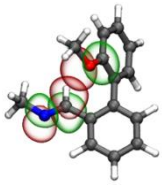 -0.66	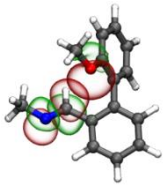 -0.55	**-1.21**
1-butylamine	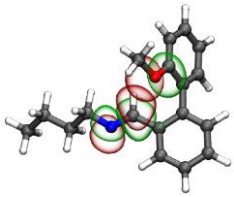 -0.68	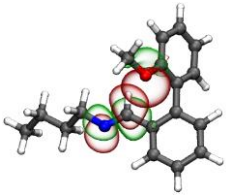 -0.54	**-1.22**

Table S7. The values of second order stabilization energy (kcal/mol) for each natural bond orbital and their sums for conformer 1 of **2**(X).

2(X)		NBO1	NBO2	NBO3	SUM
I	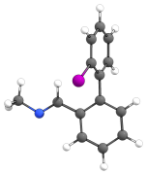	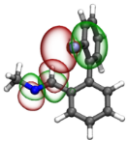 -0.61	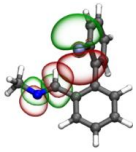 -0.19	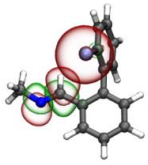 -0.09	**-0.89**
Br	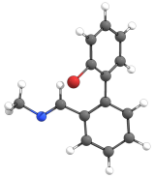	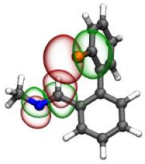 -0.64	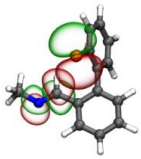 -0.24	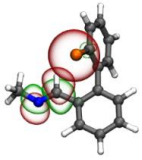 -0.12	**-0.98**
Cl	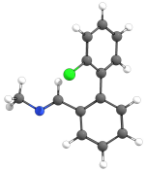	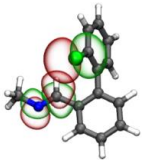 -0.62	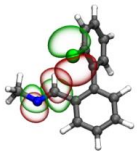 -0.29	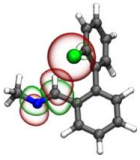 -0.15	**-1.06**
F	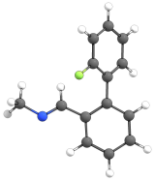	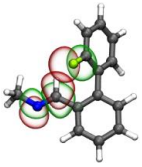 -0.41	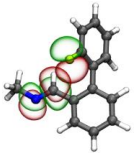 -0.29	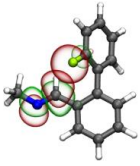 -0.24	**-0.94**

SMe		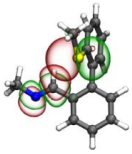 -0.86	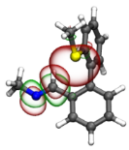 -0.23	**-1.09**
OMe	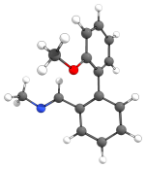	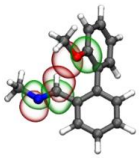 -0.66	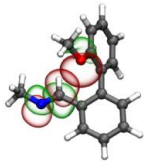 -0.55	**-1.21**
NMe_2	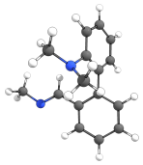	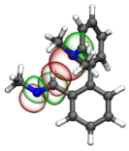 -2.11		**-2.11**

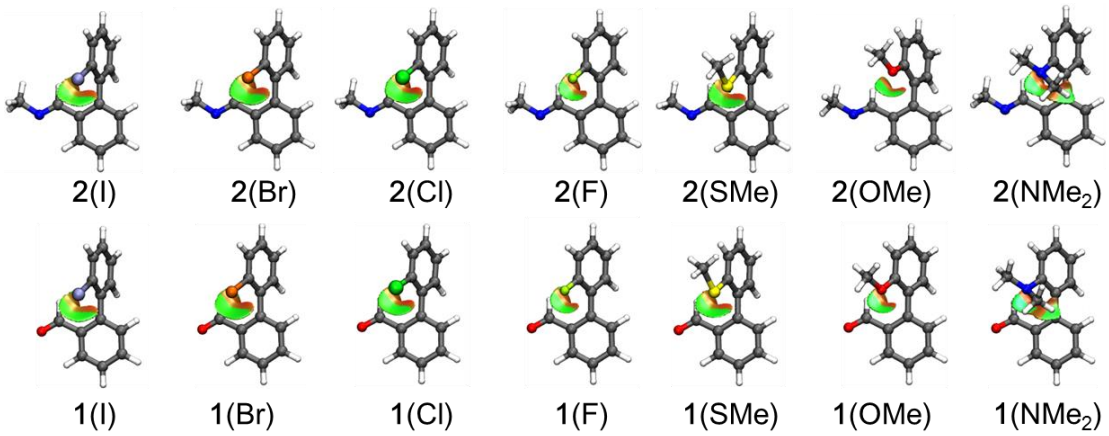

Figure S57. The NCI plot of conformer 1 for **1**(X) and **2**(X). For clarity only focused interactions were shown.

Table S8. The values of the sterimol parameters (L and B1, in 10^{-10} m), the stabilization energy difference ($\triangle\triangle E^{(2)}$ [a]) between conformer 1 of **1**(X) and **2**(X) for multivariate correlation, as well as predicted and measured $\triangle G$ [b] of imine exchange. The units of $\triangle E^{(2)}$ and $\triangle G$ are kcal/mol. The predicted $\triangle G$ value was calculated based on multivariate linear correlation of measured $\triangle G$ versus L, B1, and $\triangle\triangle E^{(2)}$.

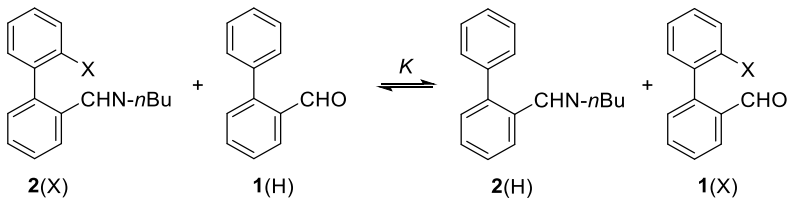

X	L	B_1	$\triangle E^{(2)}$-**1**(X)	$\triangle E^{(2)}$-**2**(X)	$\triangle\triangle E^{(2)}$ [a]	Predicted $\triangle G$	Measured $\triangle G$ [b]
F	2.65	1.35	-1.05	-0.94	-0.11	-0.095	-0.103
Cl	3.52	1.80	-1.33	-1.06	-0.27	-0.052	-0.035
Br	3.83	1.95	-1.29	-0.98	-0.31	-0.038	-0.023
I	4.23	2.15	-1.07	-0.89	-0.18	0.014	-0.012
NMe_2	3.53	1.50	-4.59	-2.11	-2.48	-0.521	-0.524
SMe	4.30	1.70	-1.68	-1.09	-0.59	-0.209	-0.195
OMe	3.98	1.35	-1.74	-1.21	-0.53	-0.285	-0.293

[a] $\triangle\triangle E^{(2)} = [\triangle E^{(2)}\text{-}\mathbf{1}(X)] - [\triangle E^{(2)}\text{-}\mathbf{2}(X)]$

[b] Measured $\triangle G = -0.281 - 0.0900L + 0.328B1 + 0.167\triangle\triangle E^{(2)}$

The quality of multivariate linear regression of measured $\triangle G$ versus L, B_1, and $\triangle\triangle E^{(2)}$ was supported by a good linear relationship (Measured $\triangle G = 1.0001*(\text{Predicted } \triangle G) + 8.06*10^{-7}$, $R^2 = 0.993$, as shown in Figure 4f) between the experimental and the predicted data. By using a standardization method of regression coefficient, the distribution of L, B_1, and $\triangle\triangle E^{(2)}$ can be determined by their corresponding values of regression coefficient of -0.270, 0.535, 0.742, respectively.

5. Solvent Effect

(1) Solvent effect on thermodynamics

Aldehydes **1**(H) and **1**(OMe) (20 mM each, 1.0 equiv.) were mixed with 1-butylamine (24 mM, 1.2 equiv.) in different solvents (0.6 mL), and the mixture was stirred overnight in the presence of molecular sieves and characterized by ^{1}H NMR. For reactions in aqueous media, aldehydes **3**(H) and **3**(OMe) (40 mM each) were used. The equilibrium constant of imine exchange was next calculated. The data is listed in Table S9, with representative NMR spectra shown in Figures S58-S64.

Table S9. Solvent parameters,[S15] *K*, measured ΔG of exchange reactions. Solvent mixtures are reported in v/v %. Cohesive energy density (*ced*) for solvent mixtures are calculated assuming these values scale linearly with the v/v % solvent composition.

Solvent	***ced*** (cal/cm^3)	**α**	***K***	**$\Delta G_{exp.}$** (kcal/mol)
Toluene	79.4	0	0.71	0.203
Chloroform	85.4	0.2	0.72	0.194
Dichloromethane	93.7	0.13	0.78	0.147
60% $CDCl_3$ 40% CD_3CN	106.8		1.03	-0.017
Pyridine	112.4	0	1.24	-0.127
20% $CDCl_3$ 80% CD_3CN	128.2		1.47	-0.228
Acetonitrile	138.9	0.19	1.64	-0.293
DMF	139.2	0	2.10	-0.439
DMSO	168.6	0	2.99	-0.648
Isopropanol	132.3	0.76	1.70	-0.314
Ethanol	161.3	0.86	1.46	-0.224
Methanol	209	0.98	1.22	-0.118
80% CD_3OD 20% D_2O	277.2		1.04	-0.023
60% CD_3OD 40% D_2O	345.4		0.88	0.076
40% CD_3OD 60% D_2O	413.6		0.68	0.228
20% CD_3OD 80% D_2O	481.8		0.53	0.375
D_2O	550	1.17	0.44	0.486

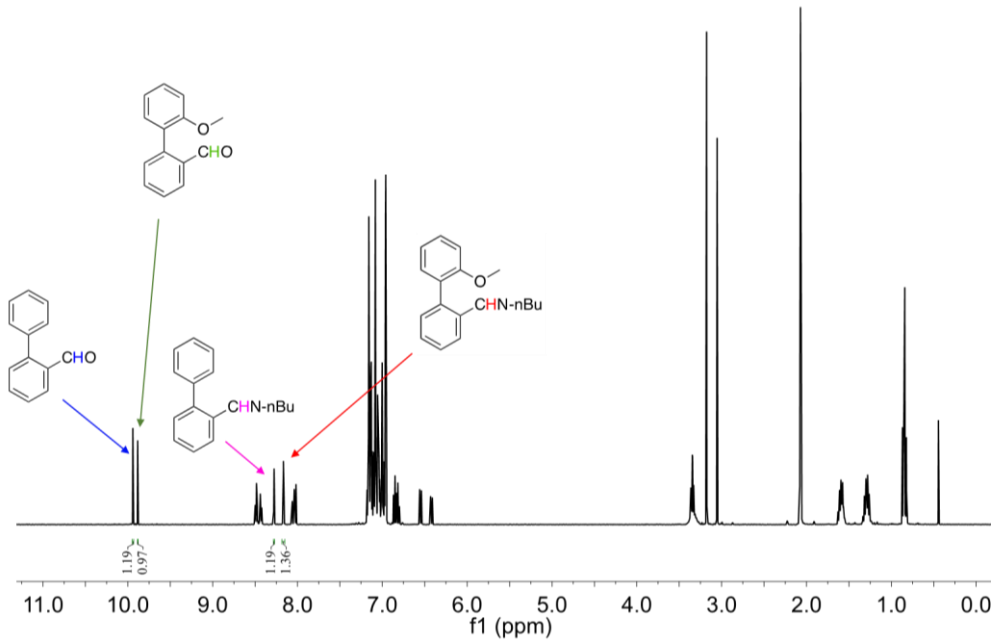

Figure S58. ^{1}H NMR spectrum of the competition between **1**(H) and **1**(OMe) for the reaction with 1-butylamine in toluene-d_8.

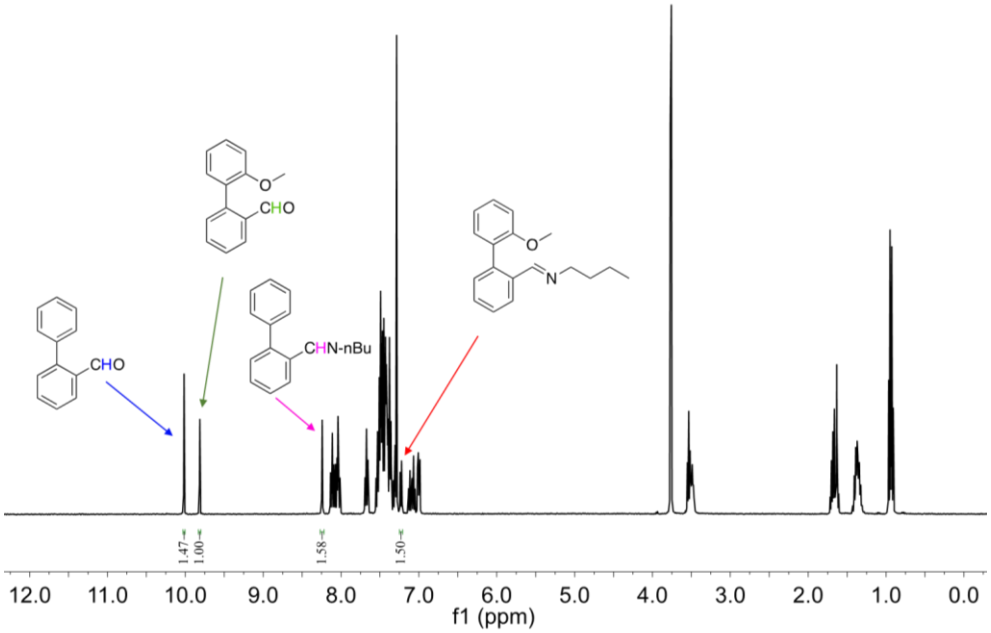

Figure S59. ^{1}H NMR spectrum of the competition between **1**(H) and **1**(OMe) for the reaction with 1-butylamine in $CDCl_3$.

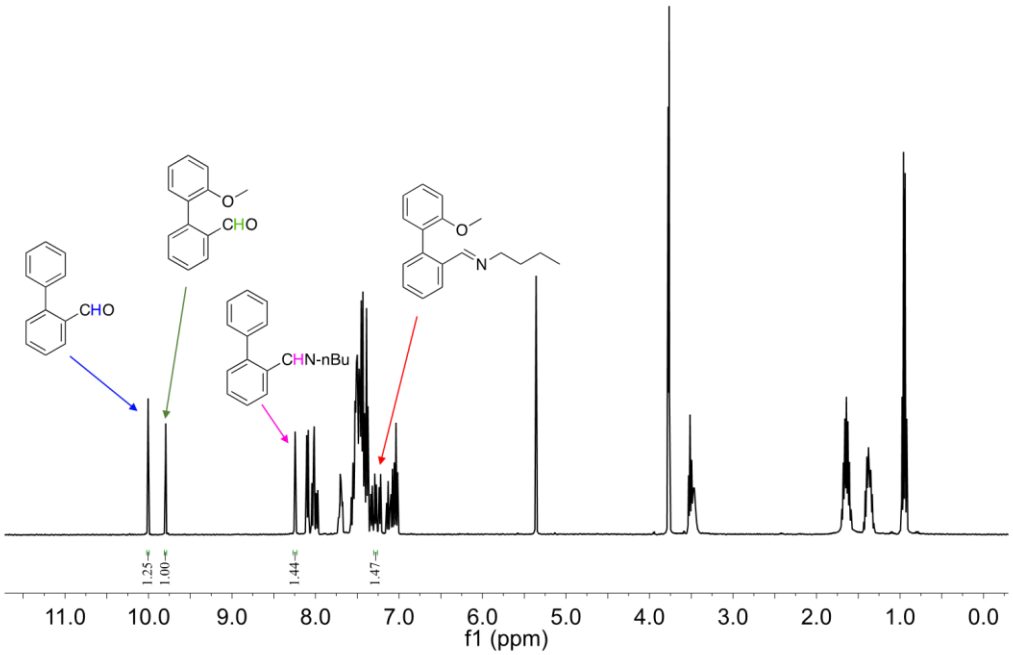

Figure S60. ^{1}H NMR spectrum of the competition between **1**(H) and **1**(OMe) for the reaction with 1-butylamine in CD_2Cl_2.

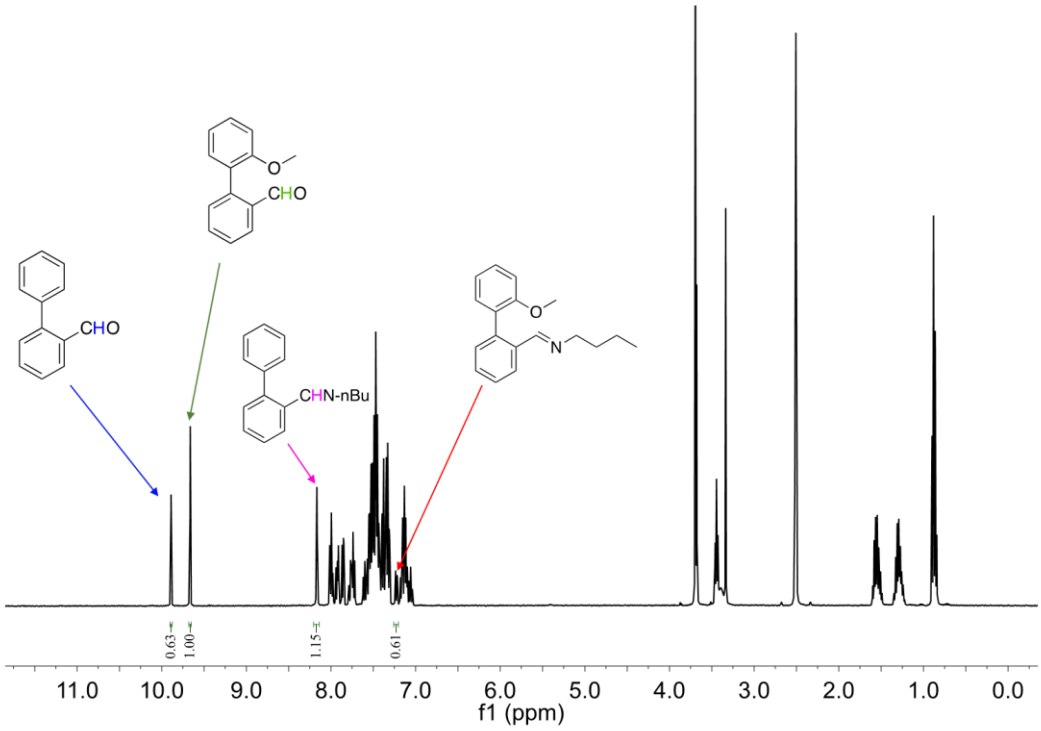

Figure S61. ^{1}H NMR spectrum of the competition between **1**(H) and **1**(OMe) for the reaction with 1-butylamine in DMSO-d_6.

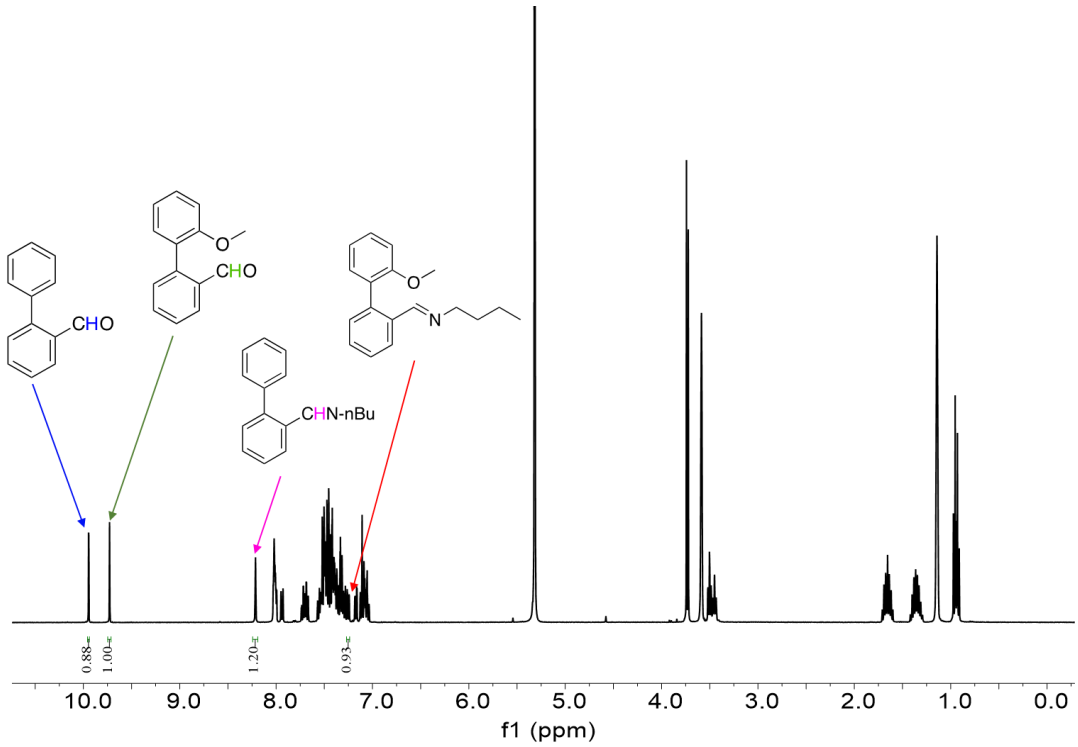

Figure S62. ^{1}H NMR spectrum of the competition between **1**(H) and **1**(OMe) for the reaction with 1-butylamine in ethanol-d_6.

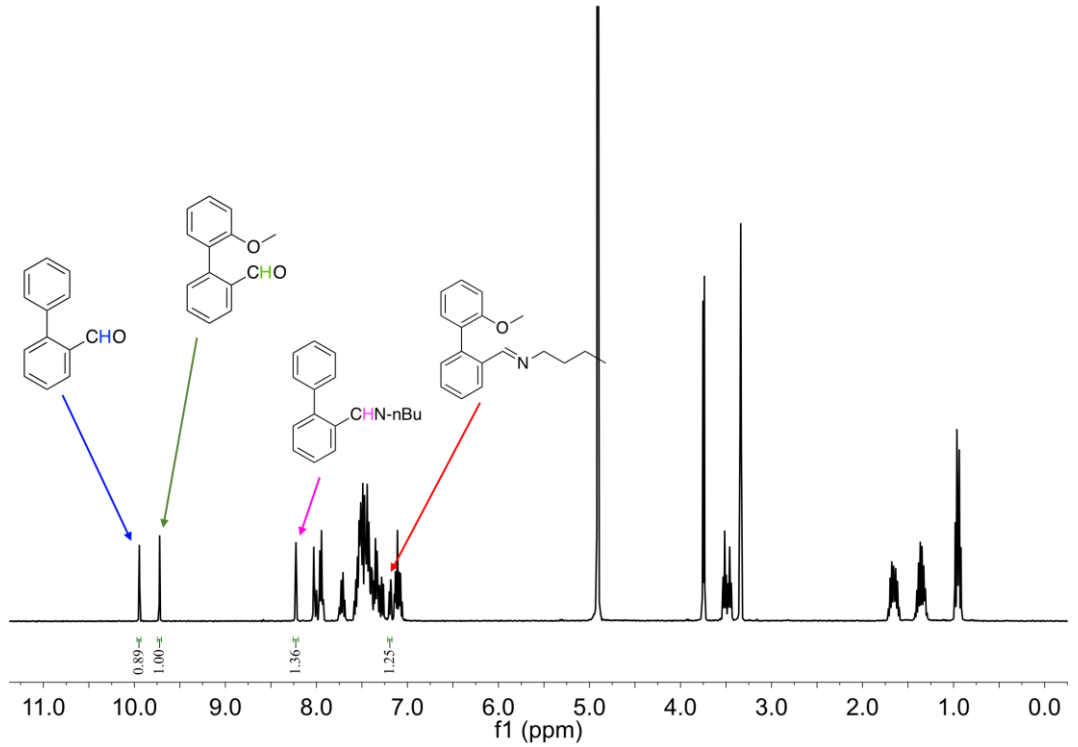

Figure S63. ^{1}H NMR spectrum of the competition between **1**(H) and **1**(OMe) for the reaction with 1-butylamine in CD_3OD (the corresponding spectra of panel c in Table S10).

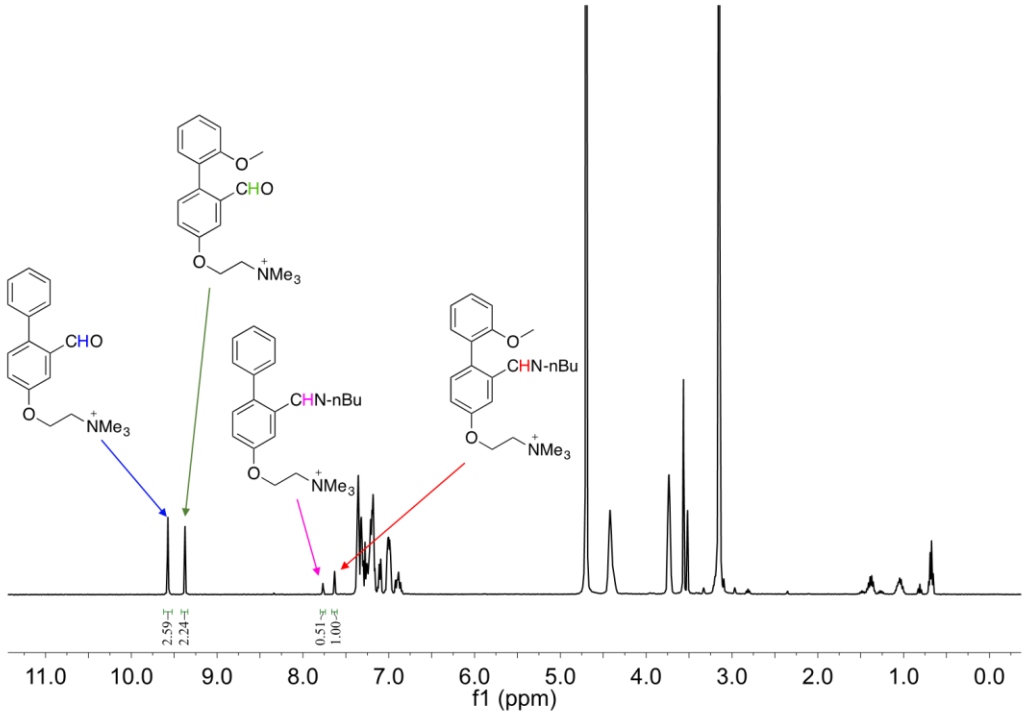

Figure S64. ^{1}H NMR spectrum of the competition between **3**(H) and **3**(OMe) for the reaction with 1-butylamine in D_2O (the corresponding spectra of panel f in Table S10).

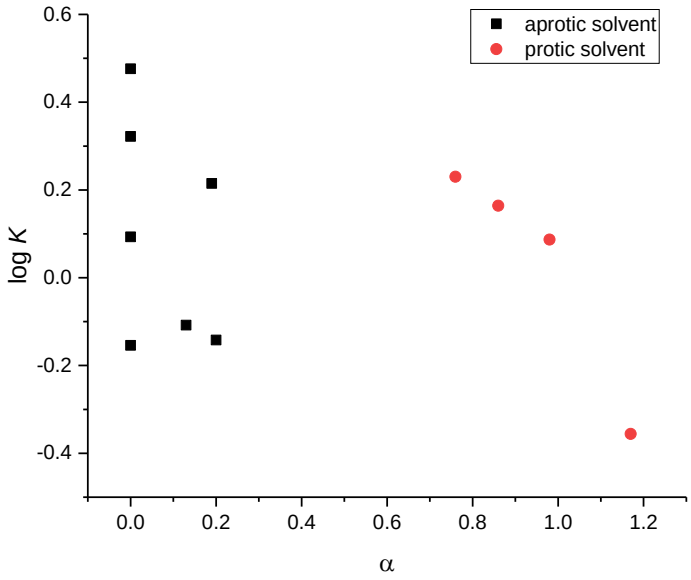

Figure S65. Plot of log *K* of imine exchange in varied solvents versus Taft parameter α.

(2) Solvent effect on kinetics

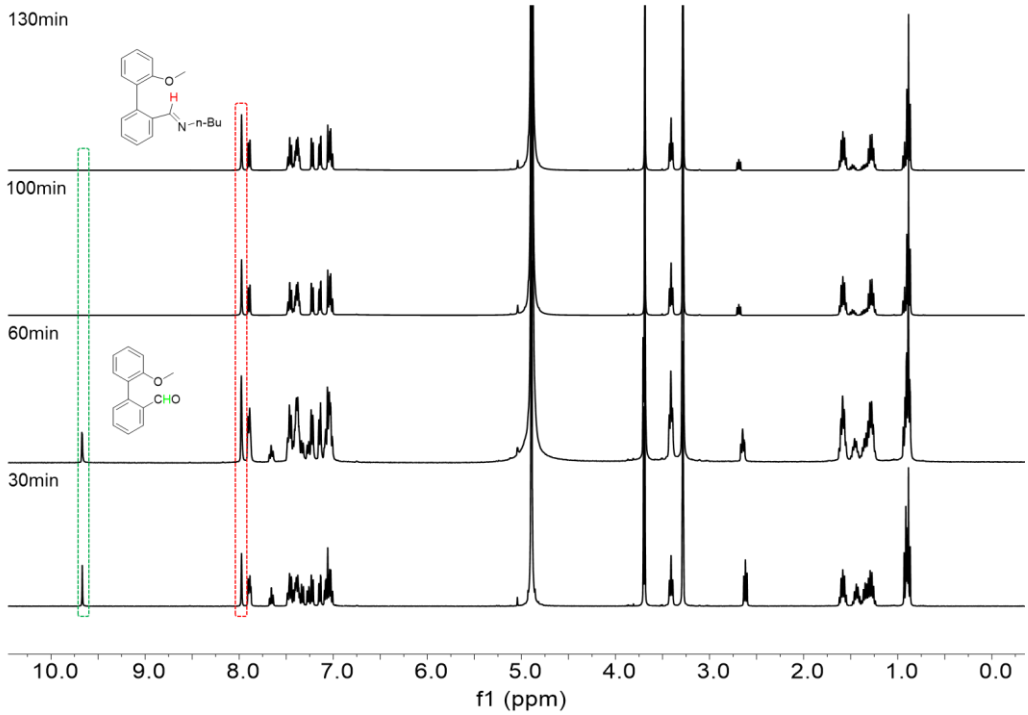

Figure S66. ^{1}H NMR spectra of the reaction between **1**(OMe) (20 mM, 1.0 equiv.) and 1-butylamine (24 mM, 1.2 equiv.) in CD_3OD. The reaction was complete in 100 min.

Table S10. The equilibrium constant and equilibrating time of the imine exchange with different sequence of reagents addition in CD_3OD or D_2O.

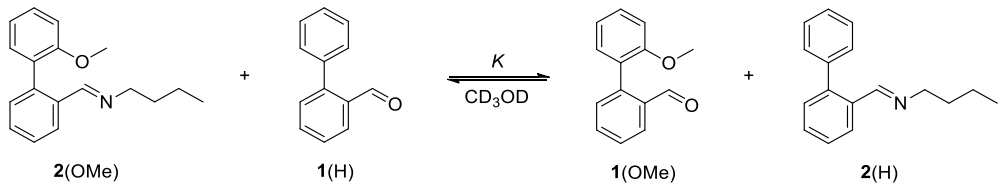

2(OMe) + **1**(H) ⇌ **1**(OMe) + **2**(H)

Panel	Sequence of adding reagents	*K*	Equilibrating time
a	Generate **2**(OMe) *in situ*, then add **1**(H)	1.22	22 day
b	Generate **2**(H) *in situ*, then add **1**(OMe)	1.23	22 day
c	**1**(H) and **1**(OMe) simultaneously reacted with 1-butylamine	1.22	1 day

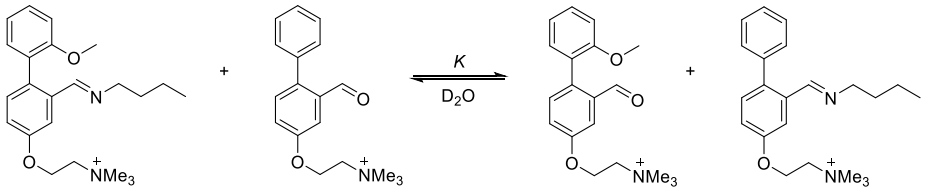

Panel	Sequence of adding reagents	*K*	Equilibrating time
d	Generate **4**(OMe) *in situ*, then add **3**(H)	0.44	15 min
e	Generate **4**(H) *in situ*, then add **3**(OMe)	0.43	15 min
f	**3**(H) and **3**(OMe) simultaneously reacted with 1-butylamine	0.43	15 min

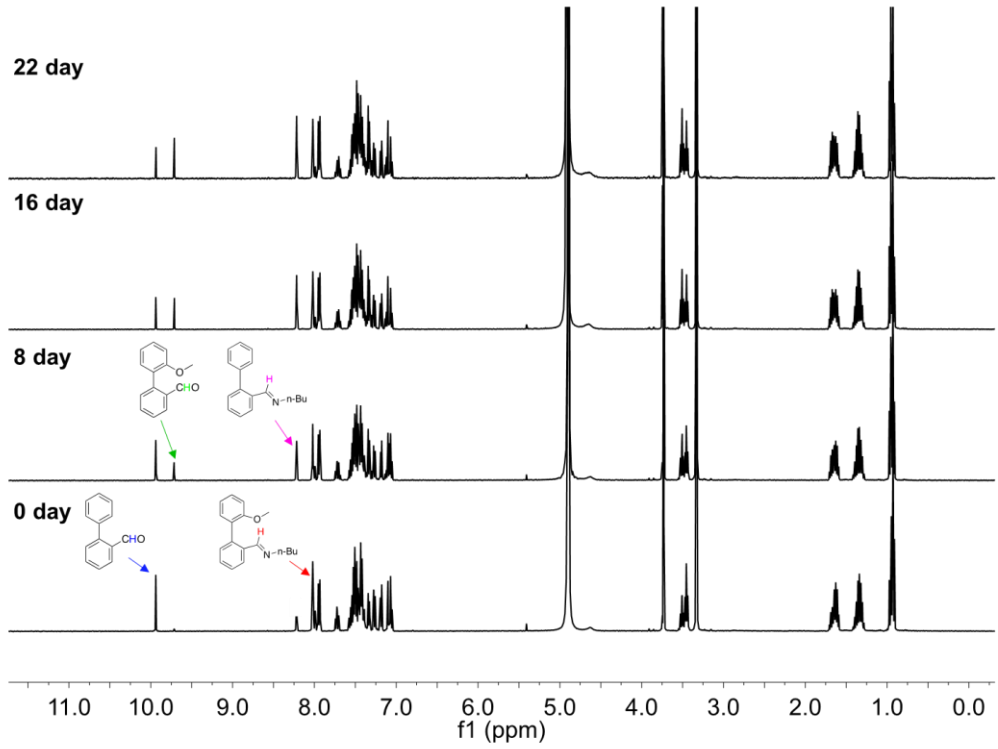

Figure S67. ^{1}H NMR spectra of the reaction of preformed **2**(OMe) and **1**(H) in CD_3OD at varied time (the corresponding spectra of panel a in Table S10).

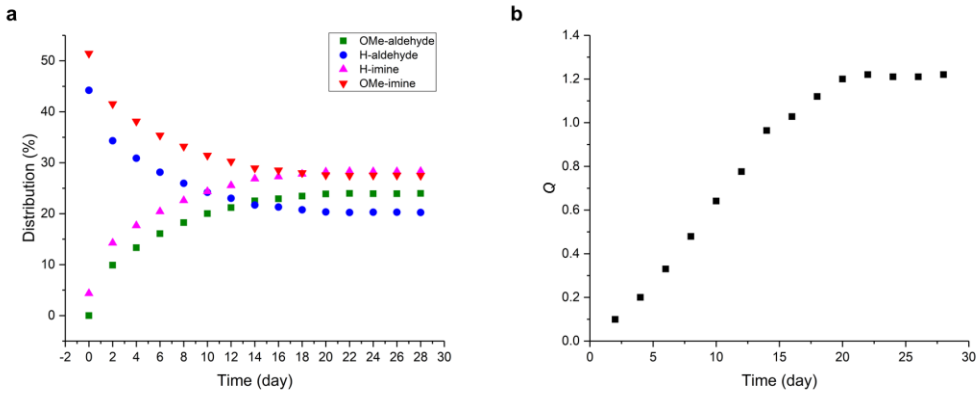

Figure S68. The kinetic profile of the reaction of preformed **2**(OMe) and **1**(H) in CD_3OD: (a) component distribution; (b) reaction quotient (Q).

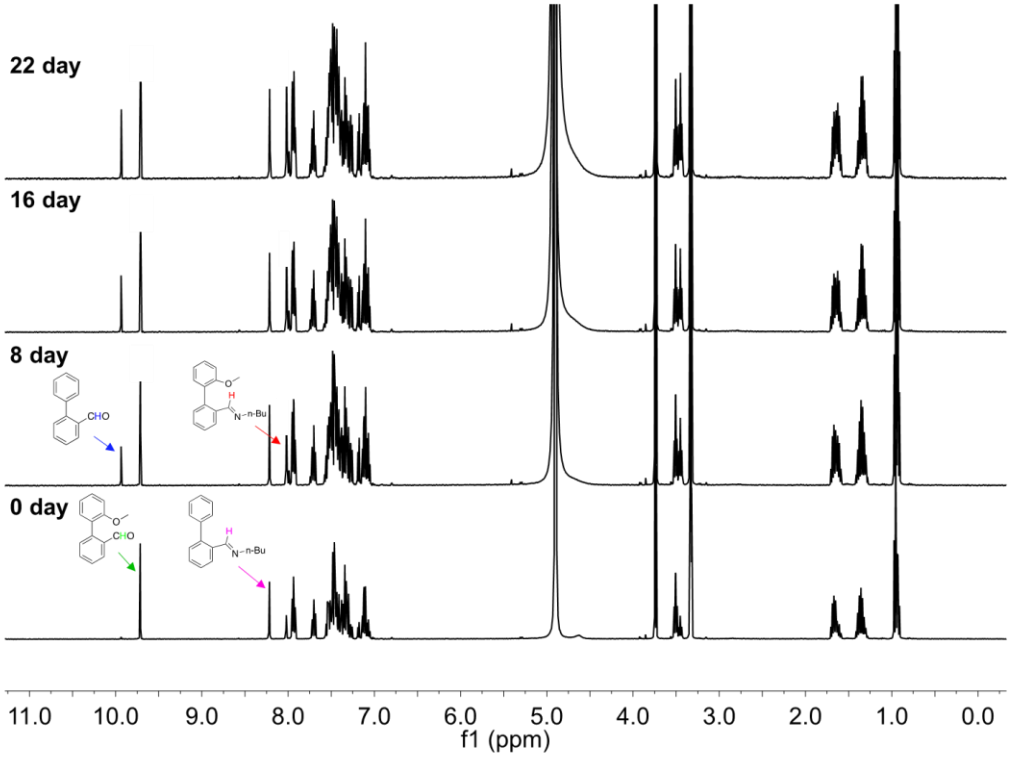

Figure S69. ^1H NMR spectra of the reaction of preformed **2**(H) and **1**(OMe) in CD_3OD at varied time (the corresponding spectra of panel b in Table S10).

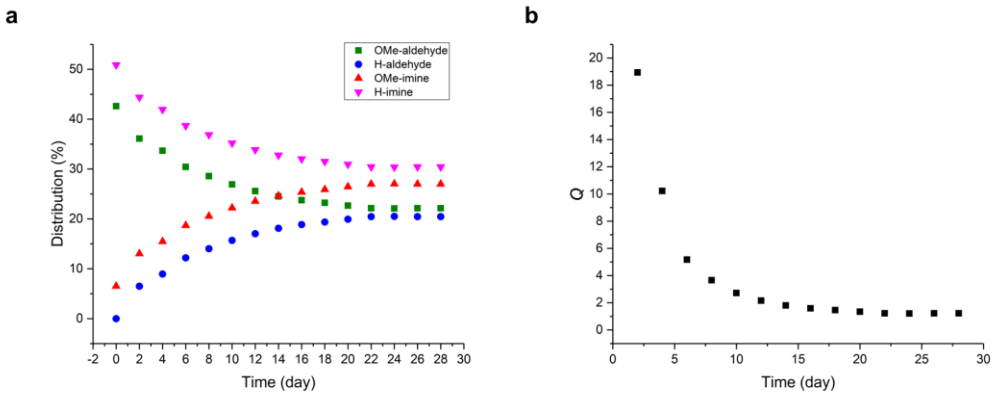

Figure S70. The kinetic profile of the reaction of preformed **2**(H) and **1**(OMe) in CD_3OD: (a) component distribution; (b) reaction quotient (Q).

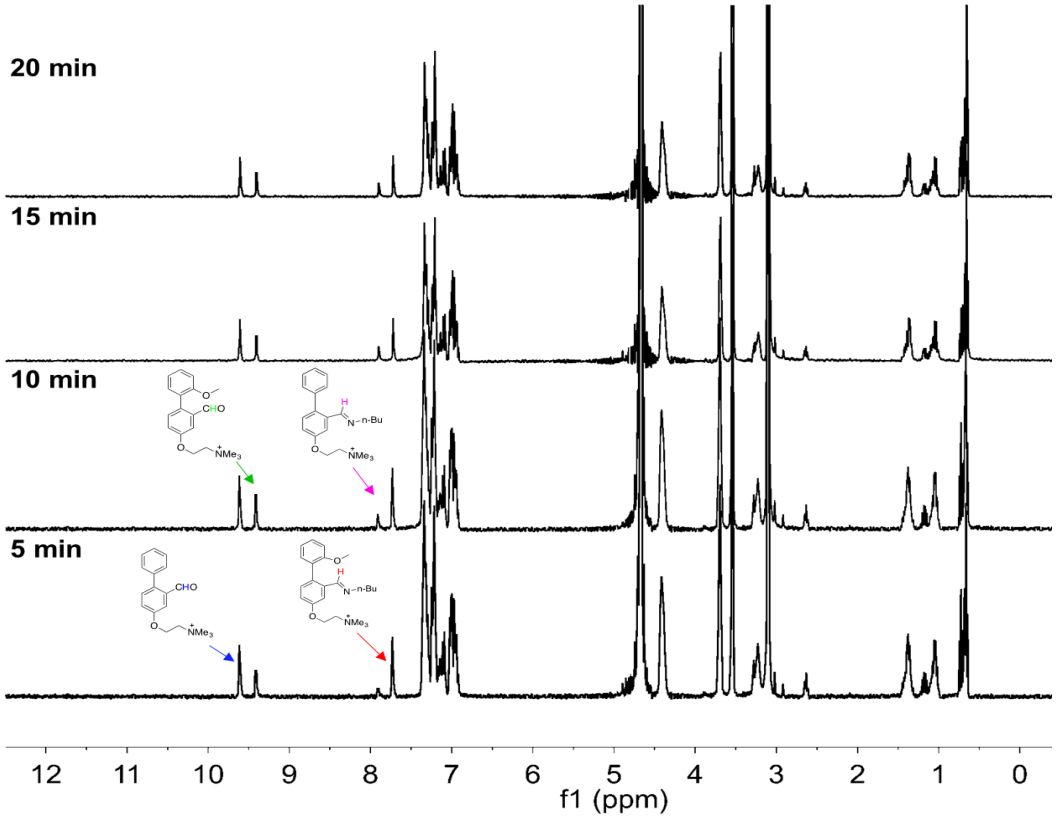

Figure S71. ^1H NMR spectra of the reaction of preformed **4**(OMe) and **3**(H) in D_2O at varied time (the corresponding spectra of panel d in Table S10).

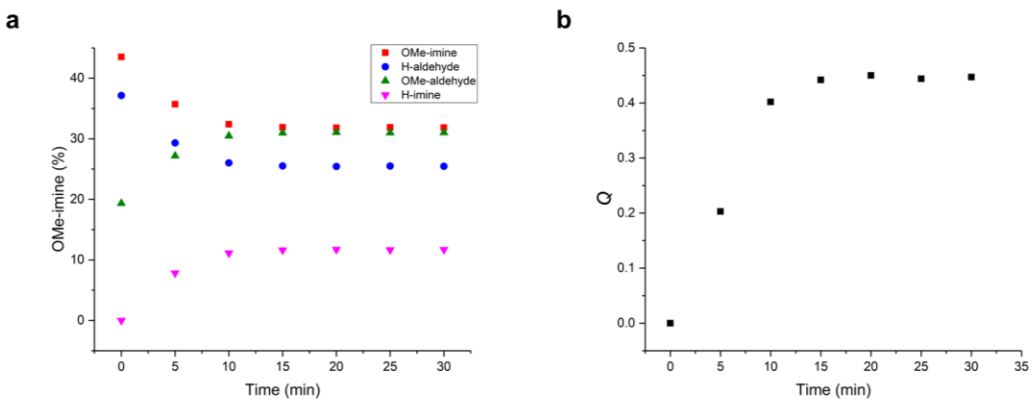

Figure S72. The kinetic profile of the reaction of preformed **4**(OMe) and **3**(H) in D_2O: (a) component distribution; (b) reaction quotient (Q).

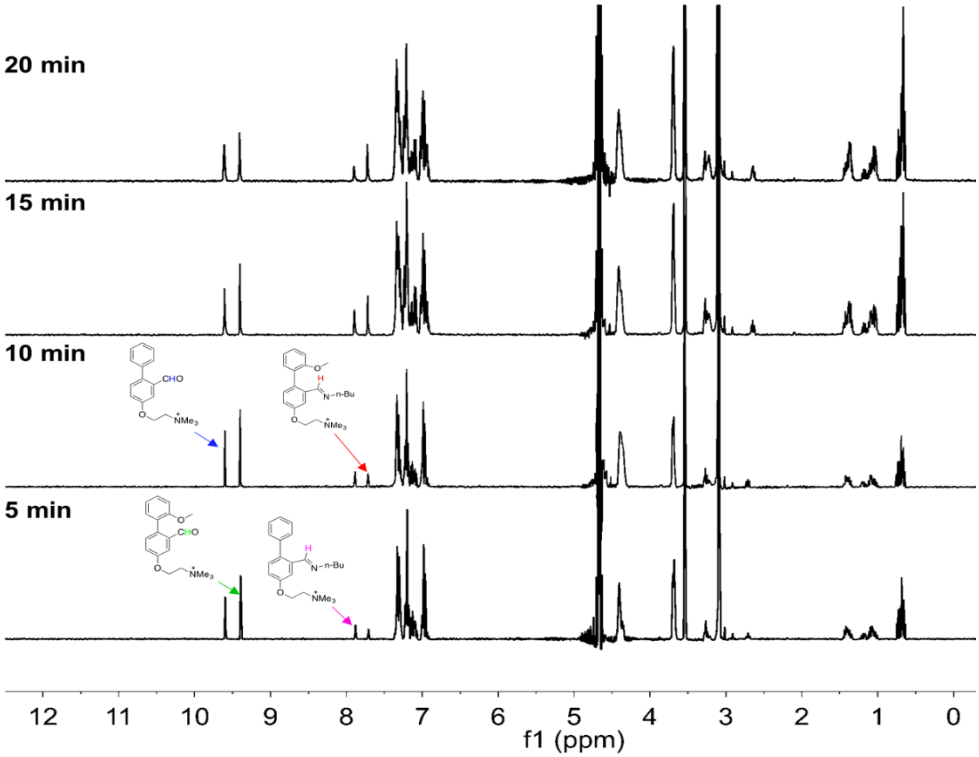

Figure S73. ^{1}H NMR spectra of the reaction of preformed **4**(H) and **3**(OMe) in D_2O at varied time (the corresponding spectra of panel e in Table S10).

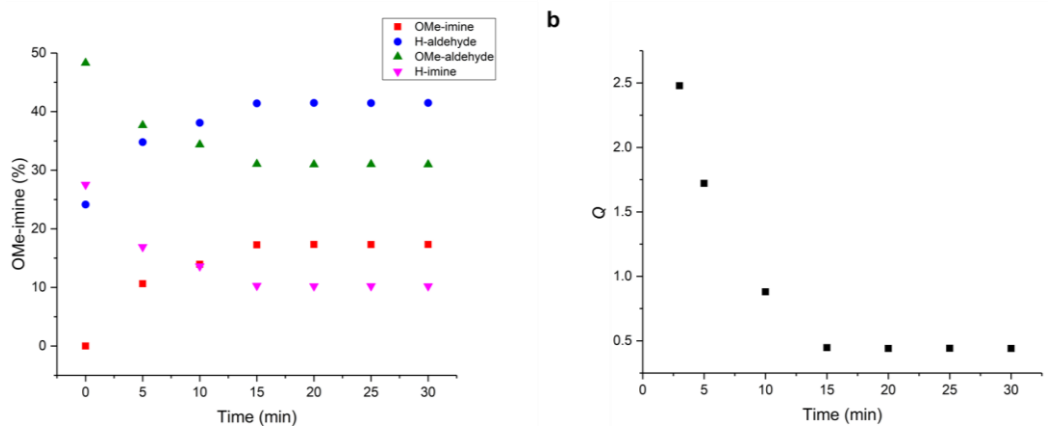

Figure S74. The kinetic profile of the reaction of preformed **4**(H) and **3**(OMe) in D_2O: (a) component distribution; (b) reaction quotient (Q).

(3) Solvent effect on $n \rightarrow \pi^*$ interaction

To explore the impact of protic solvents, one methanol molecule was added to reflect the weak interaction between the solvent and aldehyde, and this complex was subjected for computation in methanol (with PCM solvent model). The difference in free energies (△G) of conformers was summarized in Figure S75. The NBO stabilization energy ($\triangle E^{(2)}$) of $n \rightarrow \pi^*$ interaction and associated structure features are summarized in Table S11.

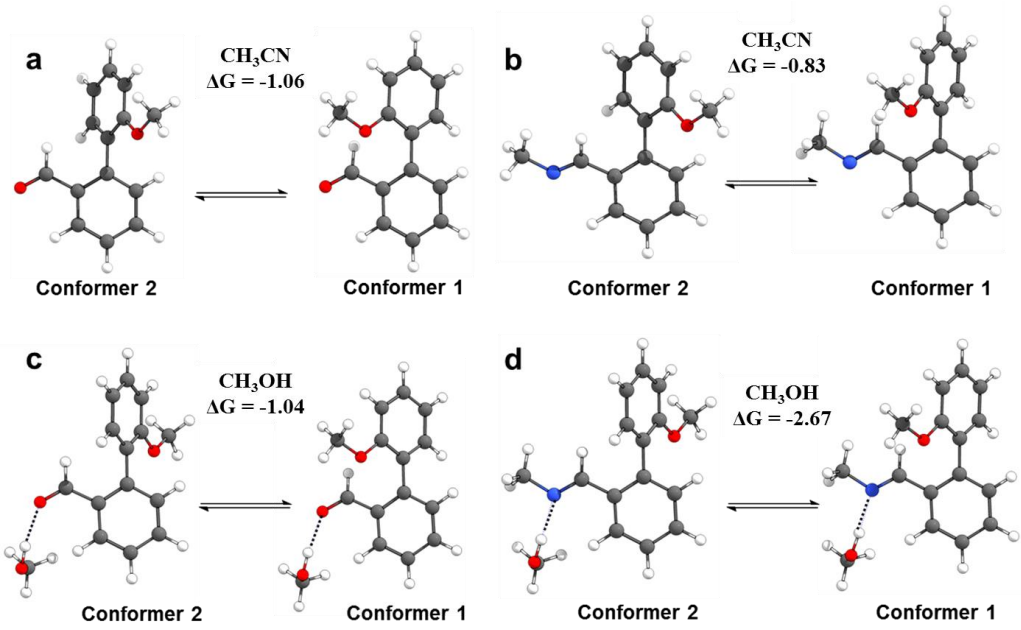

Figure S75. Calculated structures and free energy difference (kcal/mol) for

conformational equilibrium of **1**(OMe) and **2**(OMe) in acetonitrile and methanol, respectively. Based on Boltzmann distribution of conformers, △G of the exchange reaction (Figure 4A) was found to be -0.251 and -0.103 kcal/mol in acetonitrile and methanol, respectively. The trend is in agreement with measured △G of -0.293 (K = 1.64) and -0.118 (K = 1.22) kcal/mol in acetonitrile and methanol, respectively (Figure 4B and Table S9).

Table S11. The comparison of $n\rightarrow\pi^*$ interaction ($\triangle E^{(2)}$) and structural parameters of conformer 1 for **1**(OMe) and **2**(OMe) in acetonitrile and methanol, respectively.

Calculated structures of **1**(OMe) in CH_3CN or CH_3OH	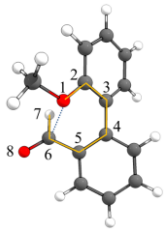 Conformer 1 (CH_3CN)	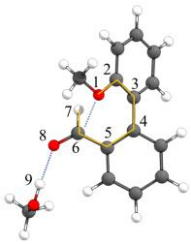 Conformer 1 (CH_3OH)
$\triangle E^{(2)}$ (kcal/mol)	-1.74	-1.81
α(2-3-4-5) (º)	54.3	54.3
β(4-5-6-7) (º)	14.4	13.1
D(1-6) (Å)	2.78	2.77
D(6-8) (Å)	1.21	1.21
D(8-9) (Å)	None	1.91
Calculated structures of **2**(OMe) in CH_3CN or CH_3OH	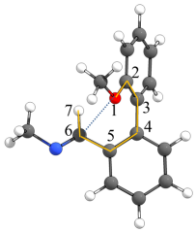 Conformer 1 (CH_3CN)	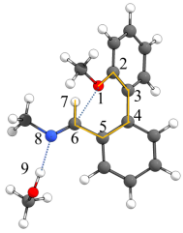 Conformer 1 (CH_3OH)
$\triangle E^{(2)}$ (kcal/mol)	-1.21	-2.34
α(2-3-4-5) (º)	57.5	46.1
β(4-5-6-7) (º)	15.0	21.0
D(1-6) (Å)	2.86	2.69
D(6-8) (Å)	1.26	1.26
D(8-9) (Å)	None	1.86

6. Imine Formation in Aqueous Phase

Imine formation in aqueous phase was performed in *situ* without isolation and purification. To a solution of **3** or **5** (20 mM, 1.0 equiv.) in D_2O (0.60 mL), was added the amine (22 mM, 1.2 equiv.). The mixture was characterized by ^1H NMR and ESI-MS after the equilibrium was reached.

For imine formation in D_2O buffer solution, **3** (20 mM, 10.0 equiv.) were dissolved in 600 μL KPi buffer in D_2O (20 mM, pH = 7.8), and a buffer solution of amine (1.09 M, pH = 7.8: 1.1 μL, 1.0 equiv.; the final concentration of amine was 2 mM) was next added. The mixture was characterized by ^1H NMR and ESI-MS.

For imine formation in buffer solution, **3** (0.20 mM, 100 equiv.) were dissolved in 600 μL KPi buffer (20 mM, pH = 7.4), and a buffer solution of amine (1.2 mM, pH = 7.4: 1.0 μL, 1.0 equiv.; the final concentration of amine was 2 μM) was next added. The mixture was characterized by ESI-MS.

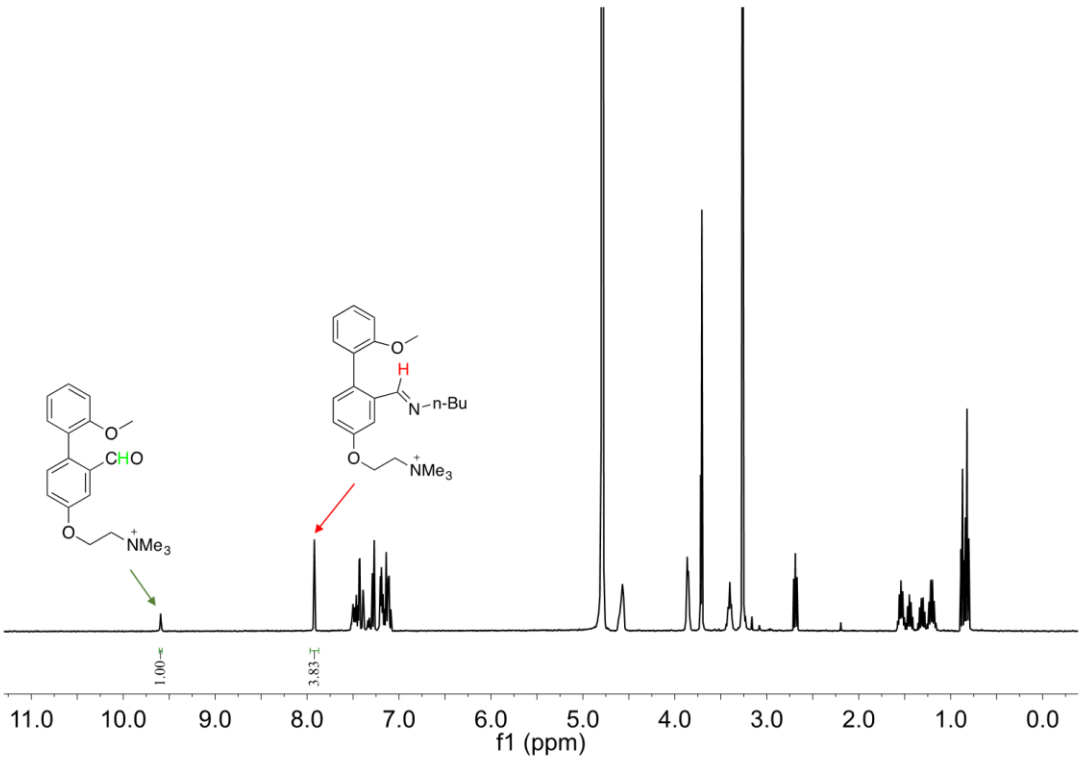

Figure S76. ^1H NMR spectrum of the reaction of **3**(OMe) (20 mM, 1.0 equiv.) and 1-butylamine (24 mM, 1.2 equiv.) in D_2O. The yield of imine is 79%.

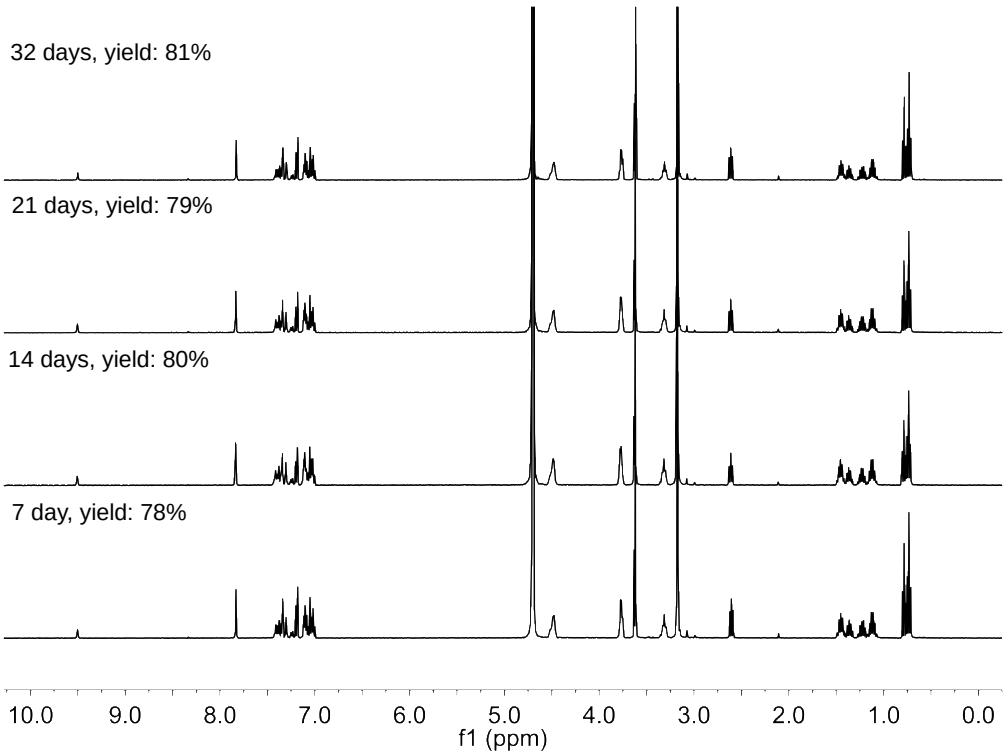

Figure S77. ^{1}H NMR spectra of the reaction of **3**(OMe) (20 mM, 1.0 equiv.) and 1-butylamine (1.2 equiv.) in D_2O at varied time. No decomposition of imine occurred.

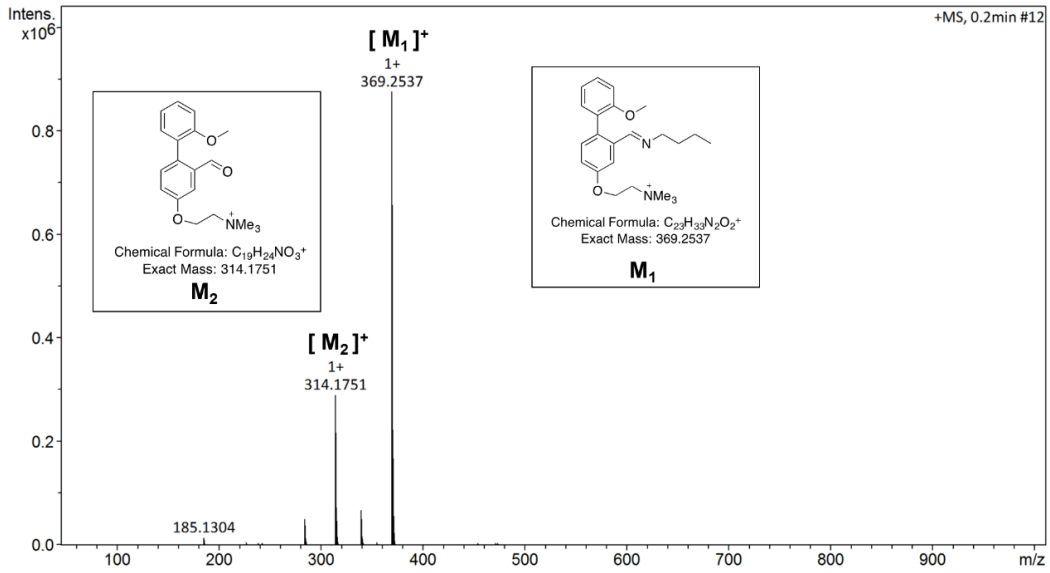

Figure S78. ESI-MS spectrum of the reaction of **3**(OMe) (20 mM, 1.0 equiv.) and 1-butylamine (1.2 equiv.) in D_2O.

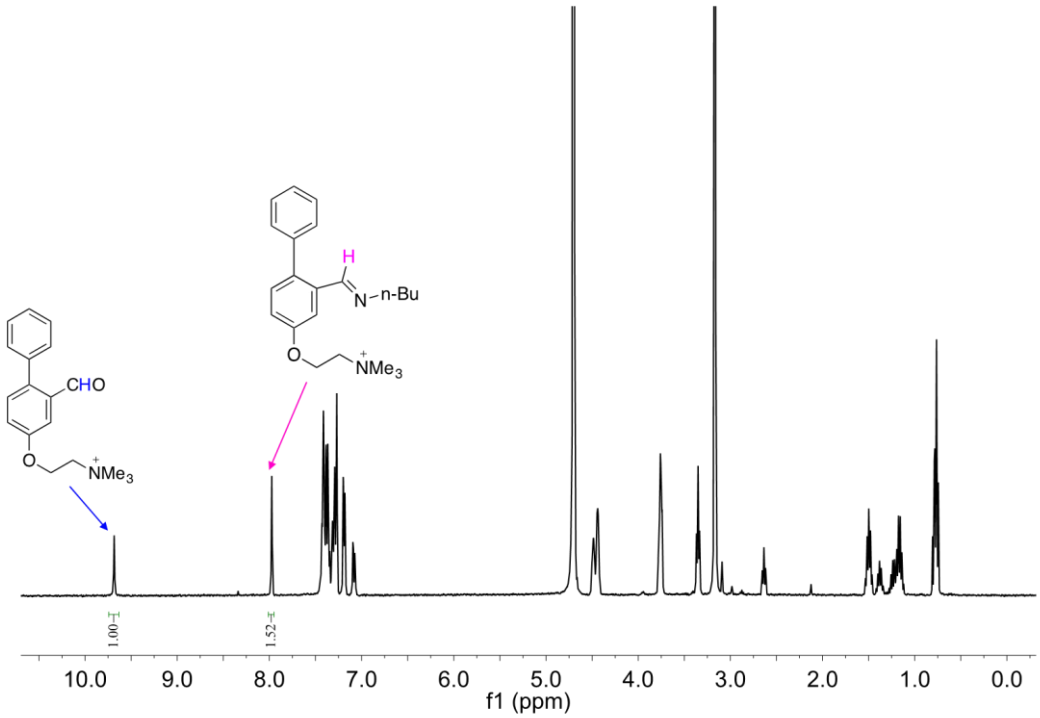

Figure S79. ^{1}H NMR spectrum of the reaction of **3**(H) (20 mM, 1.0 equiv.) and 1-butylamine (1.2 equiv.) in D_2O. The yield of imine is 60%.

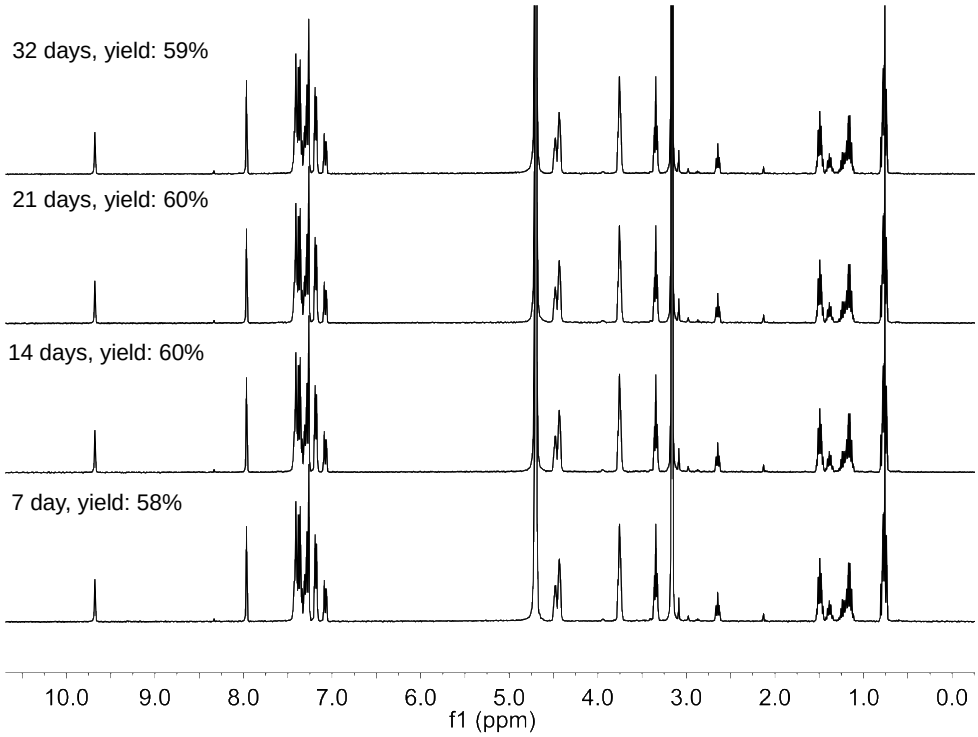

Figure 80. ^{1}H NMR spectra of the reaction of **3**(H) (20 mM, 1.0 equiv.) and 1-butylamine (1.2 equiv.) in D_2O at varied time. No decomposition of imine occurred.

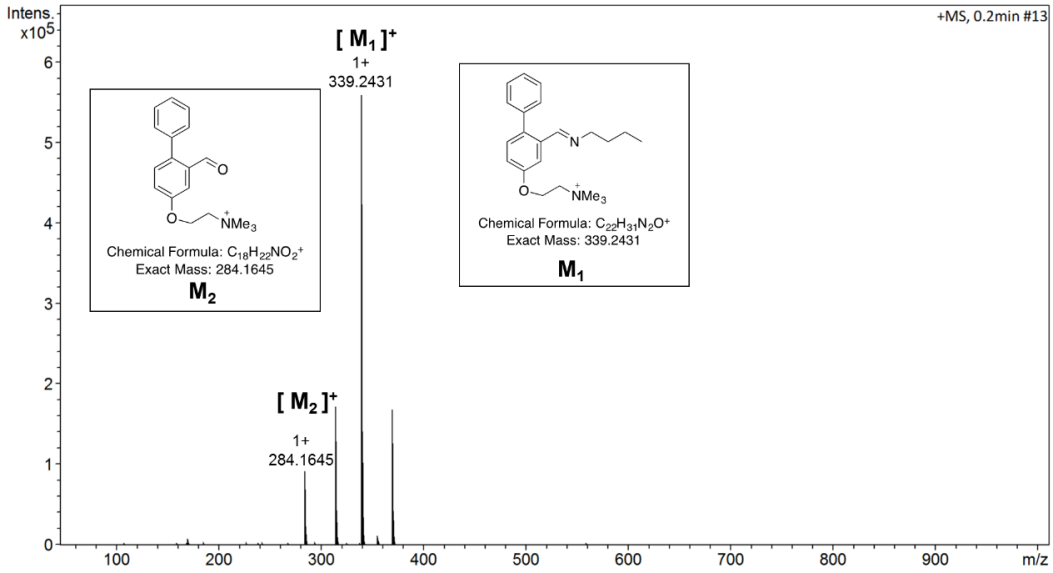

Figure S81. ESI-MS spectrum of the reaction of **3**(H) (20 mM, 1.0 equiv.) and 1-butylamine (1.2 equiv.) in D_2O.

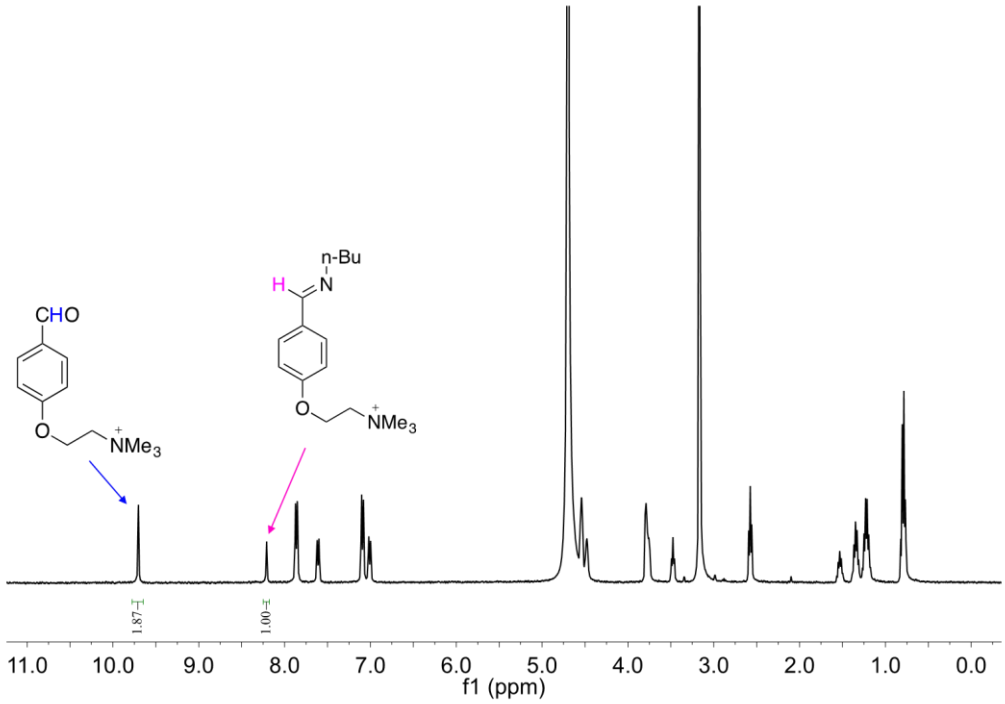

Figure S82. ^{1}H NMR spectrum of the reaction of **5** (20 mM, 1.0 equiv.) and 1-butylamine (1.2 equiv.) in D_2O. The yield of imine is 35%.

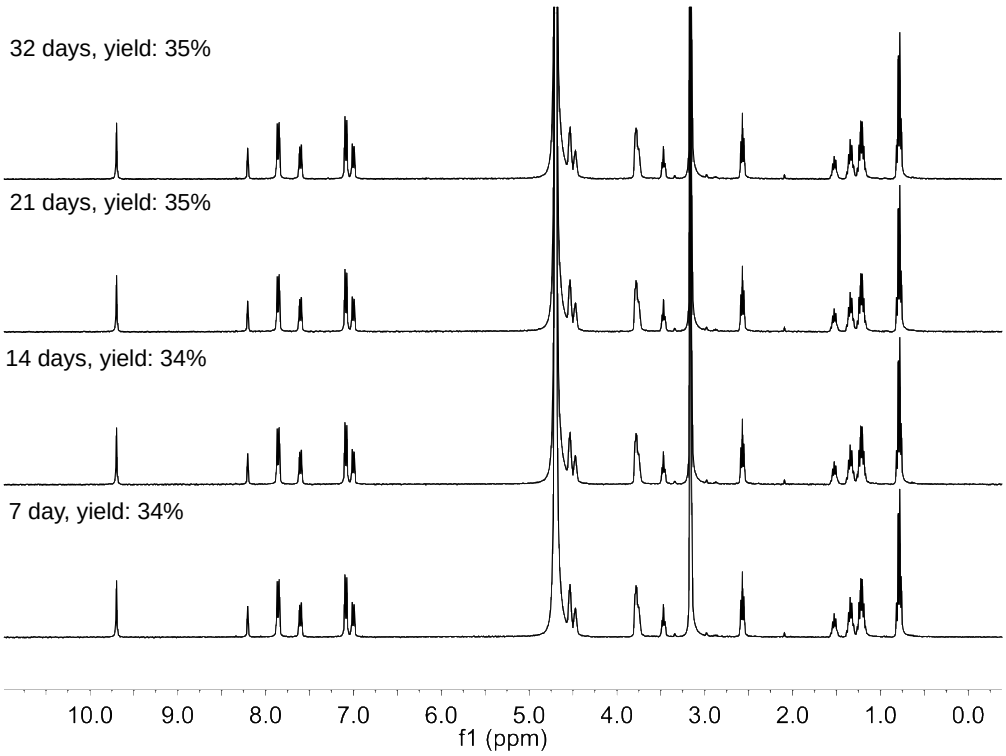

Figure S83. ^{1}H NMR spectra of the reaction of **5** (20 mM, 1.0 equiv.) and 1-butylamine (1.2 equiv.) in D_2O at varied time. No decomposition of imine occurred.

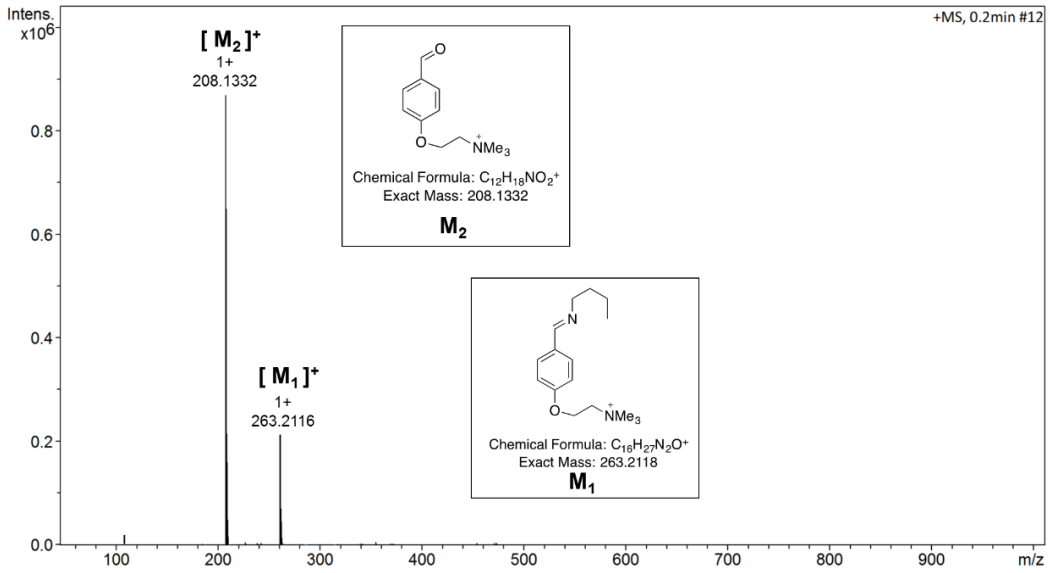

Figure S84. ESI-MS spectrum of the reaction of **5** (20 mM, 1.0 equiv.) and 1-butylamine (1.2 equiv.) in D_2O.

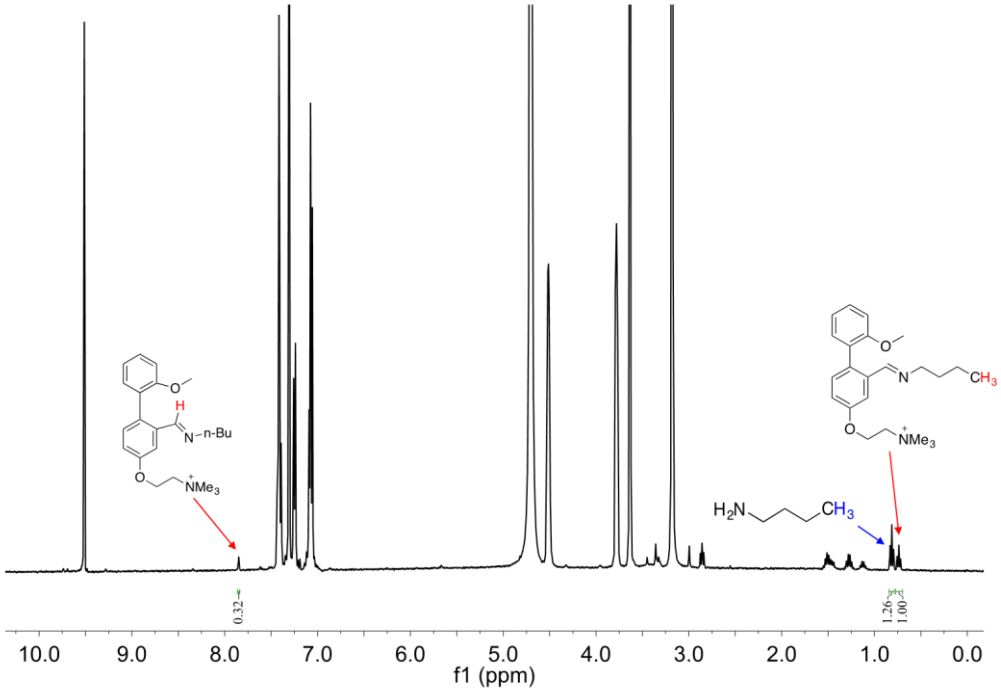

Figure S85. ^{1}H NMR spectrum of the reaction of **3**(OMe) (20 mM, 10.0 equiv.) and 1-butylamine (2 mM, 1.0 equiv.) in KPi buffer solution in D_2O (20 mM, pH = 7.8). The yield of imine is 44%.

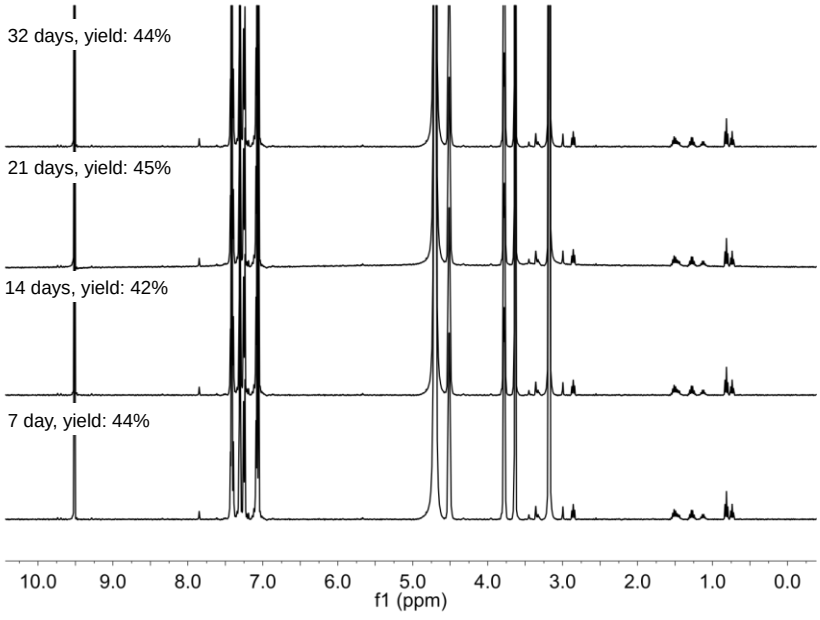

Figure S86. ^{1}H NMR spectra of the reaction of **3**(OMe) (20 mM, 10.0 equiv.) and 1-butylamine (2 mM, 1.0 equiv.) in KPi buffer solution in D_2O (20 mM, pH = 7.8) at varied time. No decomposition of imine occurred.

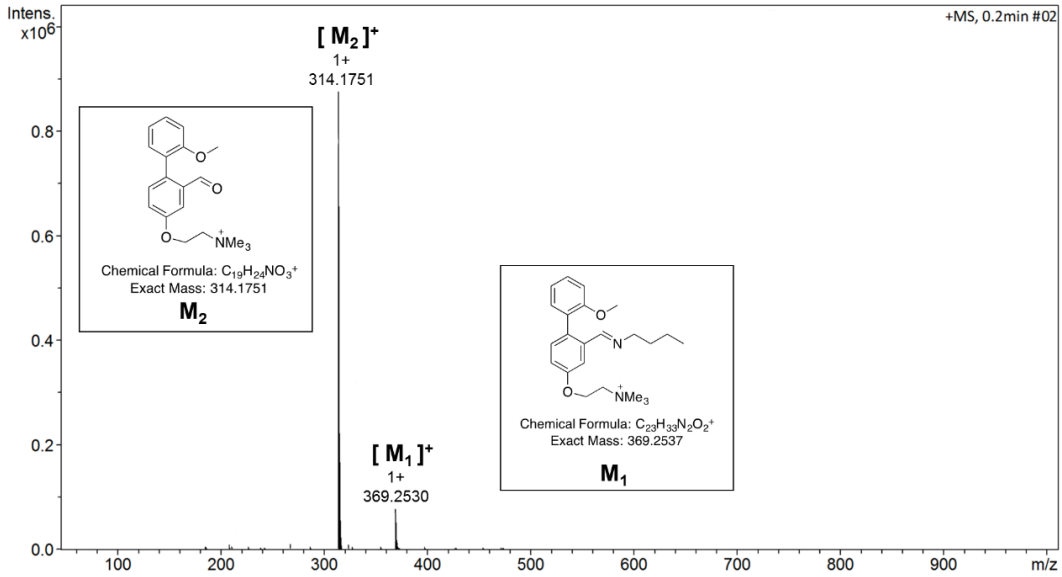

Figure S87. ESI-MS spectrum of the reaction of **3**(OMe) (20 mM, 10.0 equiv.) and 1-butylamine (2 mM, 1.0 equiv.) in KPi buffer solution in D_2O (20 mM, pH = 7.8).

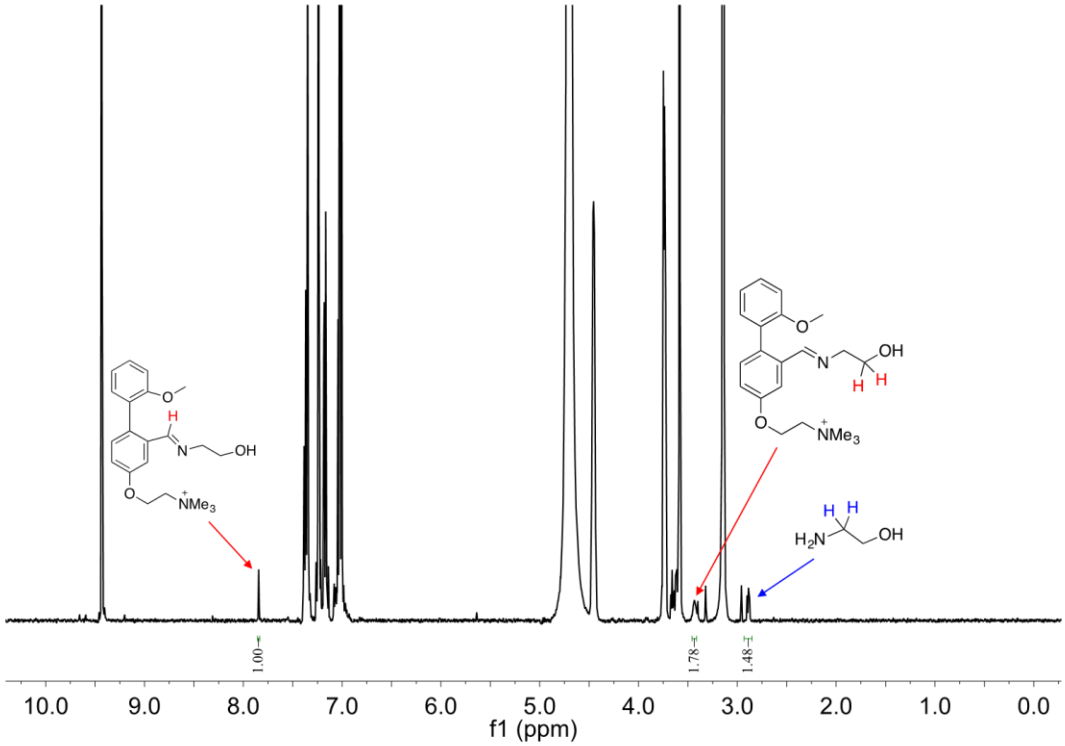

Figure S88. ^1H NMR spectrum of the reaction of **3**(OMe) (20 mM, 10.0 equiv.) and ethanolamine (2 mM, 1.0 equiv.) in KPi buffer solution in D_2O (20 mM, pH = 7.8). The yield of imine is 54%.

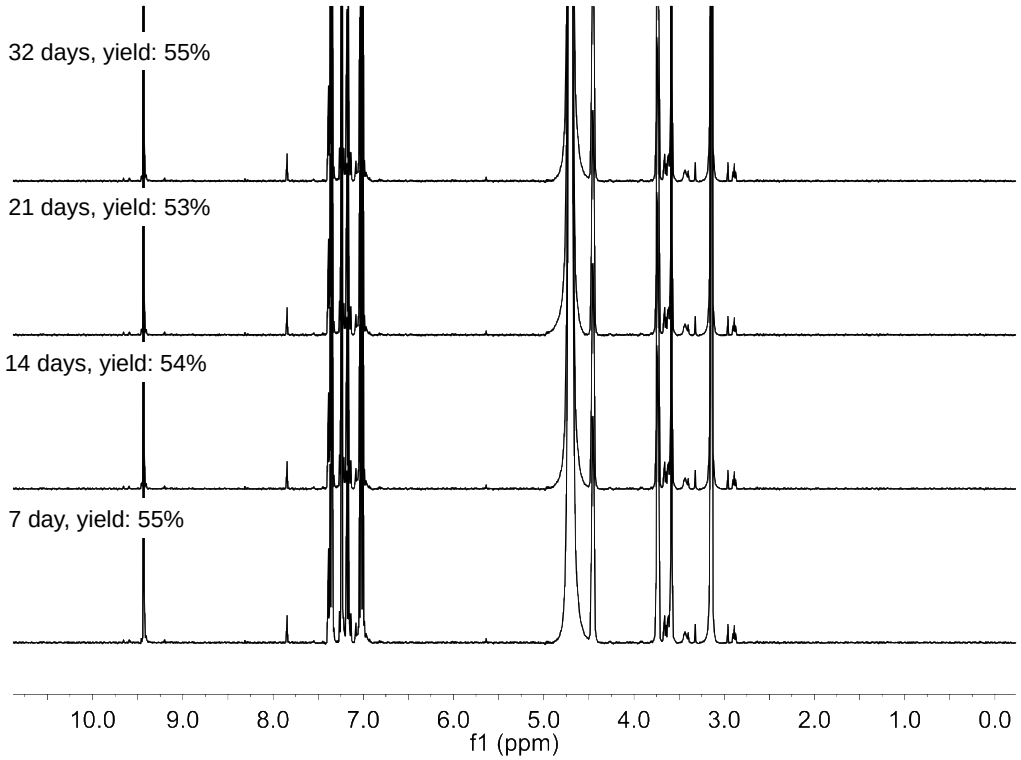

Figure S89. ^{1}H NMR spectra of the reaction of **3**(OMe) (20 mM, 10.0 equiv.) and ethanolamine (2 mM, 1.0 equiv.) in KPi buffer solution in D_2O (20 mM, pH = 7.8) at varied time. No decomposition of imine occurred.

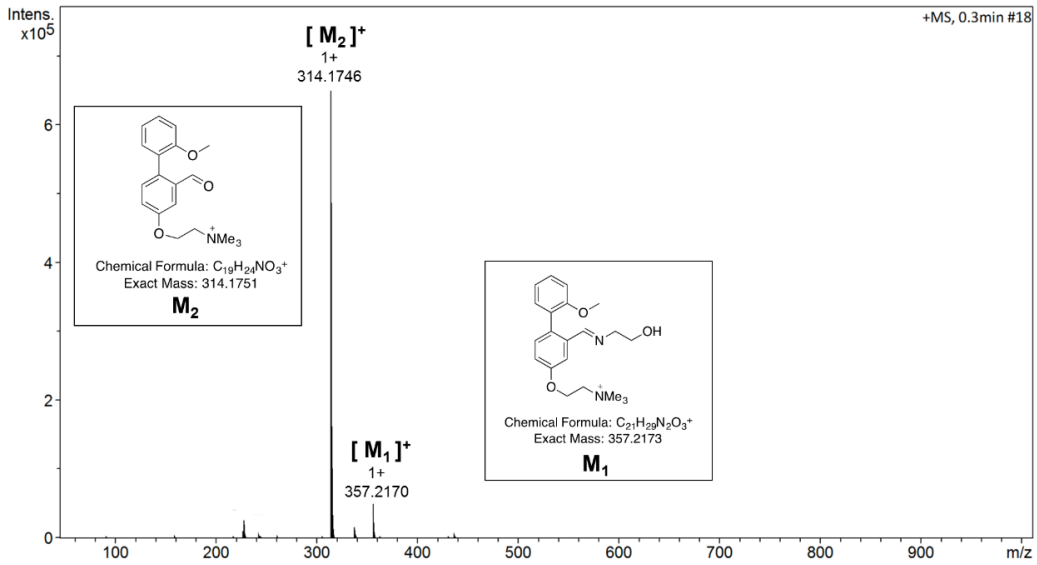

Figure S90. ESI-MS spectrum of the reaction of **3**(OMe) (20 mM, 1.0 equiv.) and ethanolamine (10 mM, 1.0 equiv.) in KPi buffer solution in D_2O (20 mM, pH = 7.8).

7. References

S1. Fürstner, A.; Mamane, V. Flexible Synthesis of Phenanthrenes by a $PtCl_2$-Catalyzed Cycloisomerization Reaction. *J. Org. Chem.* **2002**, *67*, 6264.

S2. Wallis, J. D.; O'Leary, J. Interactions and Reactions in Some 2,2′-Disubstituted Biphenyls—An Open or Shut Case. *Org. Biomol. Chem.* **2009**, *7*, 225.

S3. Sindelar, M.; Lutz, T. A.; Petrera, M.; Wanner, K. T. Focused Pseudostatic Hydrazone Libraries Screened by Mass Spectrometry Binding Assay: Optimizing Affinities toward γ-Aminobutyric Acid Transporter 1. *J. Med. Chem.* **2013**, *56*, 1323.

S4. Knowles, J. P.; O'Connor, V. E.; Whiting, A. Studies towards the Synthesis of the Northern Polyene of Viridenomycin and Synthesis of *Z*-Double Bond Analogues. *Org. Biomol. Chem.* **2011**, *9*, 1876.

S5. Fu, H.-Y.; Xu, N.; Pan, Y.-M.; Lu, X.-L.; Xia, M. Emission Behaviours of Novel V- and X-Shaped Fluorophores in Response to pH and Force Stimuli. *Phys. Chem. Chem. Phys.* **2017**, *19*, 11563.

S6. Khanapure, S. P.; Garvey, D. S.; Young, D. V.; Ezawa, M.; Earl, R. AGaston, R. D.; Fang, X.; Murty, M.; Martino, A.; Shumway, M.; Trocha, M.; Marek, P.; Tam, S. W.; Janero, D. R.; Letts, L. G. Synthesis and Structure−Activity Relationship of Novel, Highly Potent Metharyl and Methcycloalkyl Cyclooxygenase-2 (COX-2) Selective Inhibitors. *J. Med. Chem.* **2003**, *46*, 5484.

S7. Carreras, J.; Gopakumar, G.; Gu, L.; Gimeno, A.; Linowski, P.; Petuškova, J.; Thiel, W.; Alcarazo, M. Polycationic Ligands in Gold Catalysis: Synthesis and Applications of Extremely π-Acidic Catalysts. *J. Am. Chem. Soc.* **2013**, *135*, 18815.

S8. Tang, J.; Sivaguru, P.; Ning, Y.; Zanoni, G.; Bi, X. Silver-Catalyzed Tandem C≡C Bond Hydroazidation/Radical Addition/Cyclization of Biphenyl Acetylene: One-Pot Synthesis of 6-Methyl Sulfonylated Phenanthridines. *Org. Lett.* **2017**, *19*, 4026.

S9. Sheng, L.; Kurihara, K. Generation of Catalytic Amphiphiles in a Self-Reproducing Giant Vesicle. *Chem Lett.* **2016**, *45*, 598.

S10. Frisch, M. J.; Trucks, G. W.; Schlegel, H. B.; Scuseria, G. E.; Robb, M. A.; Cheeseman, J. R.; Scalmani, G.; Barone, V.; Mennucci, B.; Petersson, G. A.; Nakatsuji, H.; Caricato, M.; Li, X.; Hratchian, H. P.; Izmaylov, A. F.; Bloino, J.; Zheng, G.; Sonnenberg, J. L.; Hada, M.; Ehara, M.; Toyota, K.; Fukuda, R.; Hasegawa, J.; Ishida, M.; Nakajima, T.; Honda, Y.; Kitao, O.; Nakai, H.; Vreven, T.; Montgomery, J. A., Jr.; Peralta, J. E.; Ogliaro, F.; Bearpark, M.; Heyd, J. J.; Brothers, E.; Kudin, K. N.; Staroverov, V. N.; Kobayashi, R.; Normand, J.; Raghavachari, K.; Rendell, A.; Burant, J. C.; Iyengar, S. S.; Tomasi, J.; Cossi, M.; Rega, N.; Millam, J. M.; Klene, M.; Knox, J. E.; Cross, J. B.; Bakken, V.; Adamo, C.; Jaramillo, J.; Gomperts, R.; Stratmann, R. E.; Yazyev, O.; Austin, A. J.; Cammi, R.; Pomelli, C.; Ochterski, J. W.; Martin, R. L.; Morokuma, K.; Zakrzewski, V. G.; Voth, G. A.; Salvador, P.; Dannenberg, J. J.; Dapprich, S.; Daniels, A. D.; Farkas, Ö.; Foresman, J. B.; Ortiz, J. V.; Cioslowski, J.;

Fox, D. J. *Gaussian 09*, revision D.01; Gaussian, Inc.: Wallingford, CT, **2010**.

S11. Glendening, E. D. Reed, A. E.; Carpenter, J. E.; Weinhold, F. *NBO*, version 3.1; Gaussian, Inc.: Wallingford, CT, **2010**.

S12. Johnson, E. R.; Keinan, S.; Mori-Sánchez, P.; Contreras-García, J.; Cohen, A. J.; Yang, W. Revealing Noncovalent Interactions. *J. Am. Chem. Soc.* **2010**, *132*, 6498.

S13. Lu, T.; Chen, F. Multiwfn: A Multifunctional Wavefunction Analyzer. *J. Comput. Chem.* **2012**, *33*, 580.

S14. Humphrey, W.; Dalke, A.; Schulten, K. VMD: Visual Molecular Dynamics. *J. Mol. Graphics* **1996**, *14*, 33.

S15. Reichardt, C.; Welton, T. *Solvents and Solvent Effects in Organic Chemistry.* WILEY-VCH Verlag GmbH & Co. KGaA, Weinheim, **2011**.